AGN: mid-IR emission and the quest for heavily obscured nuclei

AGN Spectral Energy Distributions

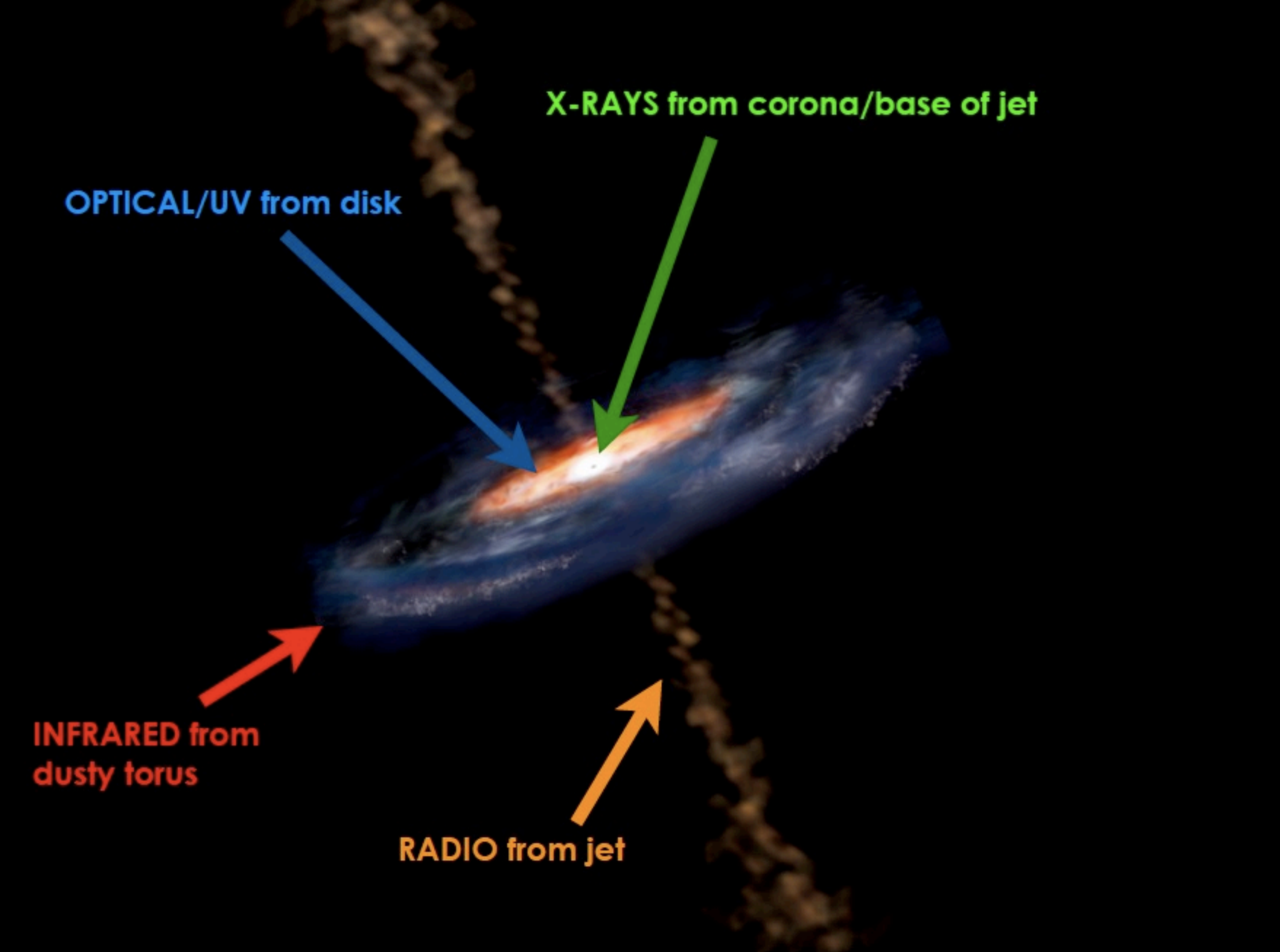
X-RAYS from corona/base of jet
OPTICAL/UV from disk
INFRARED from dusty torus
RADIO from jet

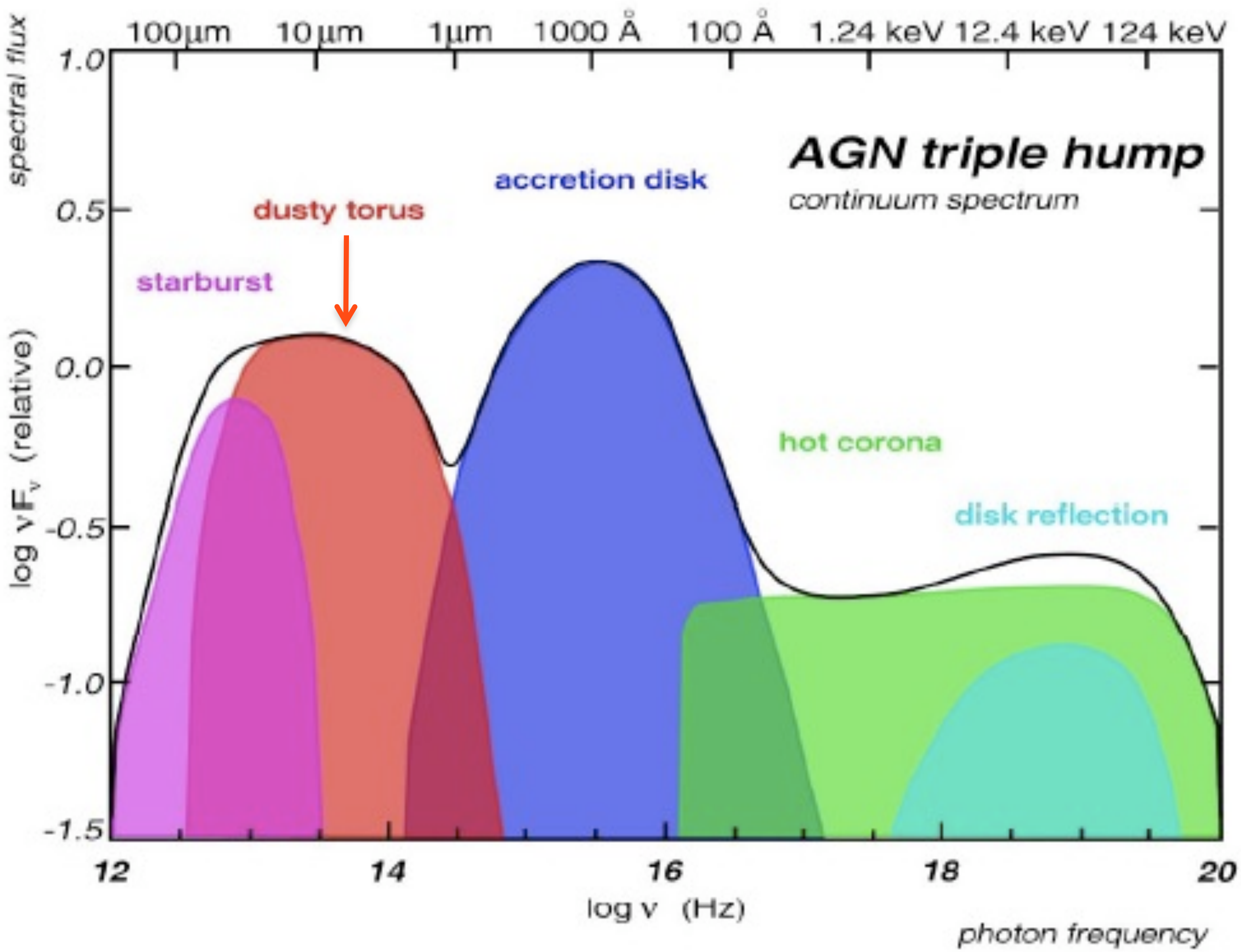
100µm
10µm
1µm
1000 Å
100 Å
1.24 keV
12.4 keV
124 keV
spectral flux
1.0
0.5
0.0
-0.5
-1.0
-1.5
log νF_ν (relative)
AGN triple hump
continuum spectrum
accretion disk
dusty torus
starburst
hot corona
disk reflection
12
14
16
18
20
log ν (Hz)
photon frequency

Broad-band spectral energy distribution of AGN:
Radio-Loud ('jetted') vs. Radio-Quiet QSOs

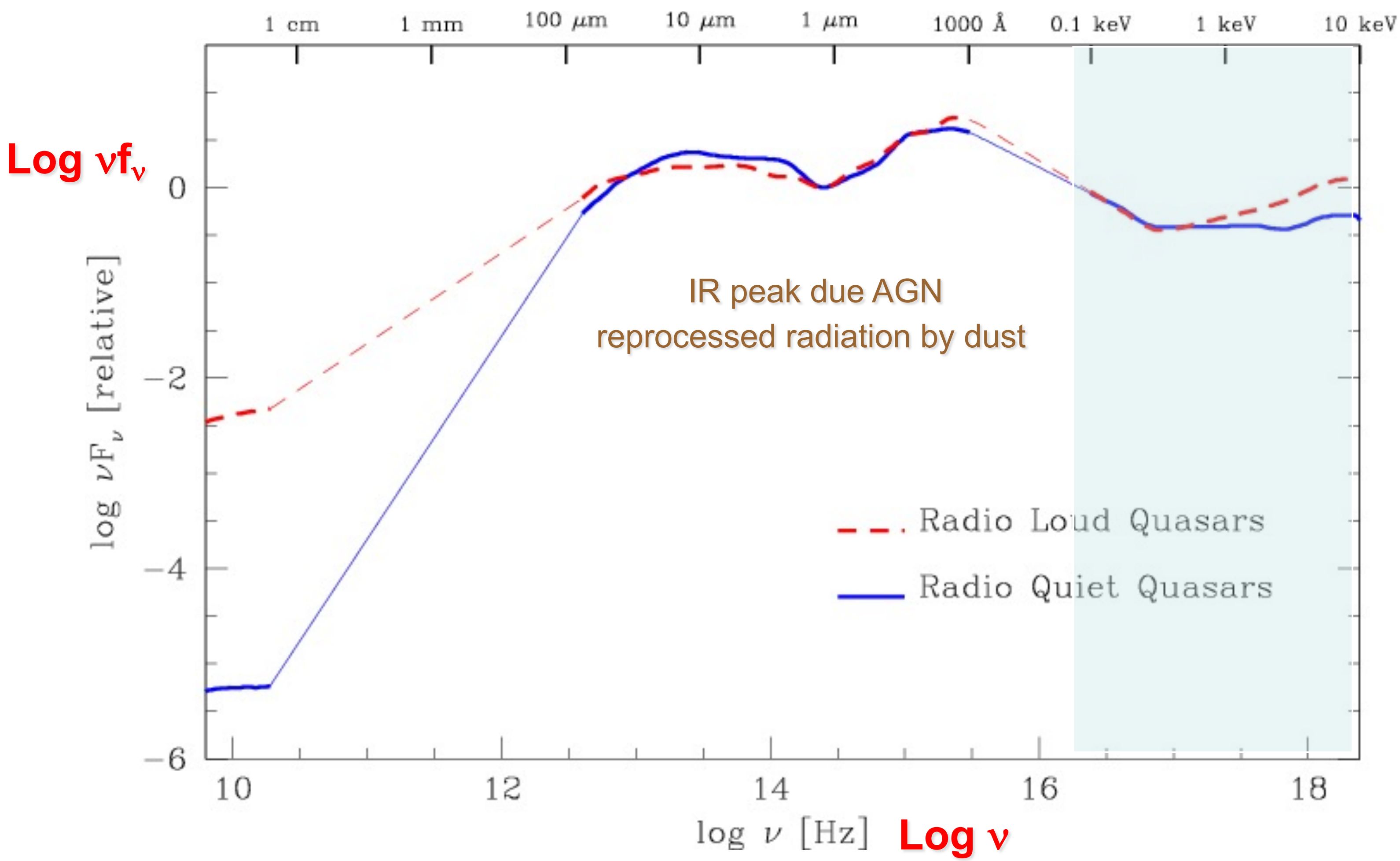

Elvis et al. 1994

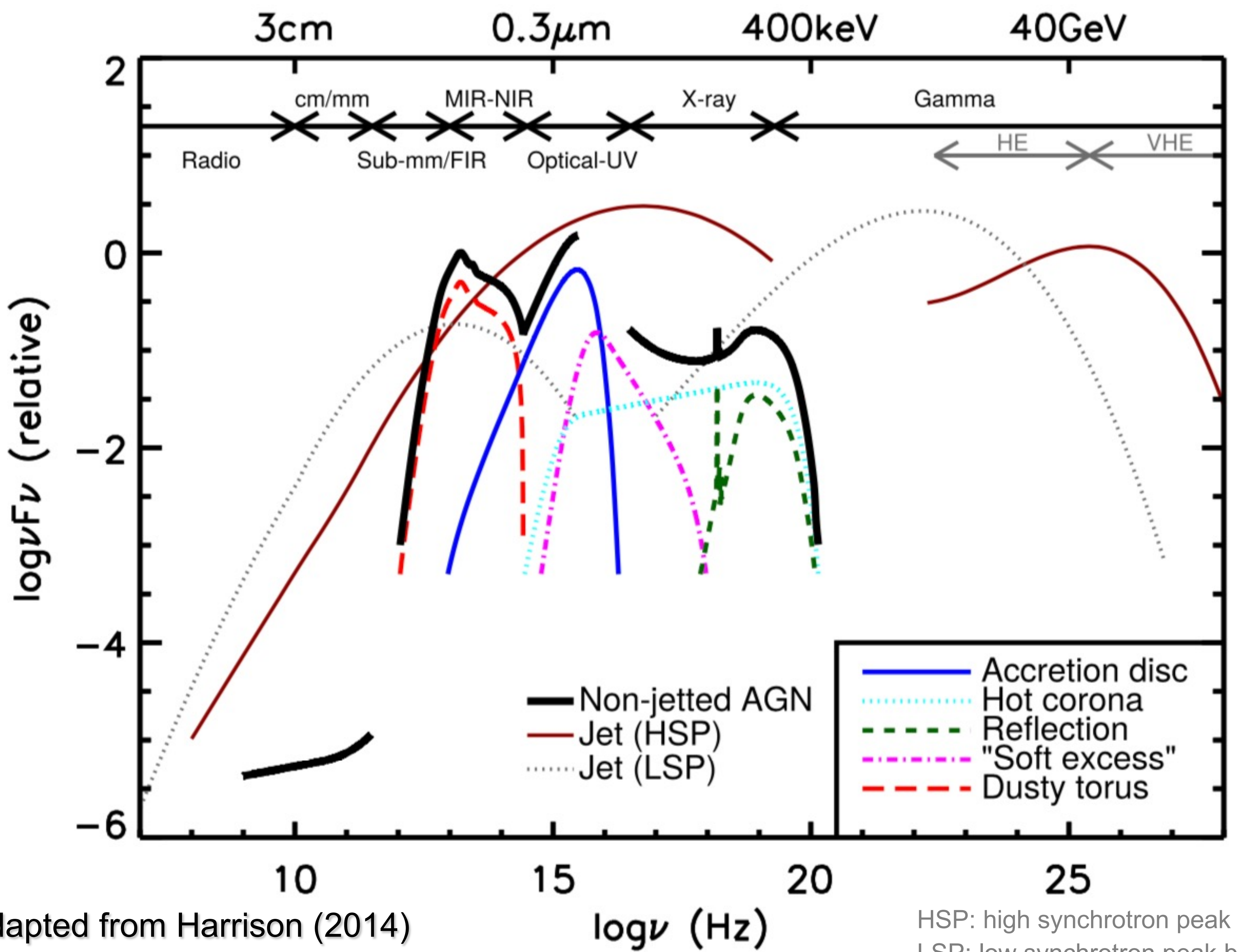

adapted from Harrison (2014)

HSP: high synchrotron peak blazar
LSP: low synchrotron peak blazar

From the slopes of the hypothetical powerlaw connecting e.g. the radio (optical) with the X-ray band (α_{RX}, α_{oX}), it is possible to derive hints on the emission processes and classify sources in macro-classes. For example, **α_{ox}** gives the importance of the UV (disc) emission vs. that of the corona (X-ray)

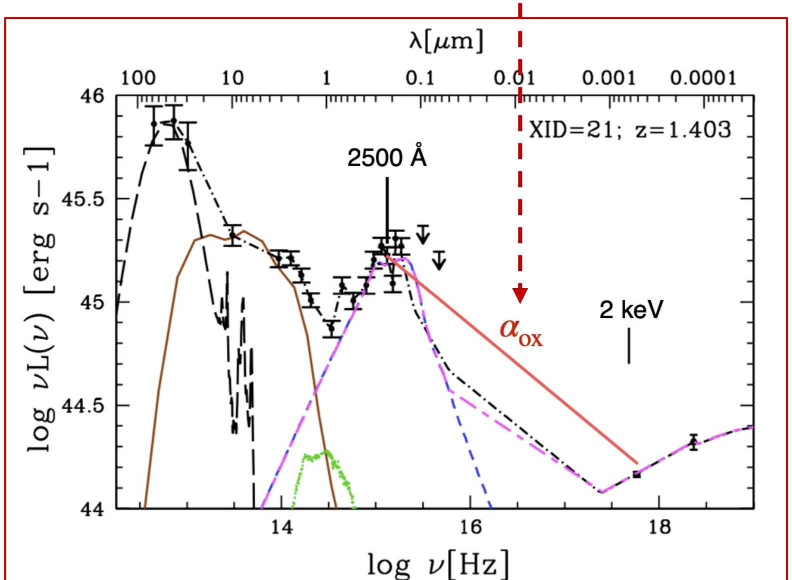

Courtesy of E. Lusso

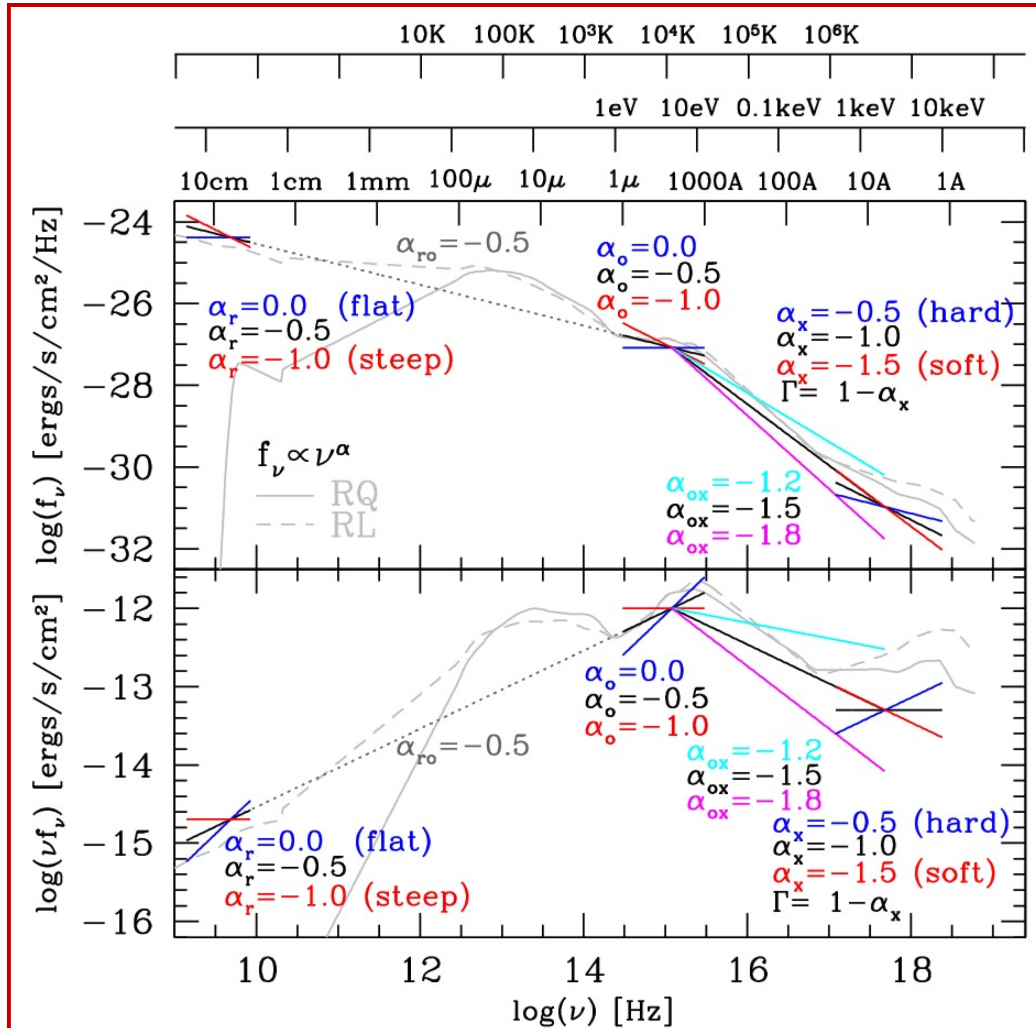

Richards et al. 2006

Mid-IR emission from AGN

Models for the infrared emission of AGN. I
‘Phenomenological’ models

Smooth dust distribution

dust grains around a central source (AGN) in a smooth distribution (e.g., Pier & Krolik ‘92, ’93)

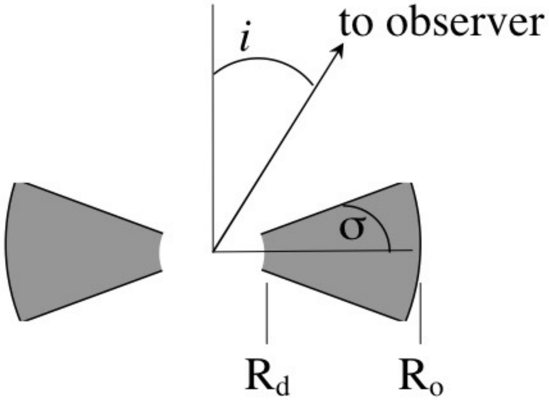

Clumpy models

dust grains in clouds (not uniform distribution) A Type 2 AGN can be seen also at large inclination angles over the equatorial plane (e.g., Nenkova et al. ‘02, ‘08)

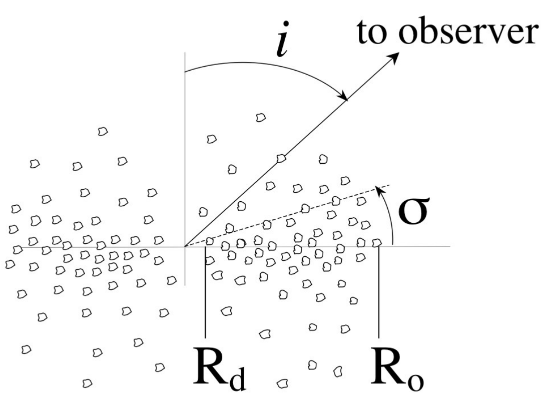

Models for the infrared emission of AGN. II
‘Phenomenological’ models

Smooth dust distribution: main properties

• The source is obscured if radiation intercepts the torus, hence obscuration is related to geometrical issues

• Dust temperature is a function of the distance from the source of the radiation field

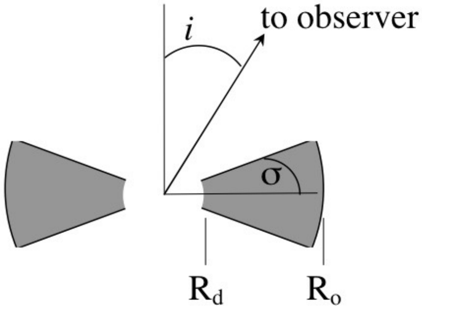

Clumpy models: main properties

• The probability of direct viewing of the AGN decreses away from the axis, but is always finite

• Different dust temperatures coexist at the same distance from the radiation source, and the same dust temperature occurs at different distances

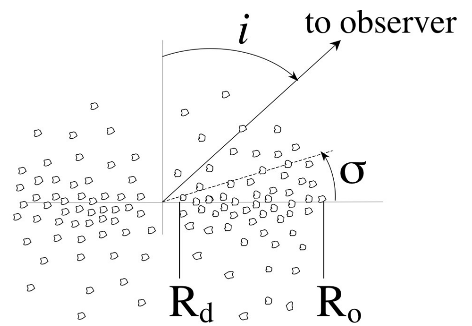

AGN type is a viewing-dependent probability

Alternative modeling: hydromagnetic disk wind

• Torus=toroidal region of a wind, structured in outflowing clouds. The acceleration is provided by magnetic field lines anchored in the disc (Blandford & Payne ‘82; Elitzur ‘08)

Models for the infrared emission of AGN. III

'Phenomenological' models

Obscuration = function of optical depth, covering factor, etc.
Proper treatment with radiative transfer models

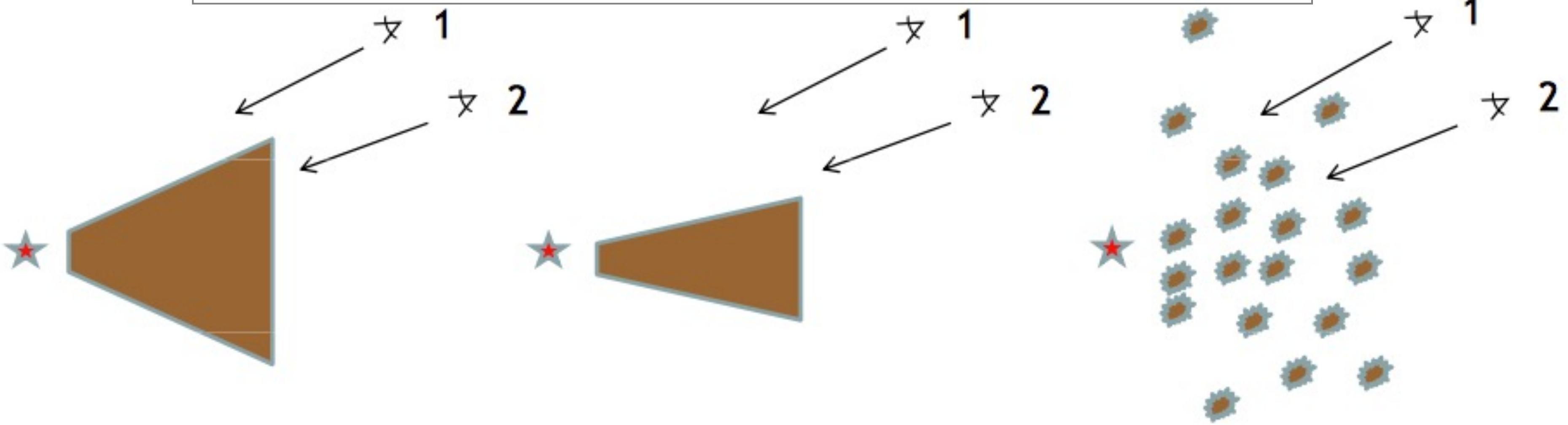

Smooth-density torus — Torus with decreased covering factor — Clumpy, soft-edge torus

The covering factor can be estimated using *SED fitting* with multiple (host galaxy and AGN) components (but model degeneracies may affect the results, i.e. different model parameters may produce similar results)

Elitzur 2011

Currently: attempts to link the properties of the absorber derived from X-rays with those of mid-IR and SED analysis in a systematic way

Dust sublimation temperatures

$$R_d \approx 0.5\ L_{46}^{1/2} (\frac{1800\ K}{T_{sub}})^{2.6}\ f(\theta)\ pc$$

$$R_d \approx 1.3\ L_{46}^{1/2} (\frac{1500\ K}{T_{sub}})^{2.6}\ f(\theta)\ pc$$

Sublimation radius for graphite and silicate dust grains

luminosity in units of 10^{46} erg/s

angle-dependent term accounting for *anisotropy of the central radiation* – angle-dependence of the emitted radiation (Netzer 2015 review; Netzer and Trakhtembrot 2014), most noticeable in smooth tori

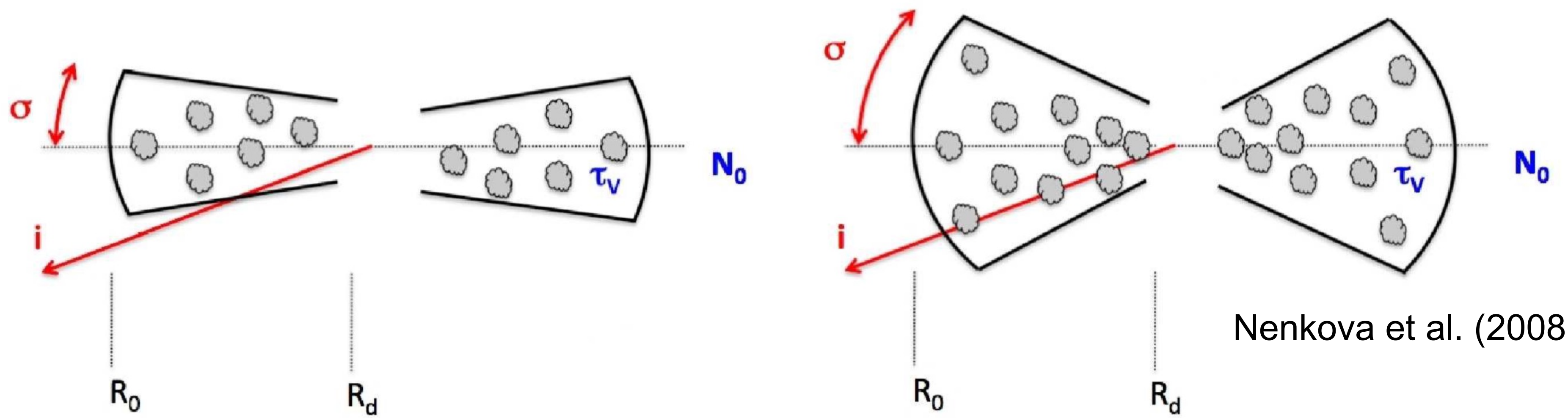

Nenkova et al. (2008)

The sublimation radius of the dust R_d represents a sort of outer boundary of the BLR clouds (dust-free) and inner radius for the dusty torus

Relative line emissivities per unit covering factor for twice solar metallicy BLR gas

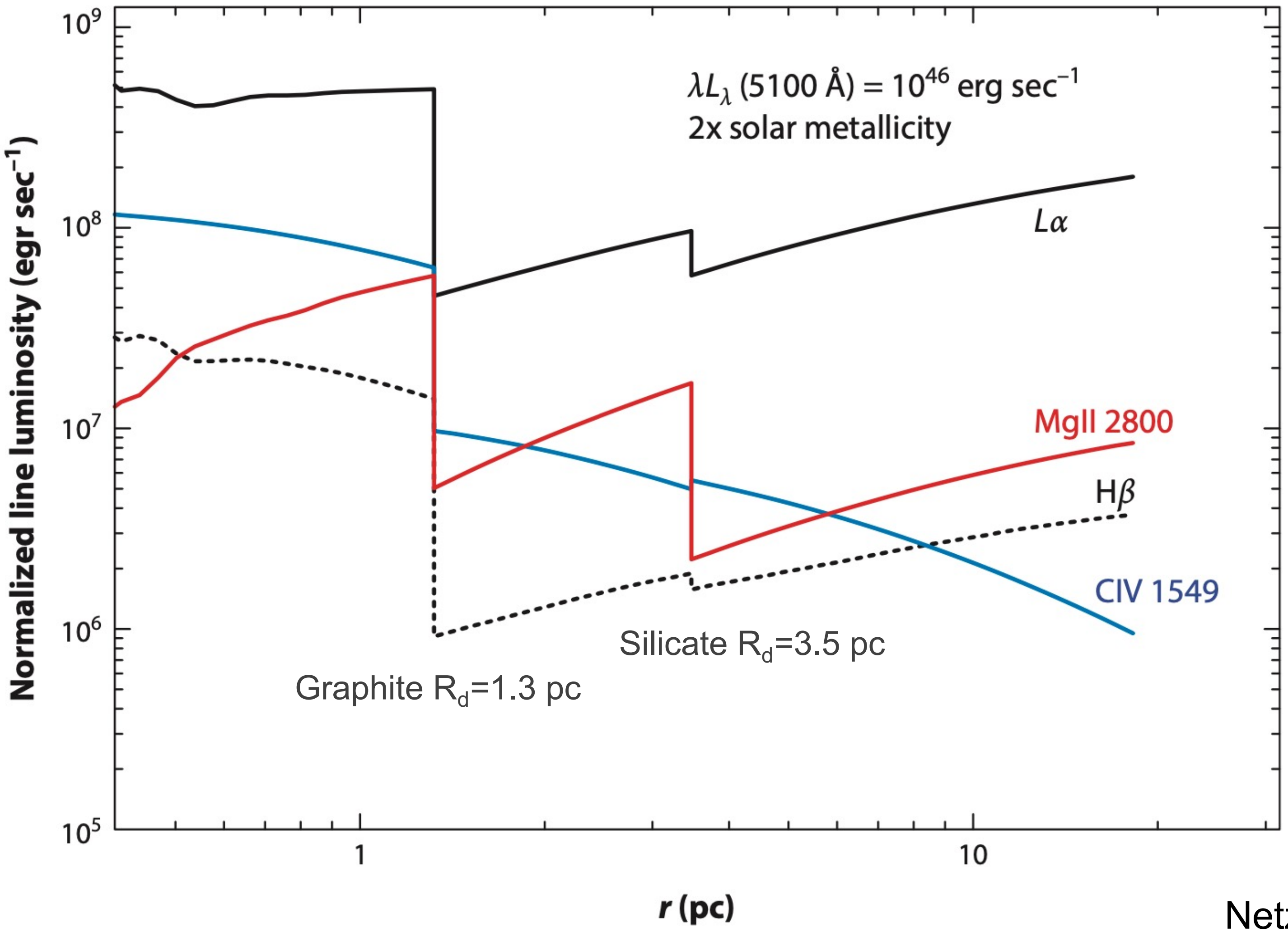

Netzer (2015)

Line intensity drops due to absorption of the ionizing radiation by the dust grains at different distances from the BH because of the different T_{subl}

Several possible configurations allowed

Main Type 1/Type 2 AGN difference is the optical depth → the silicate feature at 9.7 micron is mostly in emission/absorption in AGN1/AGN2

As the radiation propagates from the hot regions toward the observer, it passes through cooler regions, where it suffers absorption which is not balanced by the emission from cooler regions → *It is the temperature structure that primarily determines the strength of the absorption feature at large optical depth*

Dust self-absoprtion must be taken into account

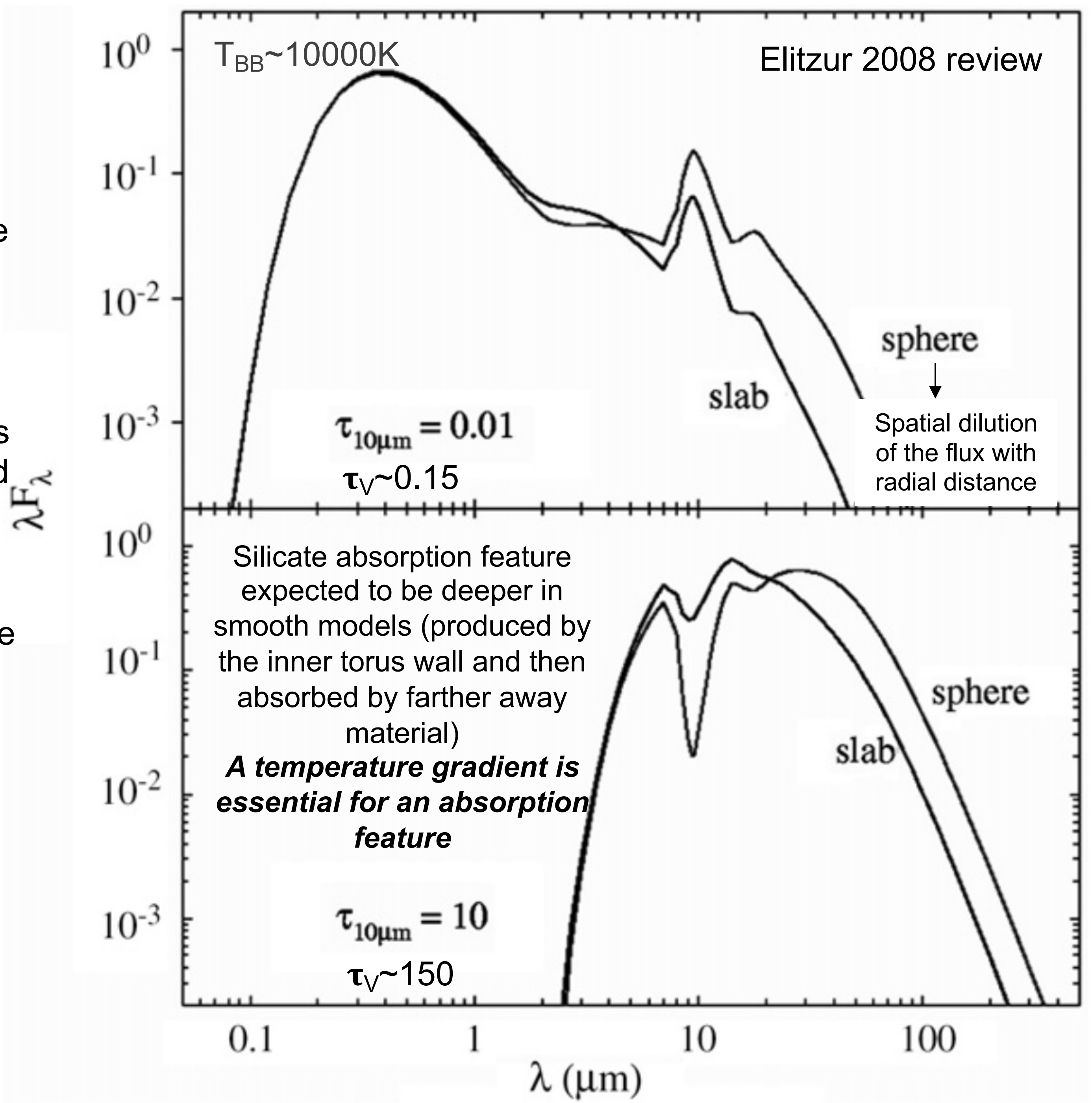

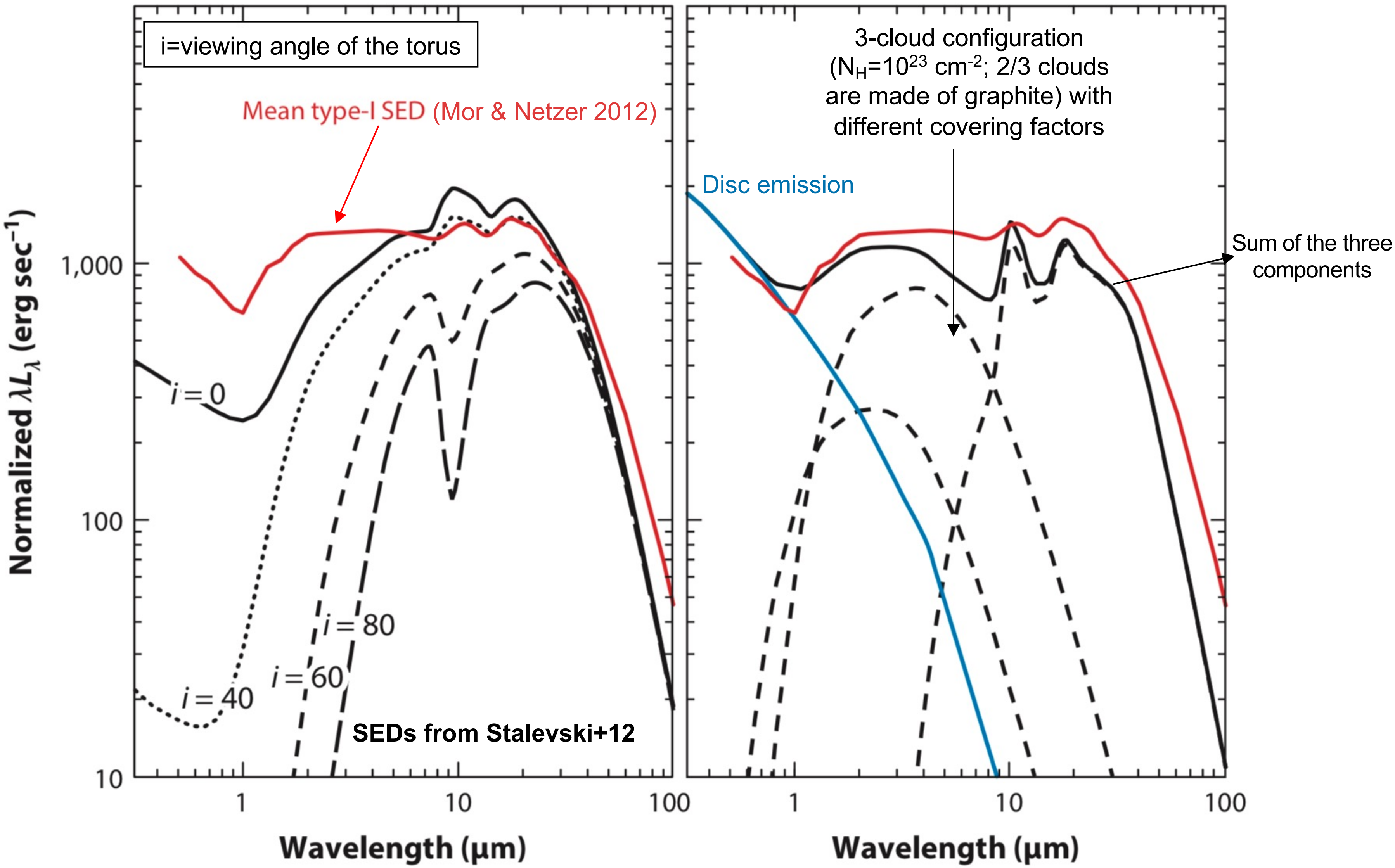

Netzer 2015 review

What is not fitting into AGN Unified Model picture in its basic form

- Presence of obscured broad-line AGN
- Presence of unobscured narrow-line AGN (called ‘true’ Type 2 AGN)

see also Hickox and Alexander (2018)

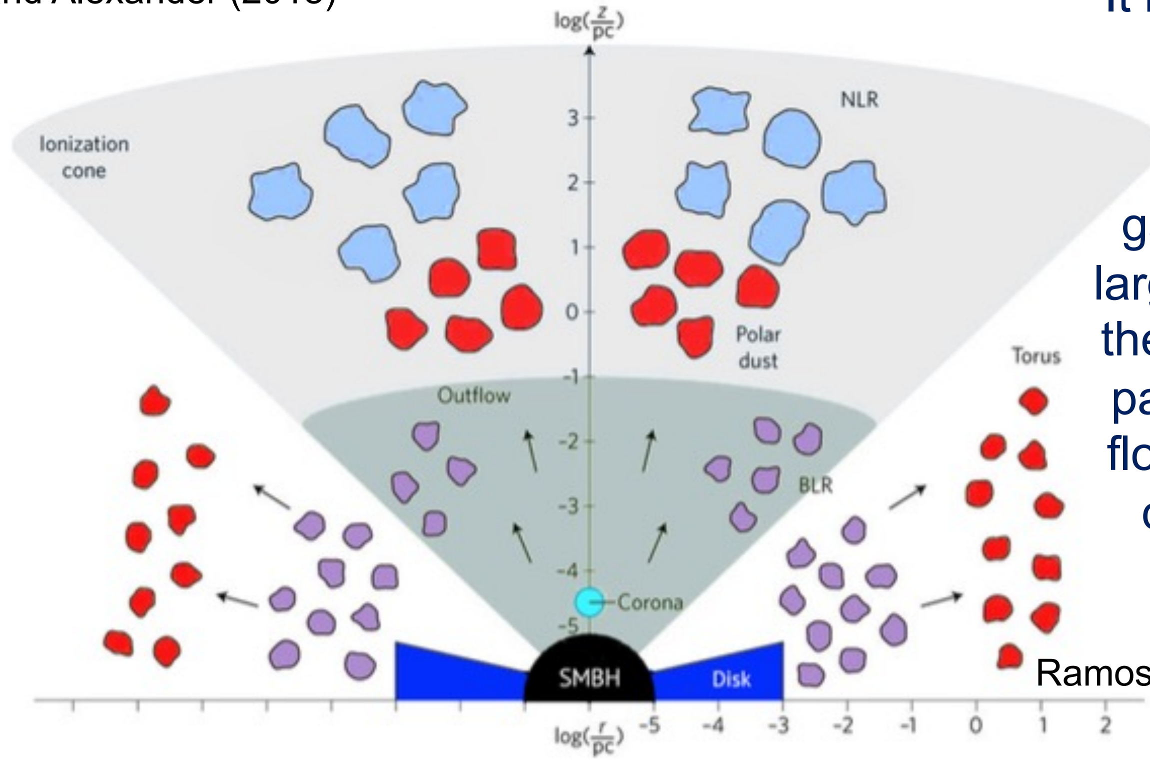

Ramos-Almeida & Ricci (2017)

It is often assumed that the torus material is gas inflow from the galaxy along with larger-scale flows in the galaxy plane → part of the general flow that continues down to the BH accretion disc

The **absorber/reprocessing material** is most likely **cloudy** and **filamentary** (e.g., Jaffe+04, Burtscher+13; Ramos-Almeida+11, Alonso-Herrero14, Garcia-Bernete+17,19)

Combes+18 – ALMA results, tori are disk-like on scales of ~10−30 pc + resonant rings at 100-pc scales; AGN non necessarily in the center

Recent studies to link the mid-IR properties of the torus with those from X-ray observations

From a physical point of view, a thick (torus) structure can be maintained if high-velocity turbulent or outflow motions are present (easier in a clumpy medium, where cloud collisions are more frequent)

Other mechanisms possibly involved: UV, optical, IR radiation pressure; magnetic winds; SF activity in the inflowing gas

Possible scheme: clumps are pushed radially by the radiation of the central source (hence, $\propto L_{AGN}/L_{Edd}$) → the dust in the clumps is heated → IR radiation towards the surrounding clumps → radiation pressure force that balances or overcomes the vertical (z) component of the BH gravity

In the end, the BH is needed to keep such a structure

In this clumps/wind scenario, clumps inside the sublimation radius are dust-free and can be seen as BLR clouds. At increasing distances from the BHs, they are observed as part of the torus

→ Disc outflow models, magnetocentrifugal winds or radiation-pressure-driven winds result in *one continuous structure* whose geometry depends on the global accretion process and whose division into dust-free and dusty regions depends entirely on the central radiation field

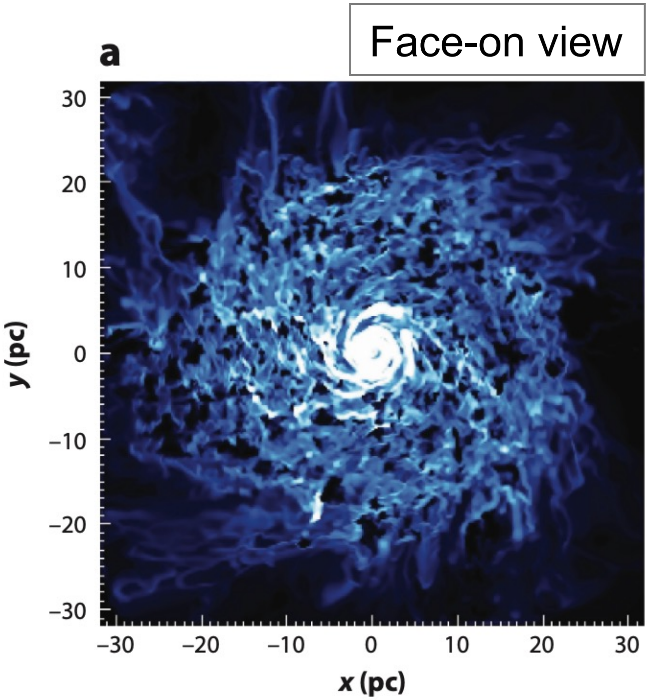

‘Torus’ density maps,
Wada et al. (2009)

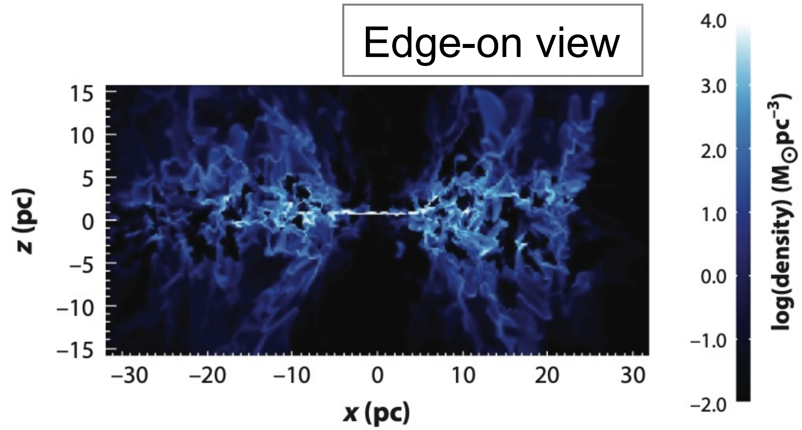

Presence of SF activity, SN explosions and stellar feedback (+ AGN feedback in Wada 2012)

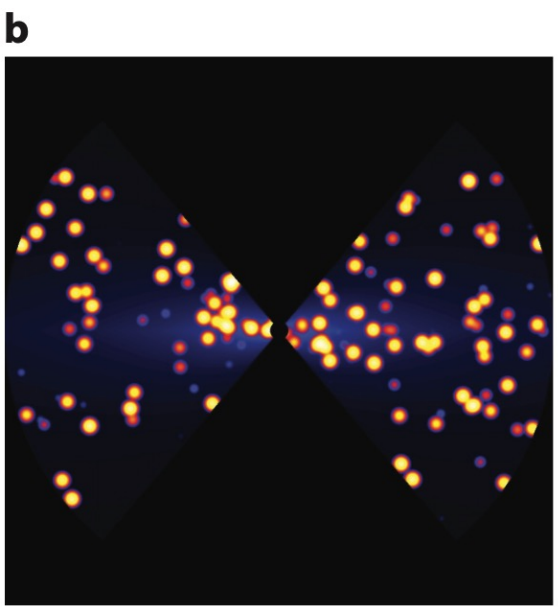

High-condensation clumps + lower-density interclump dust

Stalevski et al. (2012)

Summarizing, the dust sublimation radius sets the outer boundary of the BLR and a sort of inner radius of the dusty torus

QUESTION: *do we have an idea of the outer radius of the accretion disc?*
This may be referred to as the *self-gravity radius* which is the location where the local gravity exceeds the vertical component of the central BH gravity and the disc becomes unstable

$$R_{SG} \sim \ 1680 \ M_9^{-\frac{2}{9}} \alpha^{\frac{2}{9}} [\frac{L_{AGN}}{L_{Edd}}]^{\frac{4}{9}} [\frac{\eta}{0.1}]^{-\frac{4}{9}} \ R_g$$

$M_9 = M_{BH}/10^9\ M_\odot$
α=viscosity parameter (discussed later, AD theory; ~0.01−0.1)
η=radiation efficiency

→ R_{SG}~0.04pc in case of L_{AGN}/L_{Edd}~0.1, $10^9\ M_\odot$ BH

The disc starts fragmentation into clouds moving in the same general plane beyond R_{SG}

There are models predicting a marginally stable disc up to ~100pc owing to collisions between clouds, SF activity, and SN explosions, producing turbulence and local viscosity, allowing accretion of matter from much larger radii

Clear link with the X-ray derived column density

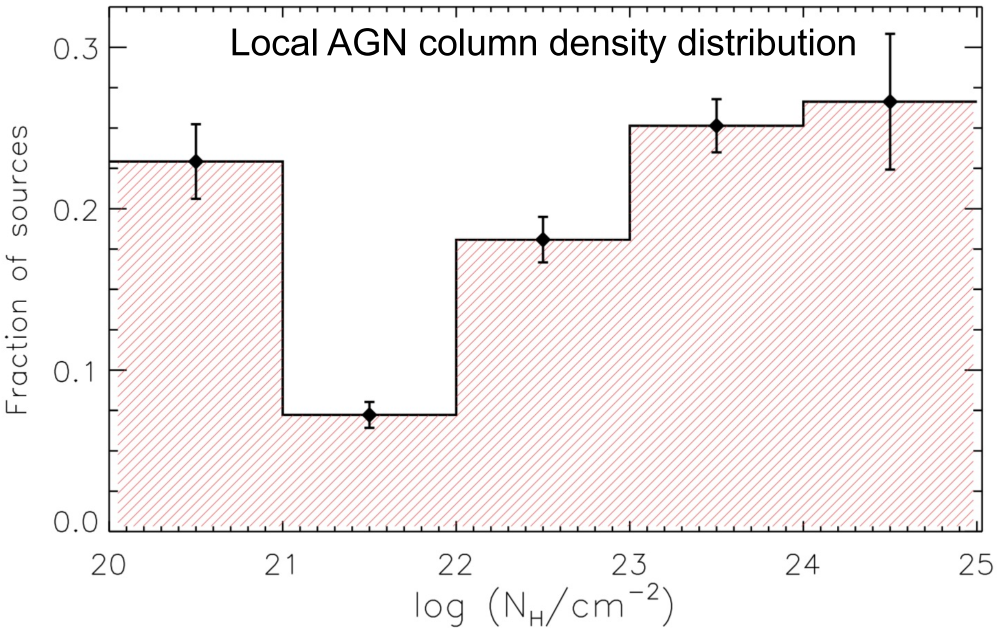

(a)

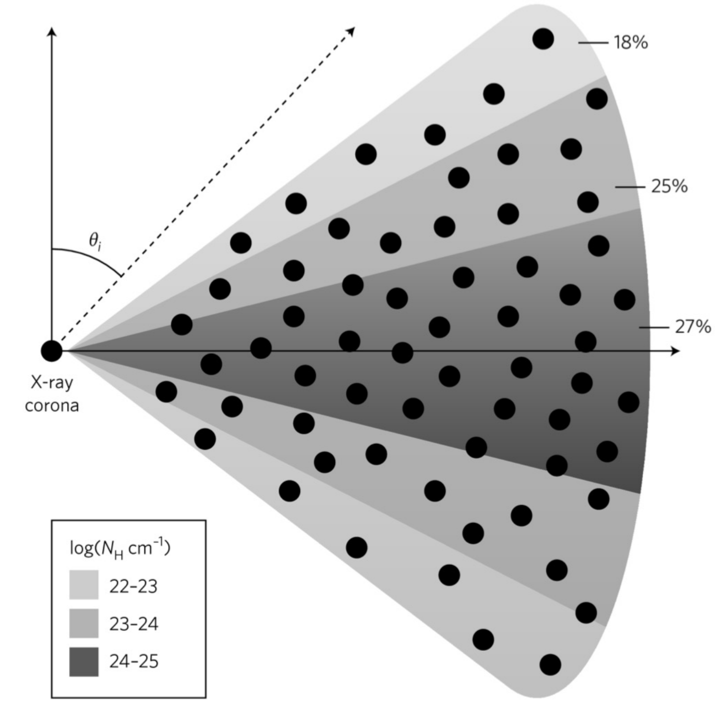

(b)

Ramos-Almeida & Ricci (2017)

- Thicker region in the equatorial plane
- Possibility that the column density along the line-of-sight is different from the average column density of the torus → proper X-ray modeling is needed to infer the clumpiness of the medium

Depth of 9.7μm silicate feature vs. X-ray obscuration. I

IRAS-12μm sample of Type 2 AGN with *Spitzer*/IRS coverage

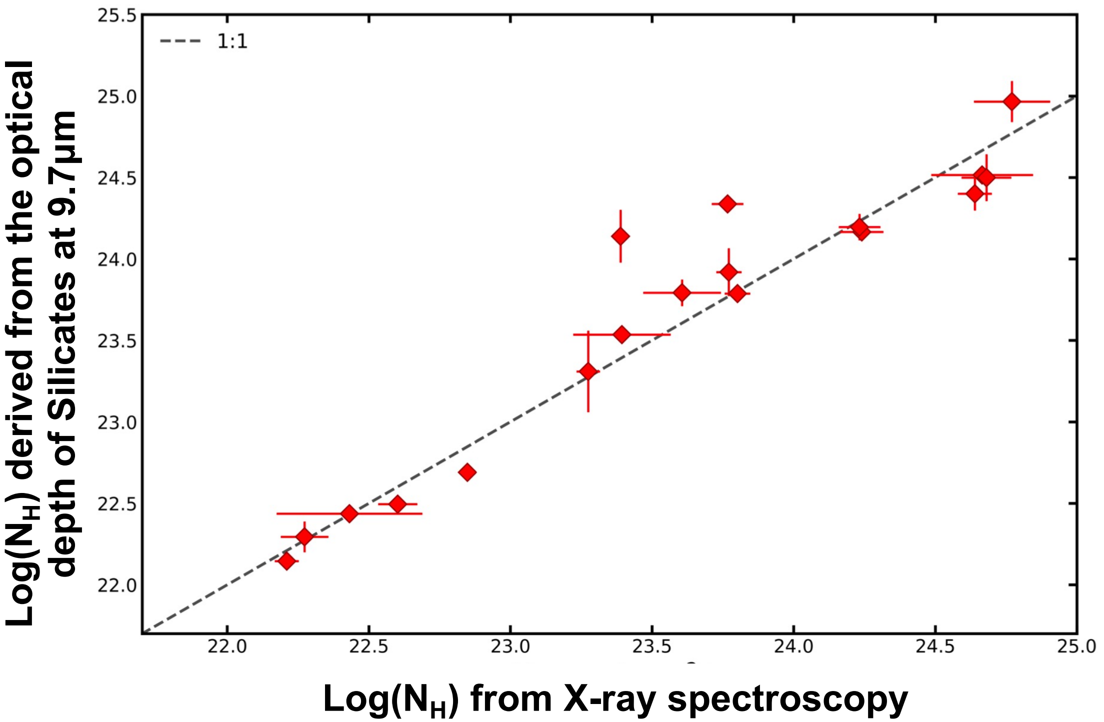

Salvestrini et al., in prep.

Is the torus the 'same' in terms of geometry and 'physical' properties in the mid-IR and X-rays?

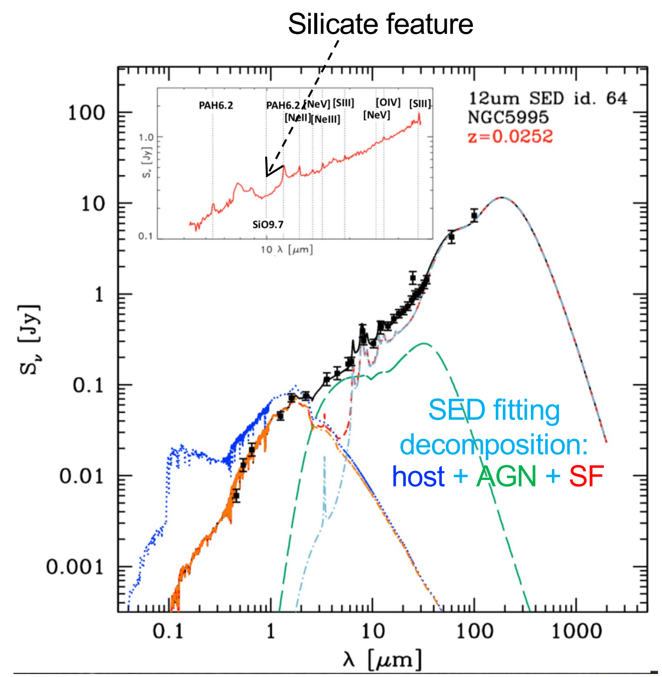

Systematic multi-wavelength study of IRAS 12-micron sample (X-ray, SED fitting, molecular gas content, gas kinematics, etc.)

Effects of the AGN on the host galaxy

see also Alonso-Herrero+ works, Mateos et al. 2016, […]

Depth of 9.7μm silicate feature vs. X-ray obscuration. II

The silicate feature properties may reflect extinction within the host galaxy (Goulding et al. 2012)

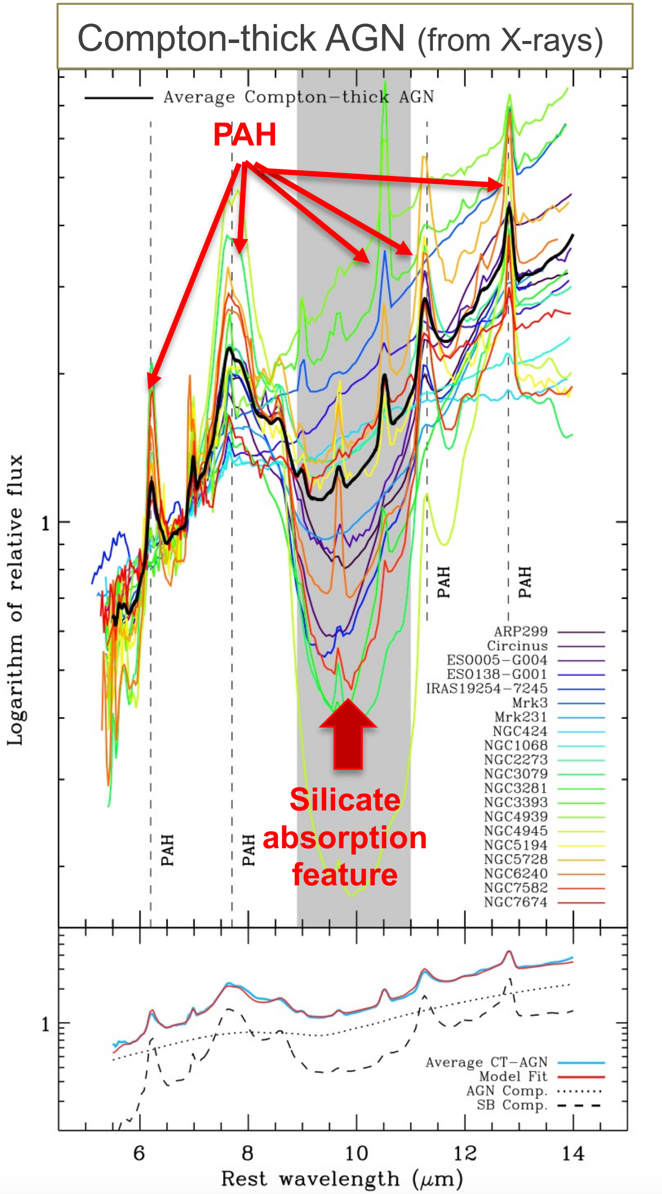

Compton-thick AGN may have different properties in the mid-IR and different shapes/depths for what concerns the silicate absorption feature

Besides, the presence of PAH (polycyclic aromatic hydrocarbon) features (main at 6.3, 7.7, 11.3, and 12.3 μm) may complicate the analysis of the silicate feature and its strength (because of the complexity of modeling the continuum)

Goulding et al. (2012)

Depth of 9.7μm silicate feature vs. X-ray obscuration. III

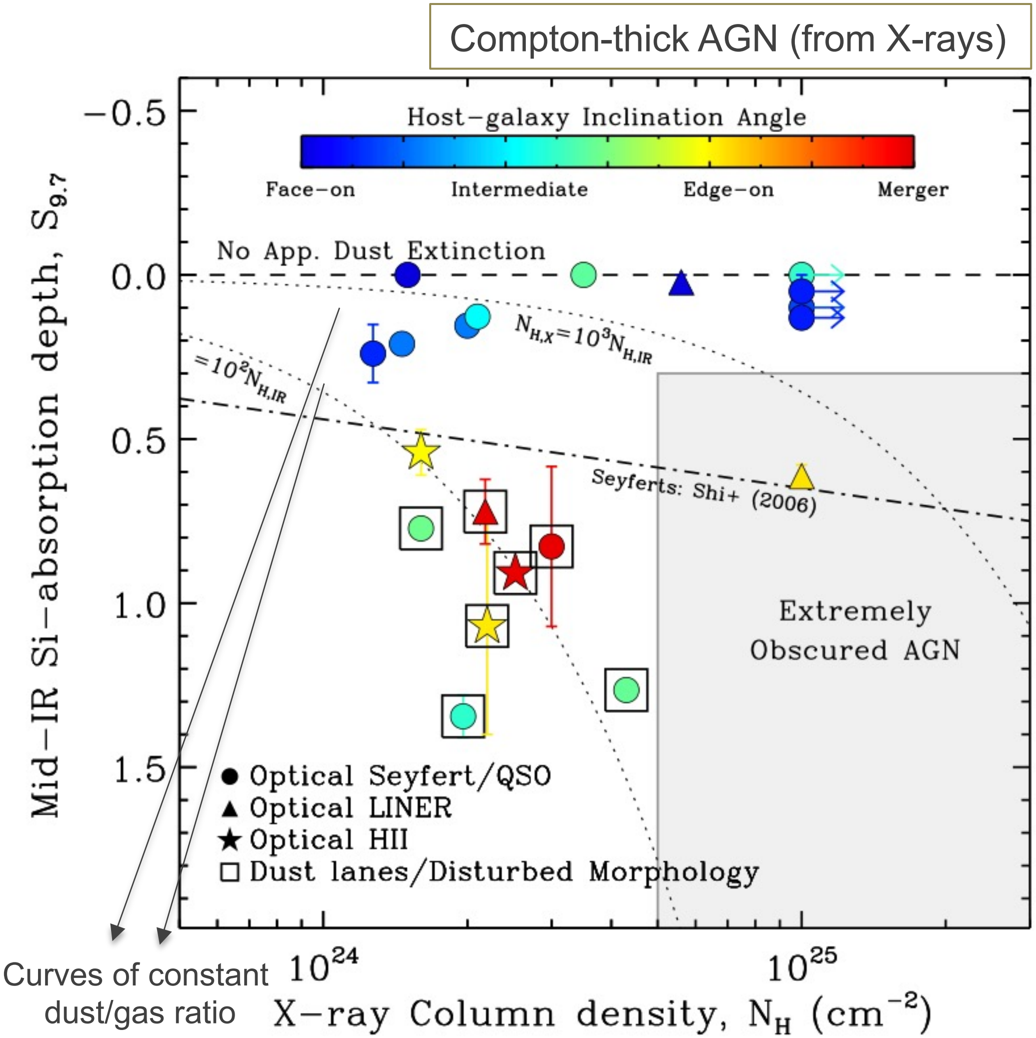

- Not so many Compton-thick AGN with deep silicate feature
- Dominant contribution to the observed mid-IR dust extinction comes from dust located in the host galaxy (possible associations with disturbed morphology, dust lanes, galaxy inclination angles…)
- Large gas/dust ratios possibly explained by gas within the sublimation radius (BLR clouds? see work by Risaliti+)

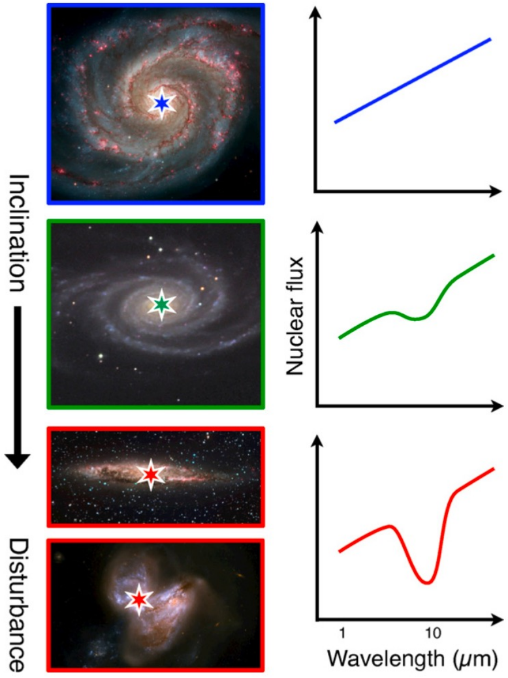

Goulding et al. (2012)

Is the truth in the middle of the two scenarios?

Contribution to obscuration from the host galaxy (e.g., dust lane) consistent with the picture of Matt (2000) − column densities up to ~10^{22} cm^{-2}

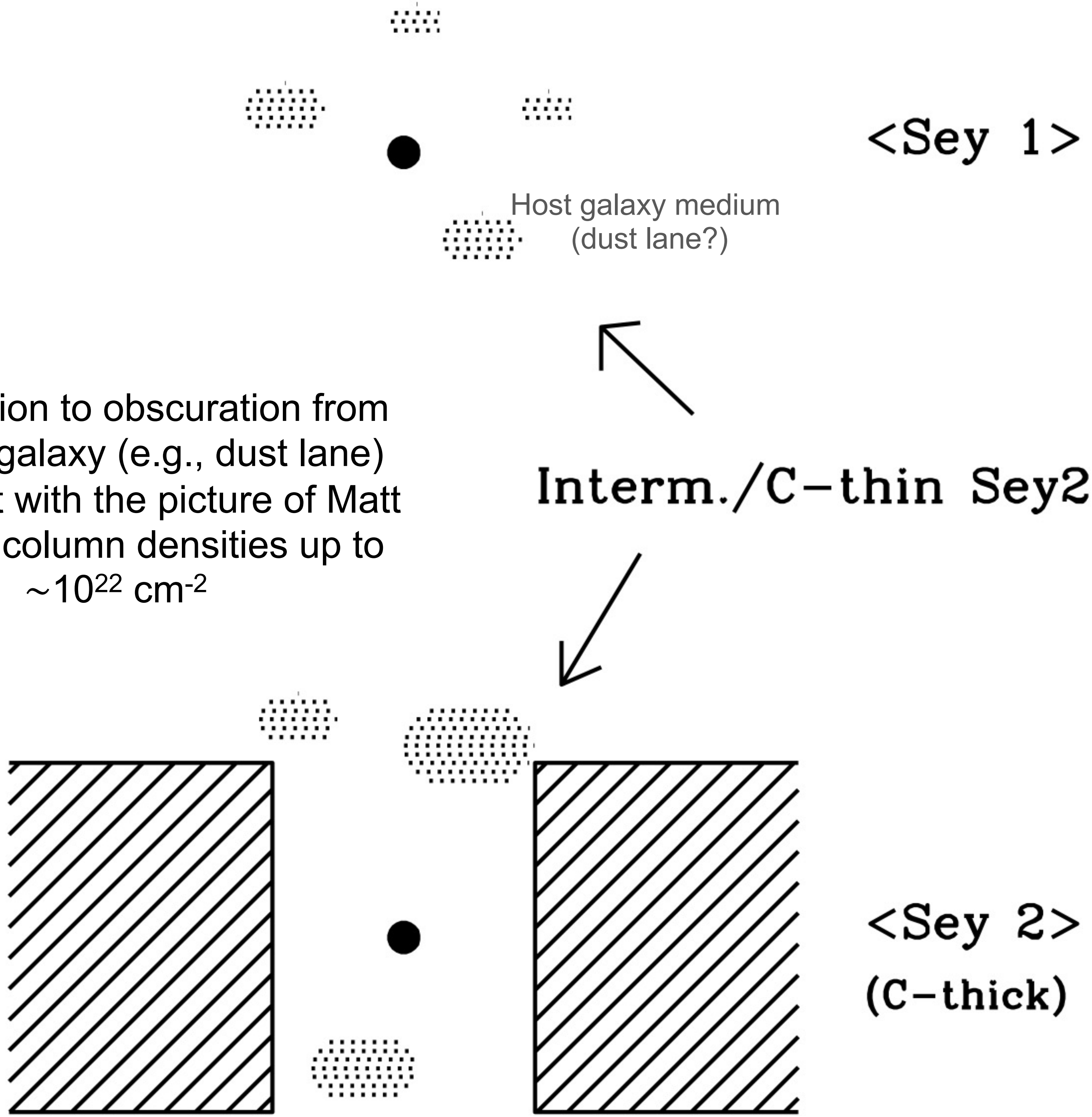

Matt (2000)

X-ray observations of local Seyfert galaxies: absorbing clouds within the BLR? I

Eclipses of the X-ray source are COMMON in nearby AGN: $\Delta N_H \sim 10^{23}-10^{24}\ cm^{-2}$

size X-ray src $<10^{14}$ cm
D $< 10^{16}$ cm

X-ray absorber "made" of BLR clouds

Risaliti et al. 2007, 2011; see also Torricelli-Ciamponi et al. 2014

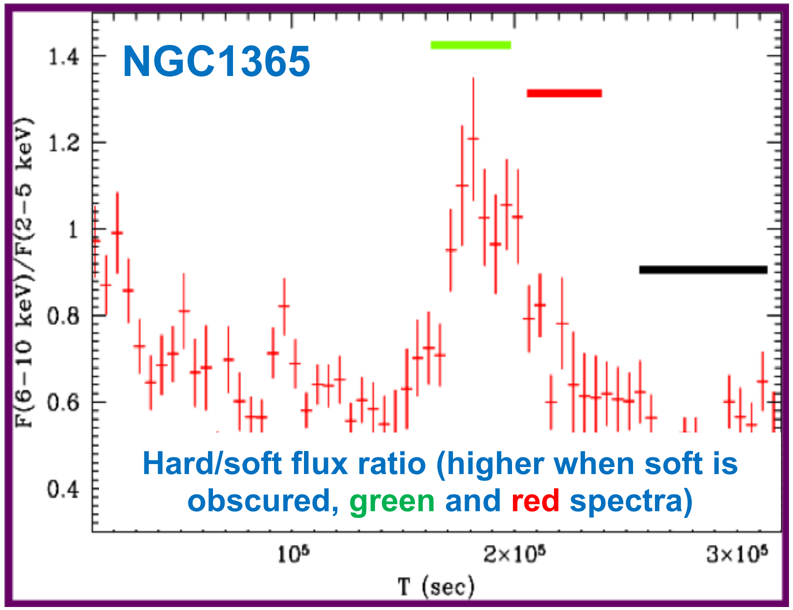

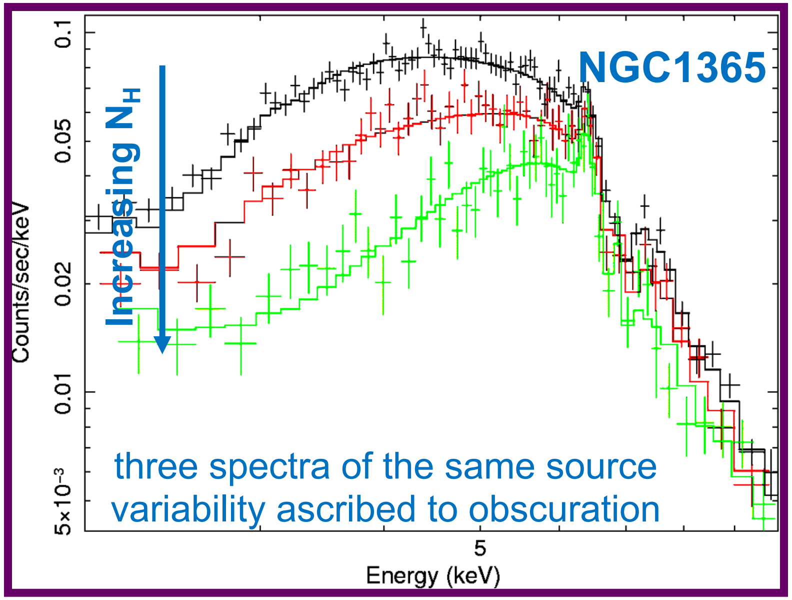

X-ray observations of local Seyfert galaxies: absorbing clouds within the BLR? II

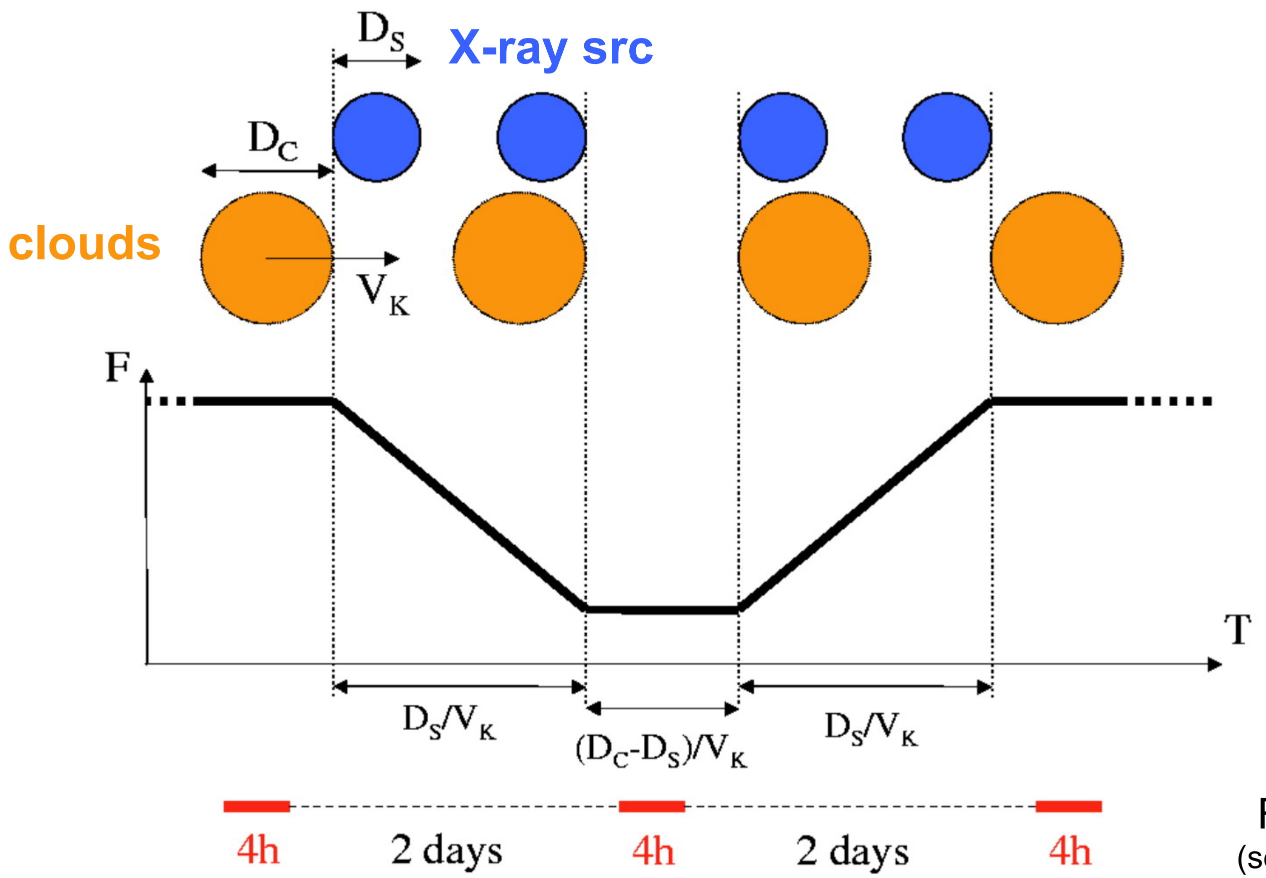

Risaliti et al. 2007
(see there for assumptions and derived values)

X-ray observations of local Seyfert galaxies: absorbing clouds within the BLR? III

High-density head, elongated lower-density tail: cometary structure?

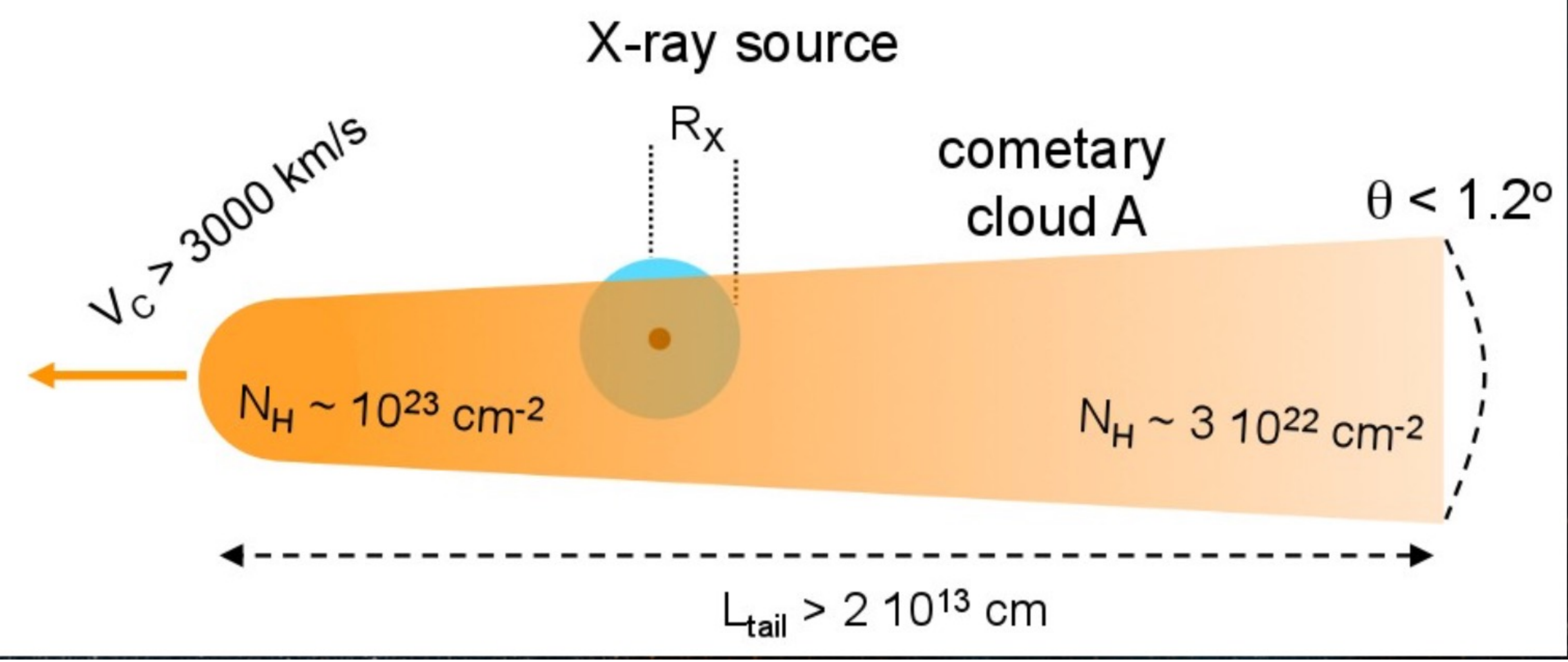

Maiolino et al. (2010)

- Occultation in NGC1365: ~48 hr (and ~48 hr for the X-ray source to emerge again)
- Cometary tails useful to explain the observed N_H 'gradients' in the eclipse event
- Obscuration by BLR clouds supported by the systematic study of Markowitz+14

Cloudy scenario confirmed by NuSTAR in NGC1068

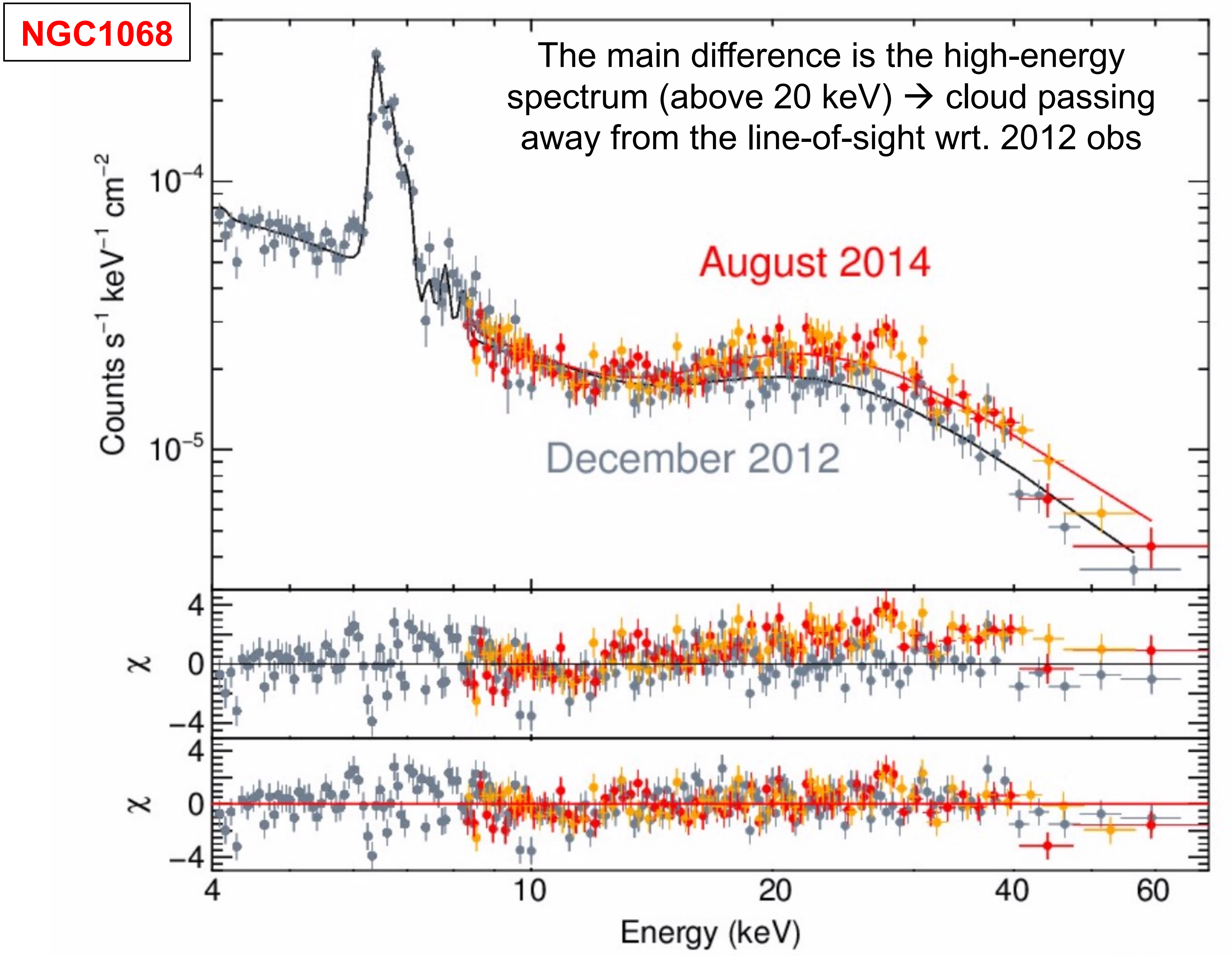

Marinucci et al. (2016)

High-resolution mid-IR observations of Seyferts (reverberation-mapping technique, time lags). I

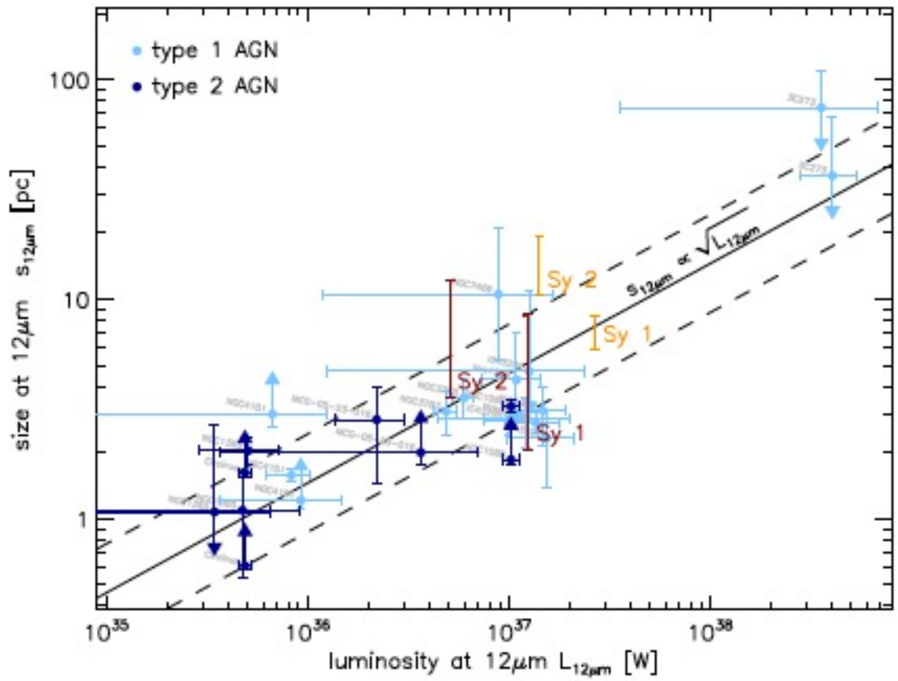

Tristram & Schartmann 2011
(see also Jaffe+04; Meisenheimer+07; Tristram+07; Tristram+09; Burtscher+13)

$R_{K=2.2\mu m} \sim 0.4\ L_{46}^{1/2}\ pc$ (Koshida et al. 2014)

- Compact (a few pc) tori with a clumpy/filamentary dust distribution (warm disk + geom. thick torus)

- No significant Sey1/Sey2 difference

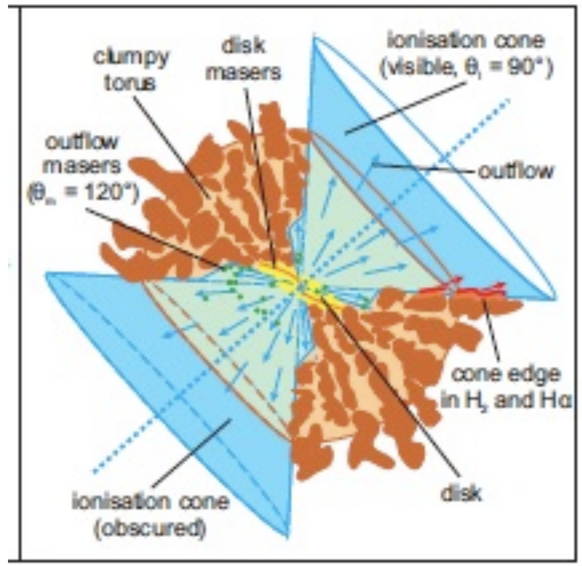

Tristram+07 - Circinus

High-resolution mid-IR observations of Seyferts. II

The situation is even more complex than expected when resolution as low as 0.1 pc are achieved in the mid-IR

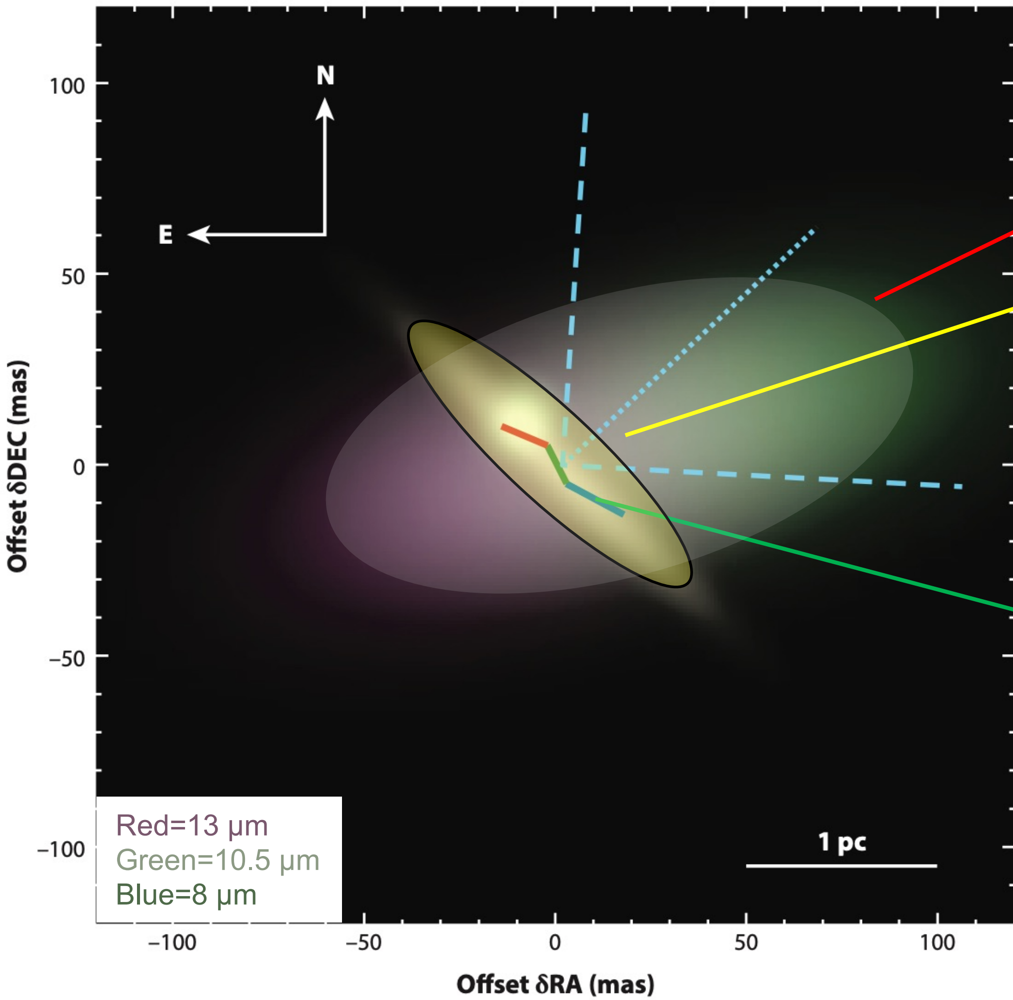

Outer torus (~0.8 × 1.9 pc^2, ~80% mid-IR emission, almost perpendicular to the inner part)

Inner torus (disc-like, ~0.2 × 1.1 pc^2, ~20% mid-IR emission)

Probed scales much smaller than the ionization cones

Maser disc

Redder extended emission in the S-E direction → Stronger extinction

Tristram+14 – Circinus
(Compton-thick Sey2 galaxy)

Modeling the mid-IR emission with “clumpy” torus

✓ Type 1 vs. Type 2 AGN difference: it is a function of the number of clouds along the line of sight, i.e., of the escape probability
✓ Same dust temperatures can be observed at different distances from the AGN

➔ Type 2 AGN: larger number of clouds and lower P_{esc} for the photons to escape

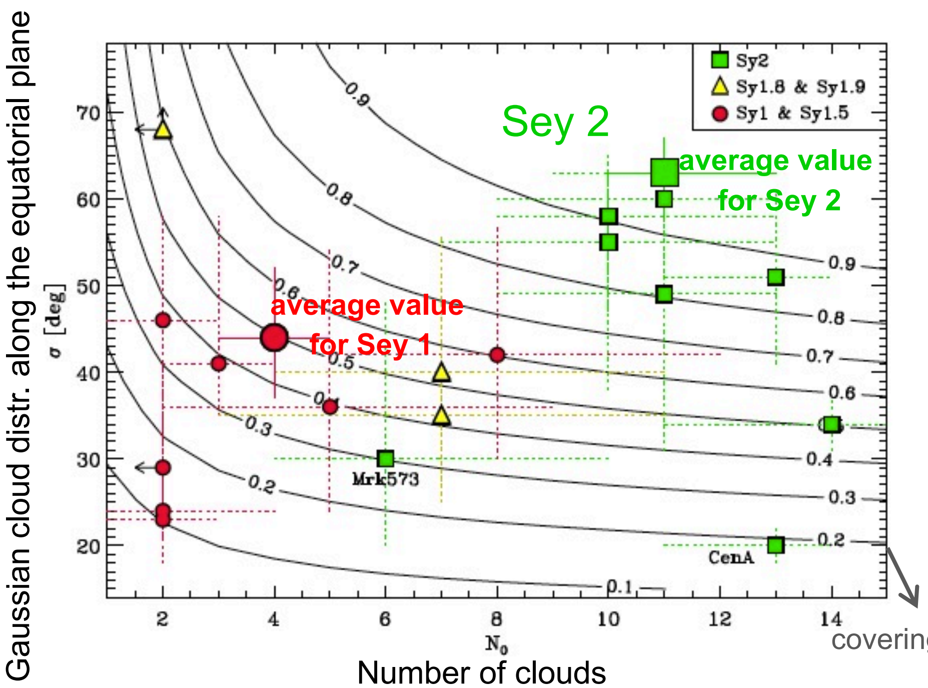

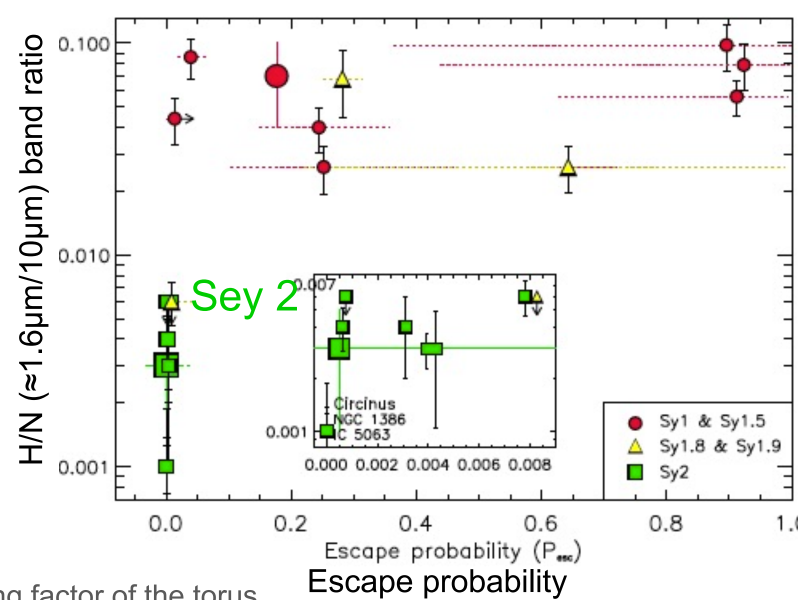

Ramos-Almeida+11; see also Garcia-Bernete+19

The complex picture provided by high-resolution ALMA observations (continuum and molecular transitions)

NGC1068

- Several gas tracers → different density (stratification of the torus)
- CND (circumnuclear disk) on scales up to 400 pc and M~10^8 $M_\odot$
- 'Inner' molecular torus of size ~130 pc and M_{gas}~3×10^5 $M_\odot$
- The wide-angle AGN wind is impacting the gas distribution but has limited impact on the higher-density torus gas on small scales (fueling can continue for at least few Myr)

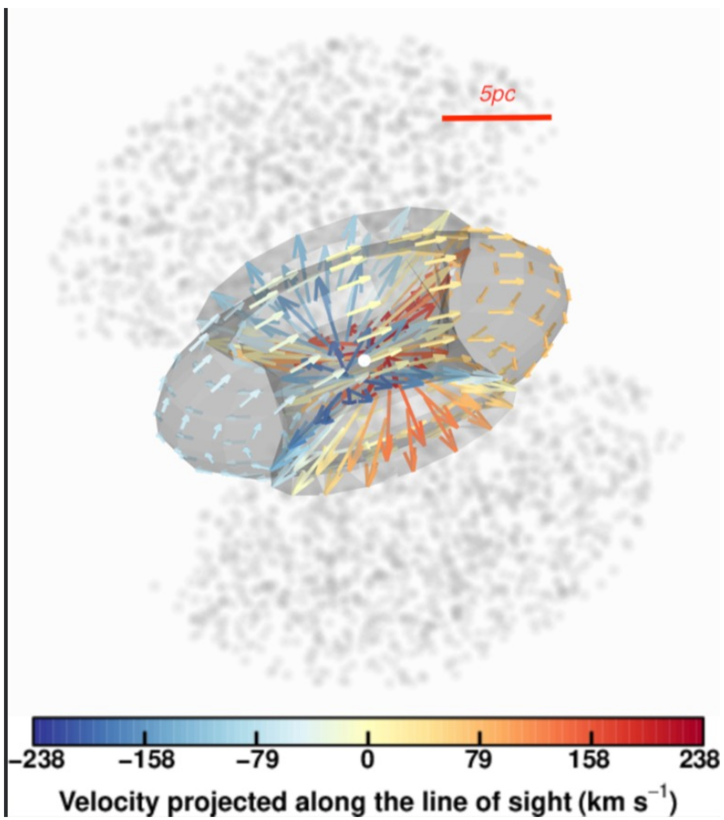

Kinematic model of the torus
(gas rotation and wind/outflow components

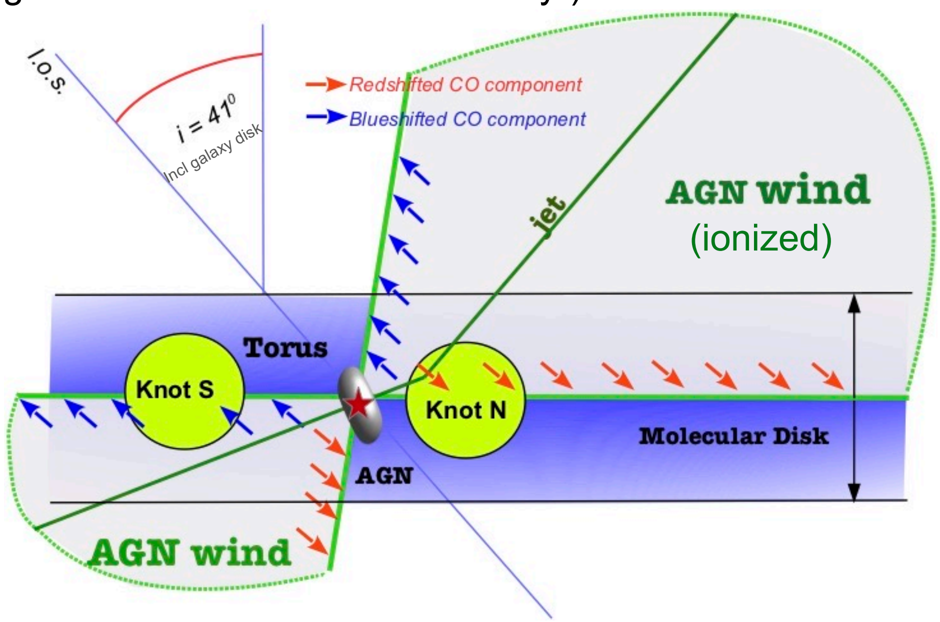

The CO line is split into blue-(red-)shifted components along the ionized outflow axis. AGN wind is extended in size

2-6 pc resolution

Garcia-Burillo et al. (2019)

The Homer Simpson's donut-like torus is not an issue anymore, although for most purposes this configuration, applied to model SEDs, works relatively well

Mid-IR to optical time lags. I

Sample of Type 1 Seyfert galaxies: time lags between UV/optical and K-band light curves (response of the thermal emission in the K band to variations of the AGN emission)

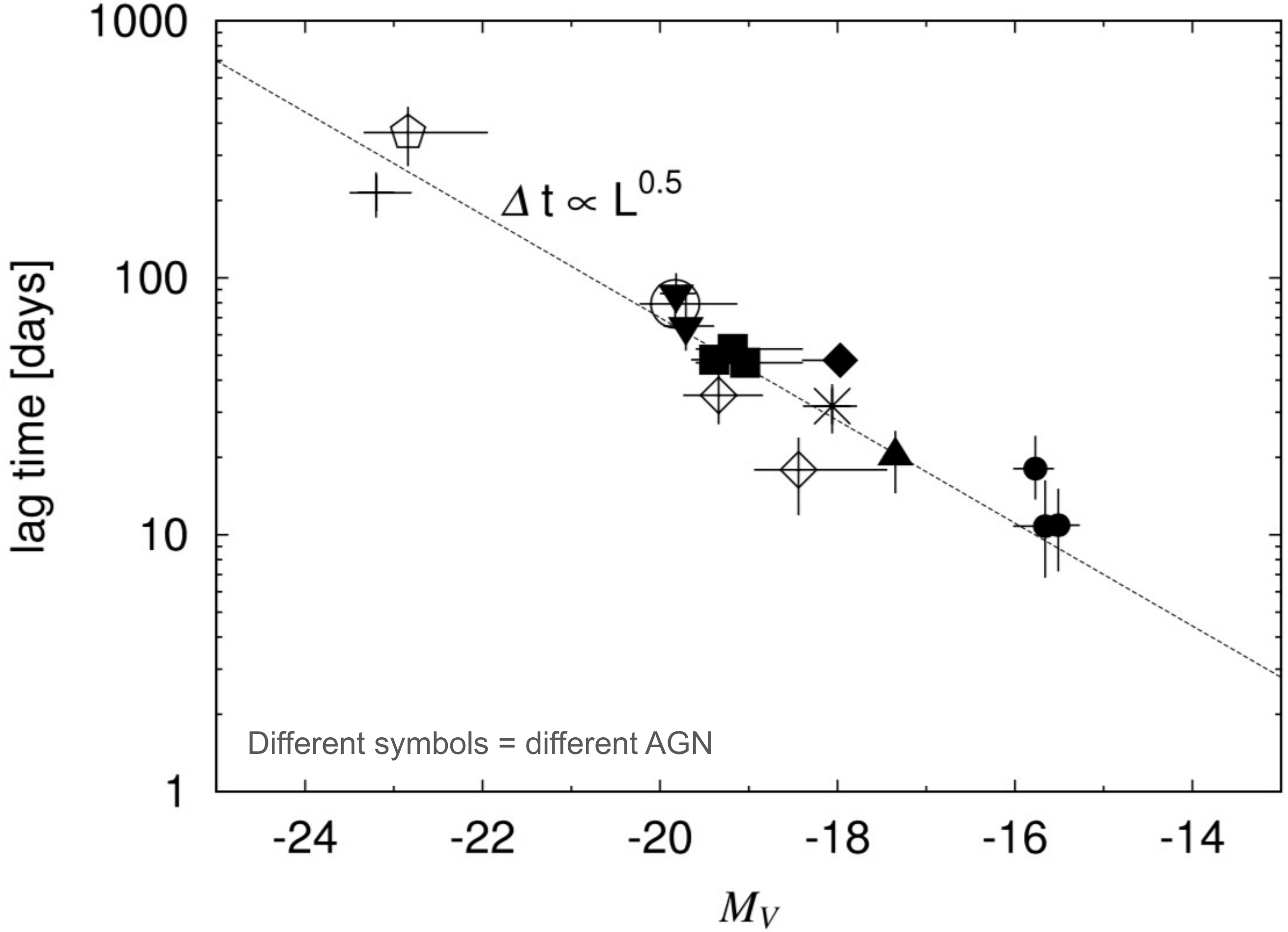

Suganuma et al. (2006)

Mid-IR to optical time lags. II

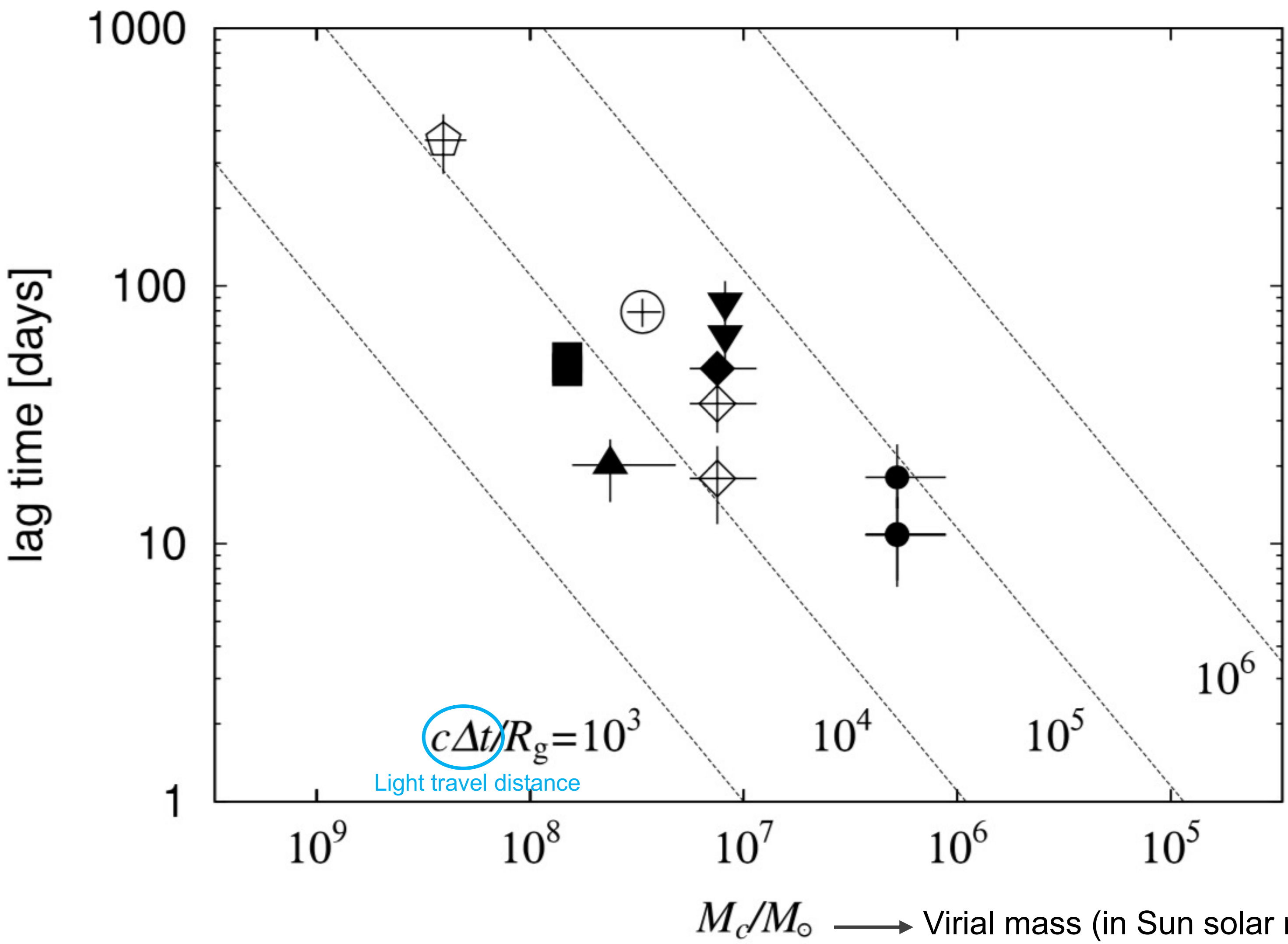

Virial mass (in Sun solar masses units) from optical reverberation studies

Suganuma et al. (2006)

Mid-IR to optical time lags. III

- The lag times are tightly correlated with the optical luminosities, as expected from dust reverberation

$$\Delta t \propto L^{0.5}$$

- The K-band time lags place an upper boundary on the similar lags of broad emission lines

→ Sort of physical transition from the BLR out to the dust that encircles the BLR (whose size is bounded by dust sublimation)

- The torus inner boundary is controlled by dust sublimation, not by dynamical processes

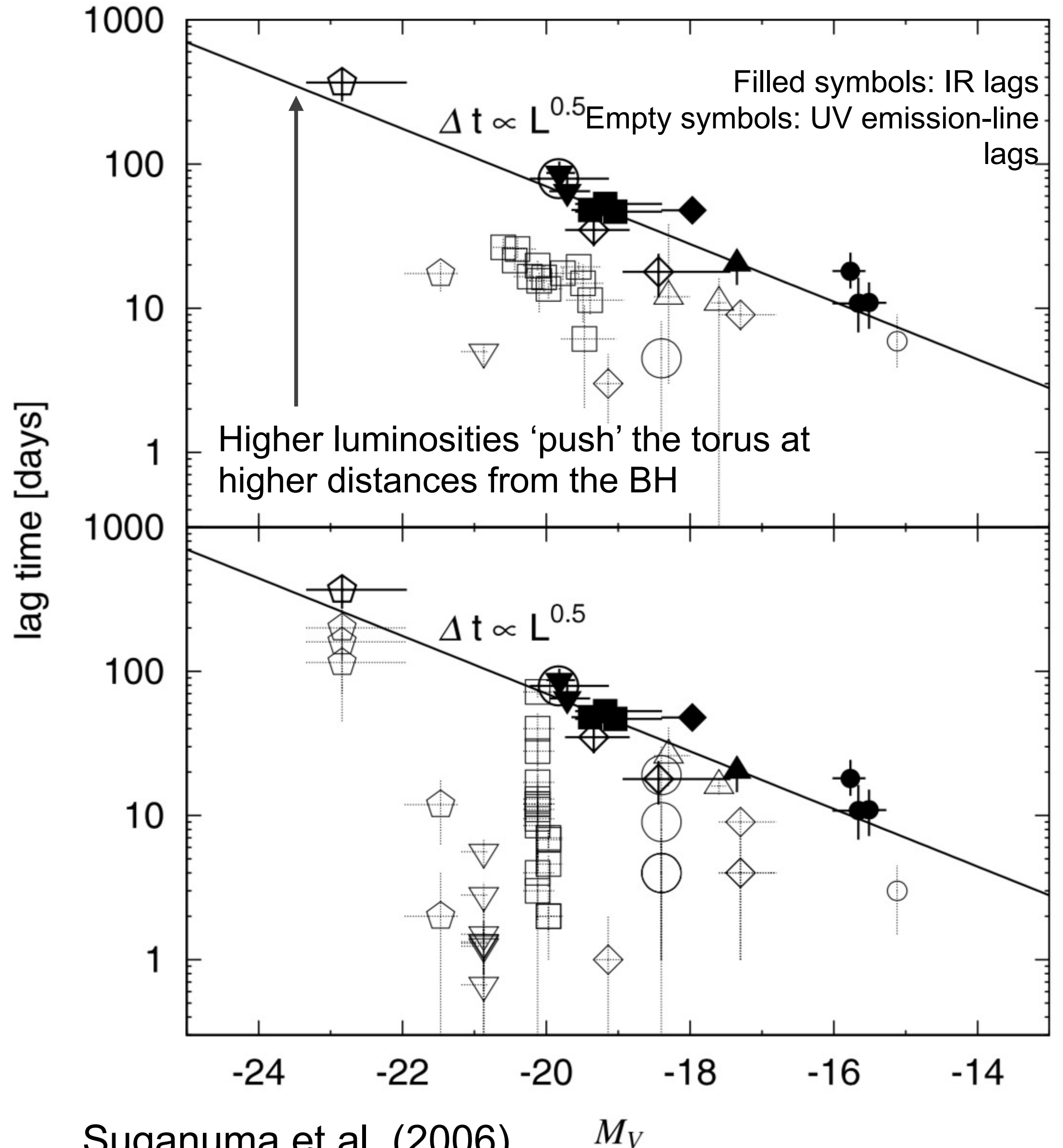

Suganuma et al. (2006)

‘Size’ of the torus from various measurements (vs. R_{BLR})
→ linear relation with AGN luminosity

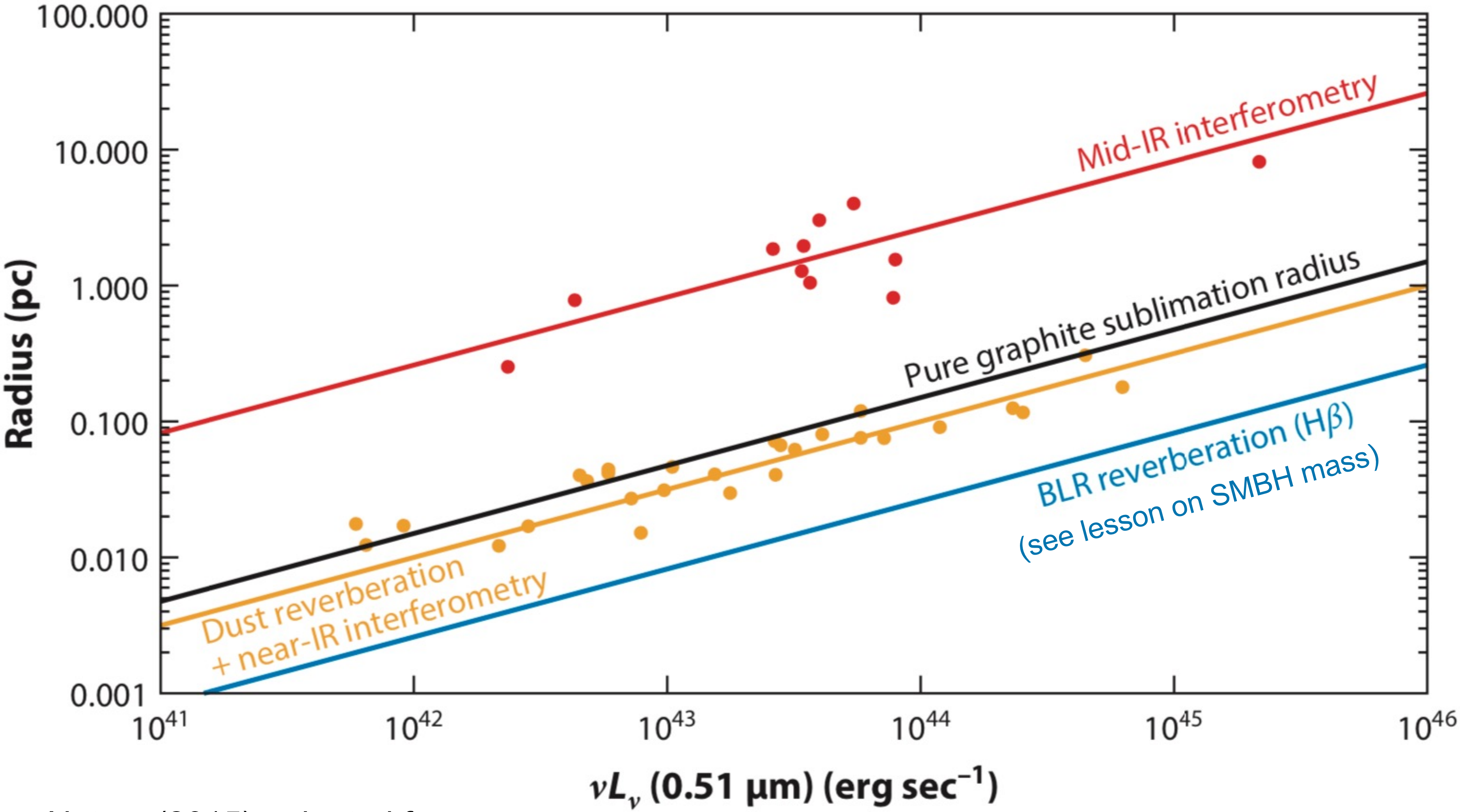

Netzer (2015), adapted from
Burtscher et al. (2013)

Some future thoughts. I

(speculative, to be investigated further)

One of the key predictions of the wind scenario (in which the torus is a sort of extension of the BLR clouds) is that *the torus disappears at* $L_{bol}<10^{42}$ *erg/s* because the mass accretion rate cannot sustain the required cloud outflow rate anymore (Elitzur 2008, Elitzur & Shlosman 2006)

Example: FRI galaxies (to be compared to FRII, which have, on average, tori and higher L_{bol})

This would explain indications of Type 2 AGN lacking obscuration at low L_{bol}.

The suppression of mass outflow spreads radially inward from the dusty, molecular region into the atomic, ionized zone → The removal of the toroidal obscuration by the dusty wind would be followed by a diminished outflow from the inner ionized zone and disappearance of the BLR at some lower luminosities

Nicastro 2000: gas outflows from the surface of the disc, outside the region dominated by radiation pressure, can lead to the *disappearing of the BLRs at very low Eddington ratios*

Some future thoughts. II

The system should release the excess accreted mass in another more efficient way, i.e. through jet emission (radio mode)

Radio loudness vs. Eddington ratio anticorrelation:
at low efficiency, the AGN are more radio loud and experience jet emission

→ The outflow decreases, jets are fed by an increasingly higher fraction of the accreted mass and finally, once the outflow is extinguished, all of the inflowing material not funnelled into the BH is channelled into the jets

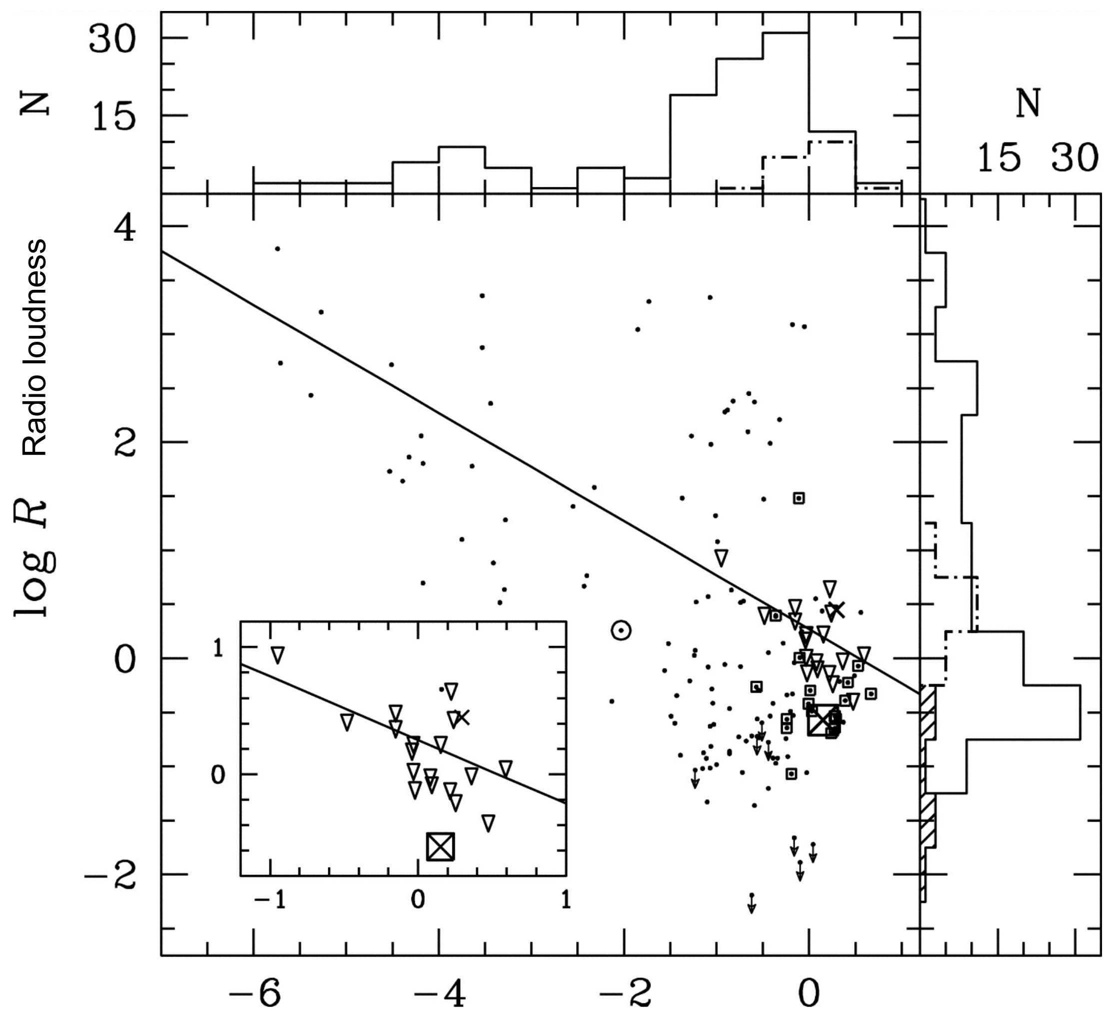

Log(λ_{Edd})=Edd. Ratio= $\log L_{bol}/L_{Edd}$

Greene et al. (2006)

Some future thoughts. III

High — Accretion Rate (L/L_{Edd}) — Low

Low — Radio Loudness — High

Full Unification Scheme;
both type 1 & 2

molecular outflow extinguished
Torus disappears; type 1 only

atomic outflow extinguished
BLR disappears; "true" type 2

Elitzur (2008 review)

Mid-IR as a proxy of the nuclear (intrinsic) AGN power

- The mid-IR emission is mostly due to reprocessing (i.e., thermalized by dust) of the intrinsic AGN emission.
  The UV/optical emission in obscured AGN is extincted but re-emerges as IR emission.

- Selecting sources extincted in the UV/optical and bright at mid-IR wavelengths provides a good tool to pick up obscured sources.

- Stacking X-ray emission and consequent comparison with expected X-ray emission provides an estimate on the amount of obscuration.

Mid-IR vs. X-ray emission of AGN

Asmus et al. (2014); see also Lutz et al. (2004) and Gandhi et al. (2009)

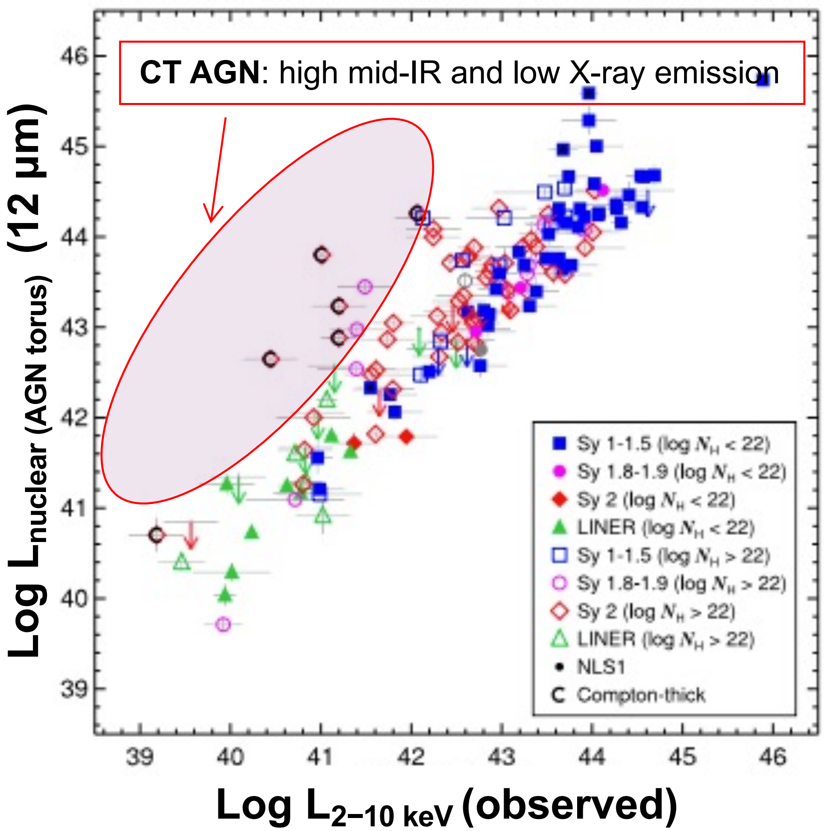

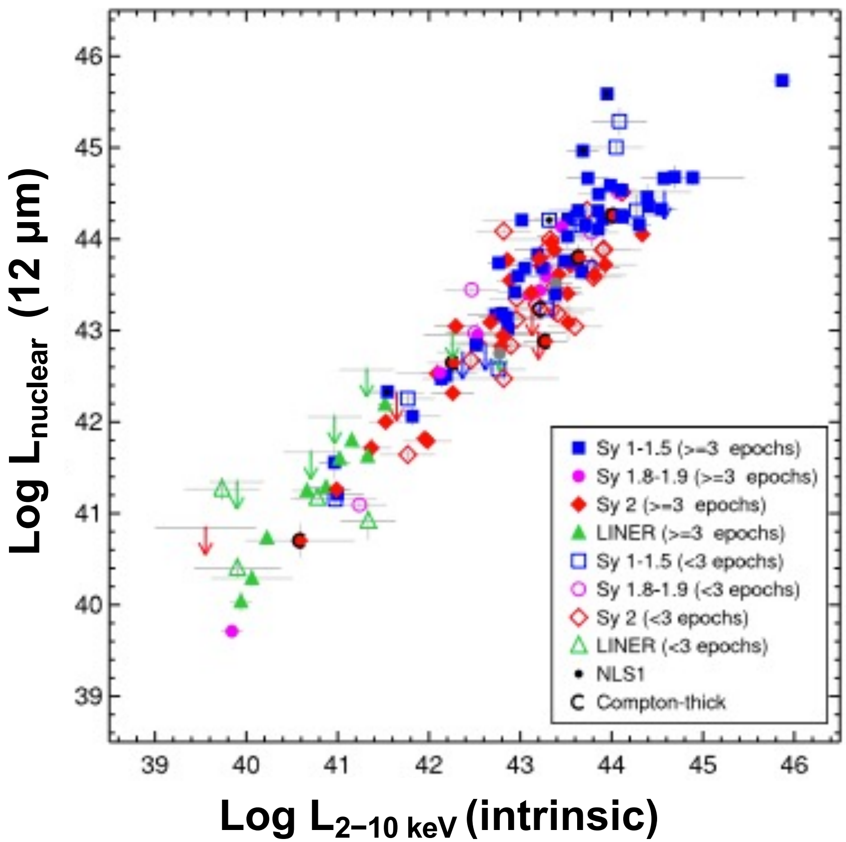

Corrected for the N_H

High mid-IR emission (from e.g. SED-fitting decomposition) coupled with low X-ray emission is suggestive of X-ray obscuration

MID-IR as a proxy of the intrinsic AGN strength

The combined optical/mid-infrared selection in the quest for Compton-thick AGN at high-z (I)

F(24 μm)/F(R) vs. L(5.8 μm)

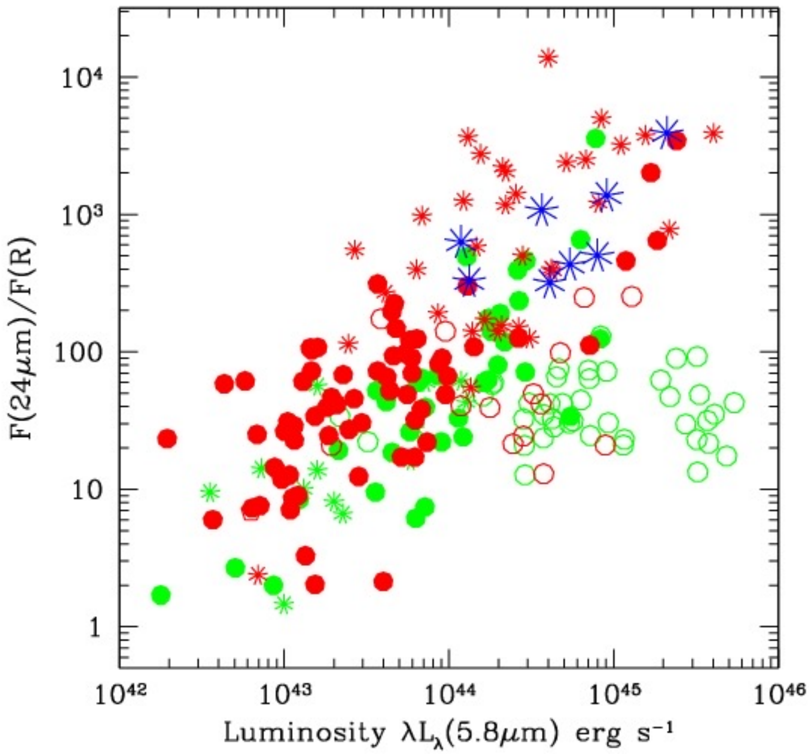

F(24 μm)/F(R) vs. F(X)/F(R)

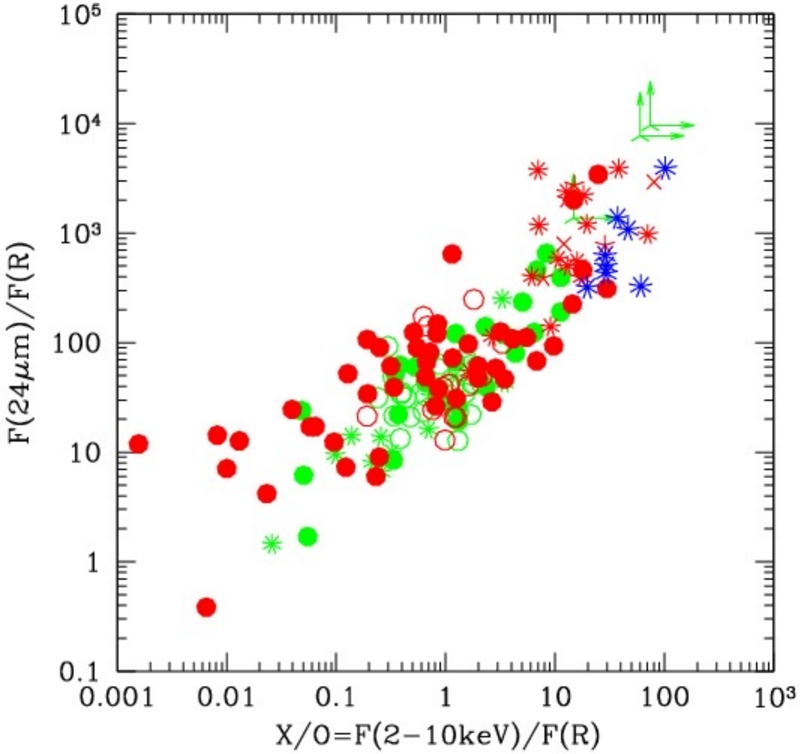

From Fiore et al. (2008)
Different symbols: different surveys
Filled symbols: Type 2 AGN candidates

In Type 2 AGN candidates, the F(24 μm)/F(R) ratio correlates with L(5.8 μm) and F(X)/F(R)
→The MIR luminosity provides an estimate of the X-ray flux

The combined optical/mid-infrared selection in the quest for Compton-thick AGN at high-z (II)

red color
bright at 24μm but faint in the optical

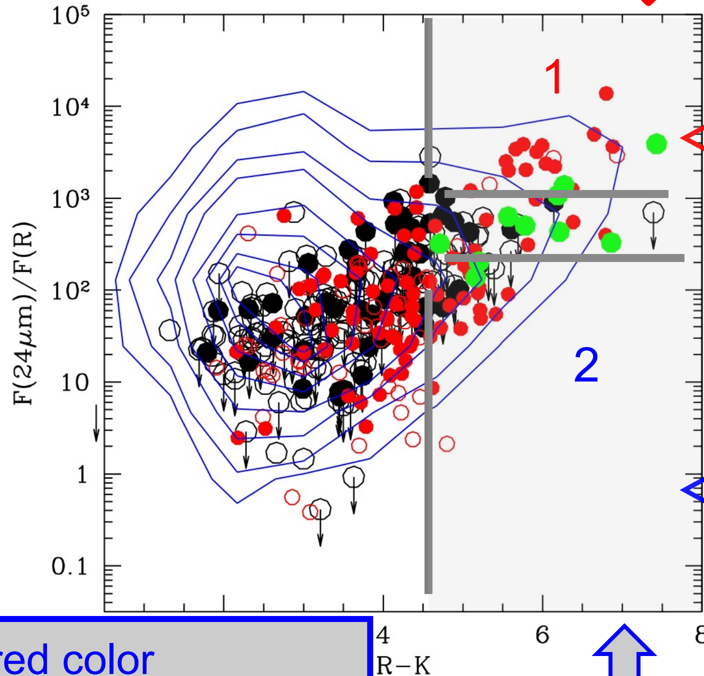

red color
Low 24μm to optical flux ratio

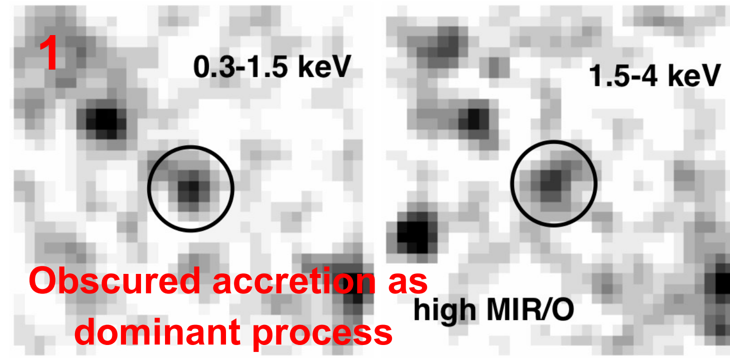

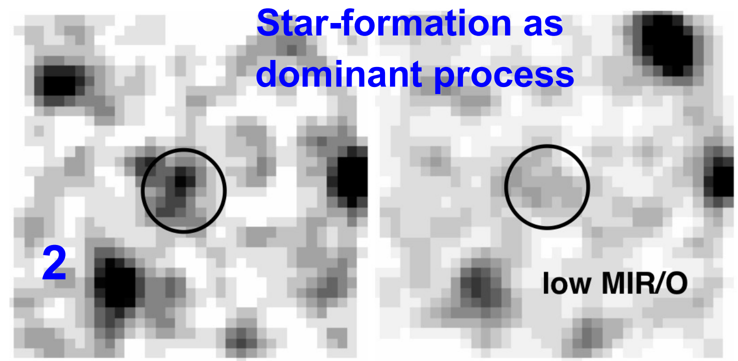

Fiore et al. 2008

CDF-S: <log L(5.8 μm)> ≈ 44.6

Log(L_X) ≈ 43 (expected) vs. 41.8 (observed from X-ray stacking analysis)

→Log N_H>24 at the z=2 (Compton-thick)

The combined optical/mid-infrared selection in the quest for Compton-thick AGN at high-z (III)

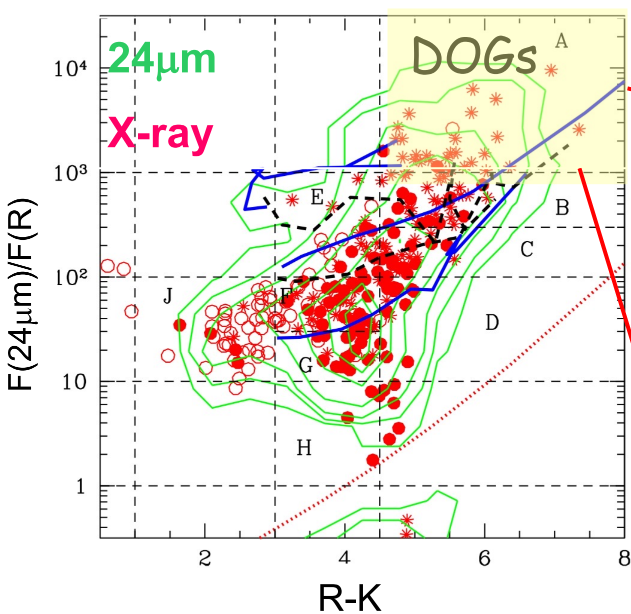

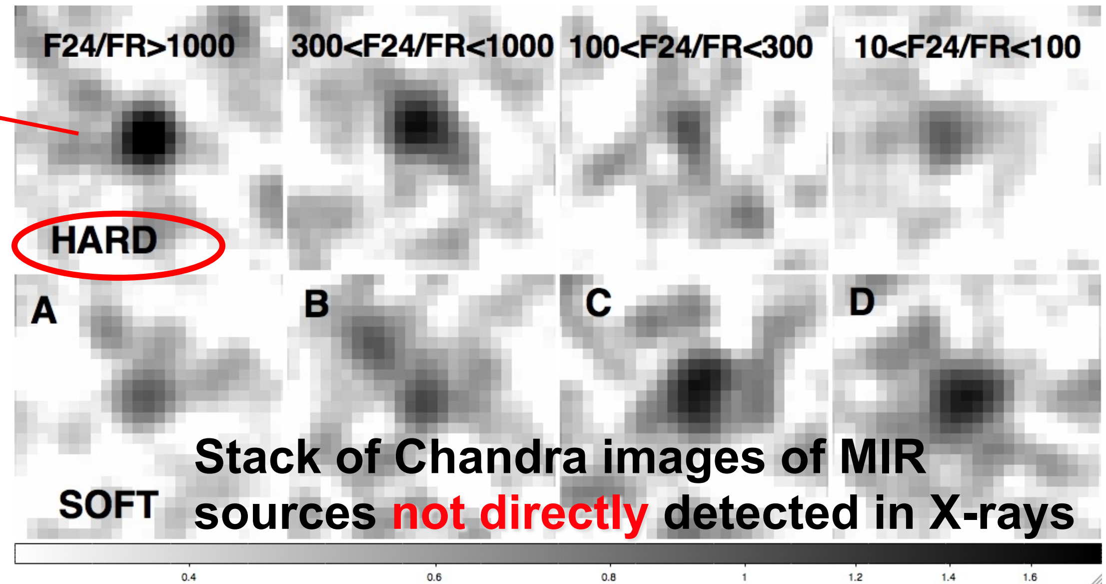

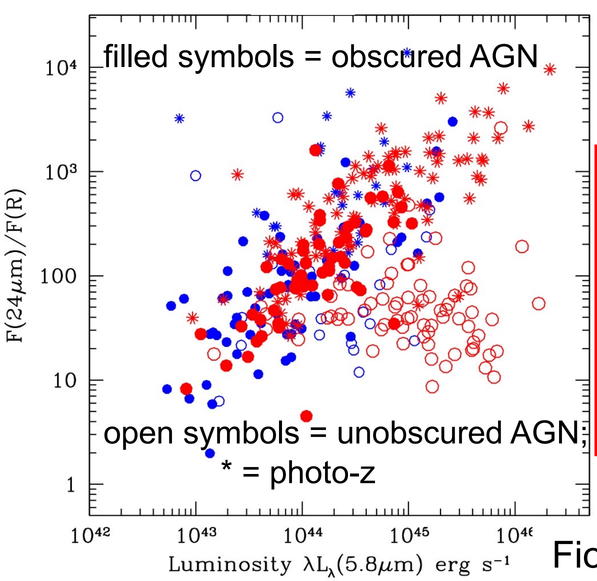

COSMOS:
large fraction of Compton-thick AGN candidates at z≈2 in cell A

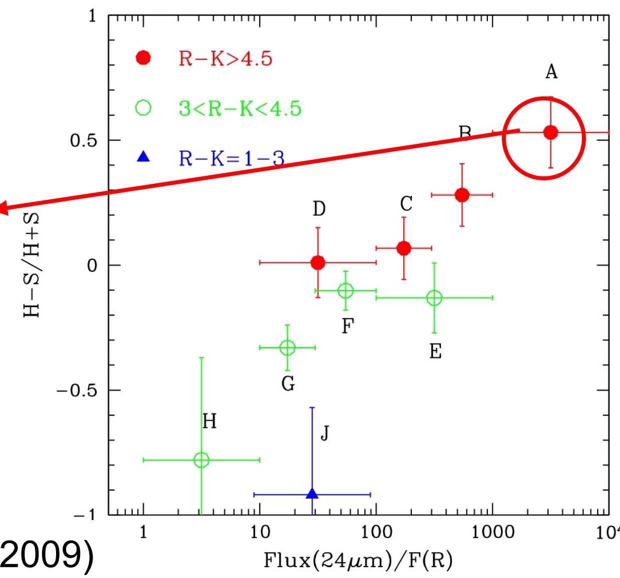

Fiore et al. (2009); Lanzuisi et al. (2009)

The combined optical/mid-infrared selection in the quest for Compton-thick AGN at high-z (IV)

MID-IR excess galaxies (Daddi et al. 2007)

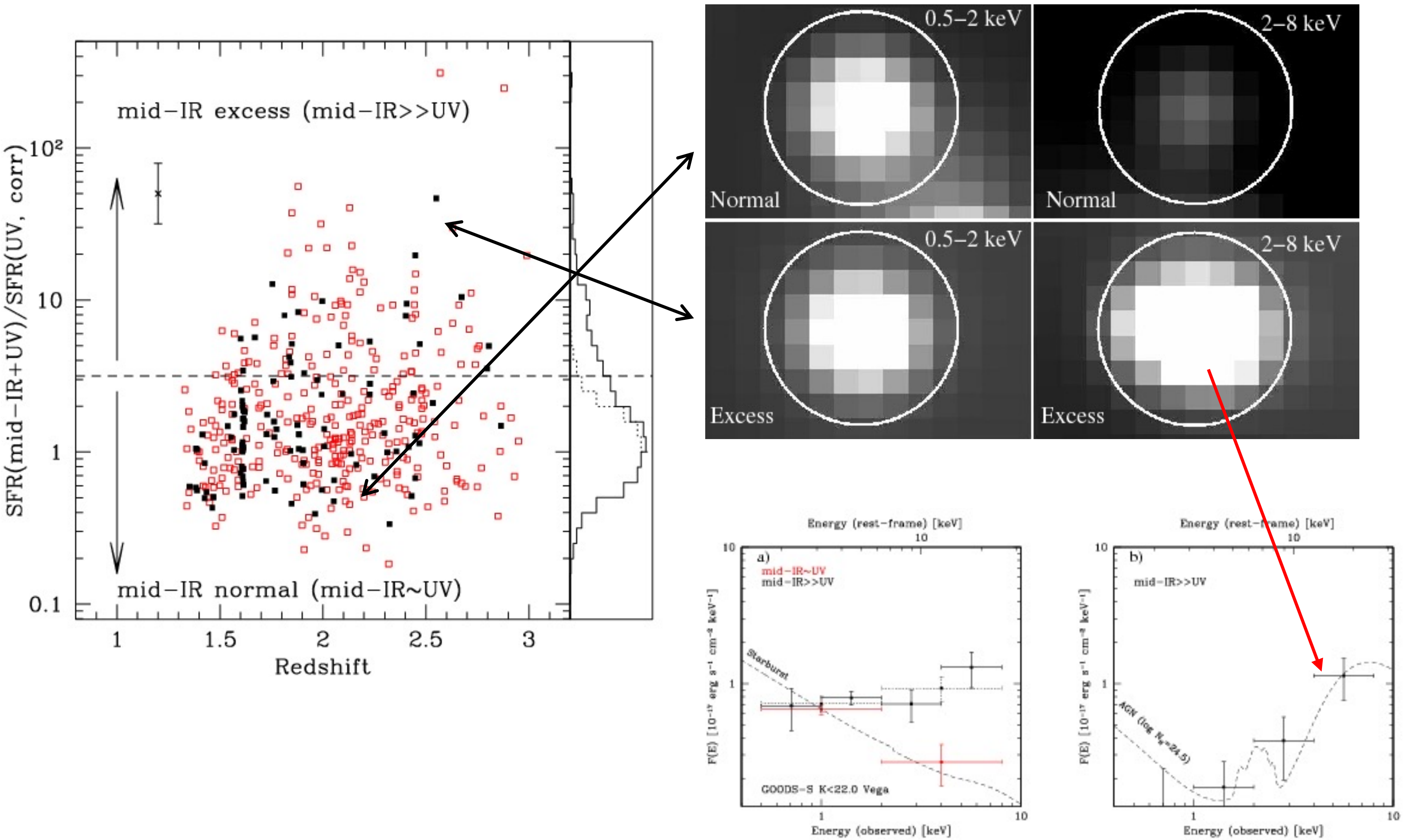

Multi-wavelength selection of AGN: pros and cons

Table 3 A multi-wavelength overview of AGN highlighting the different selection biases (weaknesses) and key capabilities (strengths)

Band	Type	Physics	Selection biases/weaknesses	Key capabilities/strengths
Radio, $f_r \gtrsim 1$ mJy	Jetted	Jet	Non-jetted sources	High efficiency, no obscuration bias
Radio, $f_r \lesssim 1$ mJy	Jetted and non-jetted	Jet and SF	Host contamination	Completeness, no obscuration bias
IR	Type 1 and 2	Hot dust and SF	Completeness, reliability, host contamination, no dust	Weak obscuration bias, high efficiency
Optical	Type 1	Disk	Completeness, low-luminosity, obscured sources, host contamination	High efficiency, detailed physics from lines
X-ray	Type 1 and (most) 2	Corona	Very low-luminosity, heavy obscuration	Completeness, low host contamination
γ-ray	Jetted	Jet	Non-jetted, unbeamed sources	High reliability
Variability	All (in principle)	Corona, disk, jet	Host contamination, obscuration, cadence and depth of observations	Low-luminosity

The definitions of some of the terms used in the bias and capability columns are as follows: *Efficiency*: ability to identify a large number of AGN with relative small total exposure times (this is thus a combination of the nature of AGN emission and the capabilities of current telescopes in a given band). *Reliability*: the fraction of sources that are identified as AGN using typical criteria that are truly AGN. *Completeness*: the ability to detect as much as possible of the full underlying population of AGN

from Padovani+17 review on AGN

Completeness vs. reliability issues

A simplified picture of AGN evolution

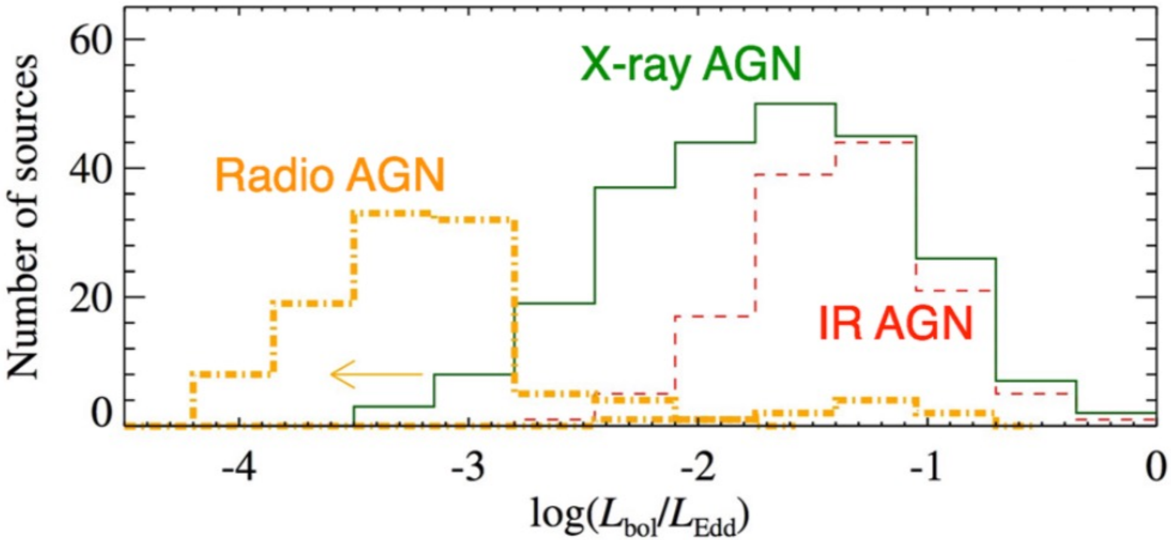

Hickox+09
situation up to z~1

Goulding+14

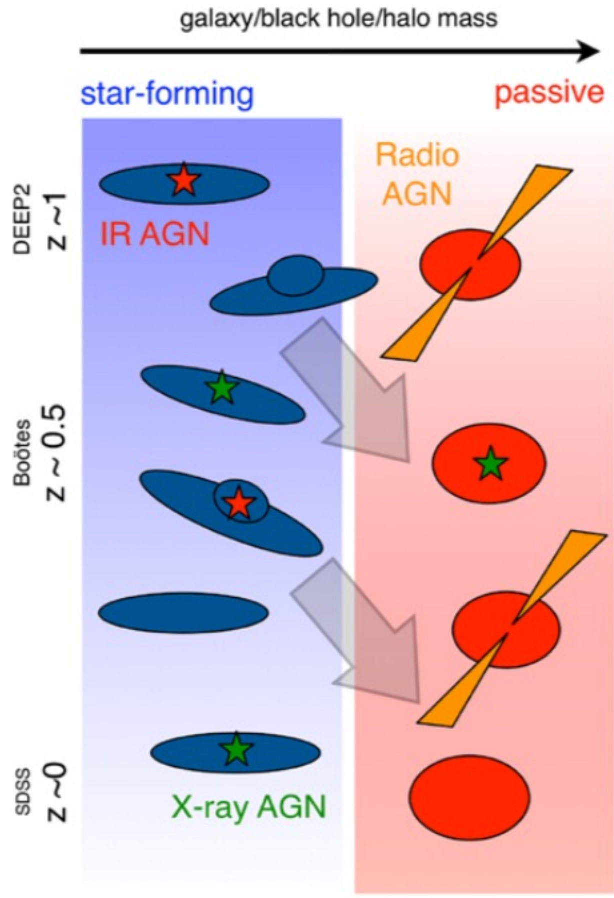

- All galaxies appear to begin as star-forming blue-cloud systems and end as passive red-sequence sources, once their dark matter halos have grown sufficiently.
- Galaxies hosting **IR**, **X-ray,** and/or **radio** AGN appear to follow a similar evolutionary path: **radiatively efficient rapid BH growth** (IR/X-ray AGN) appears to be linked with those galaxies with large supplies of cool gas, while **mechanically dominated** (radio) **accretion** is associated with passive galaxies, which may also be responsible for preventing late SF.

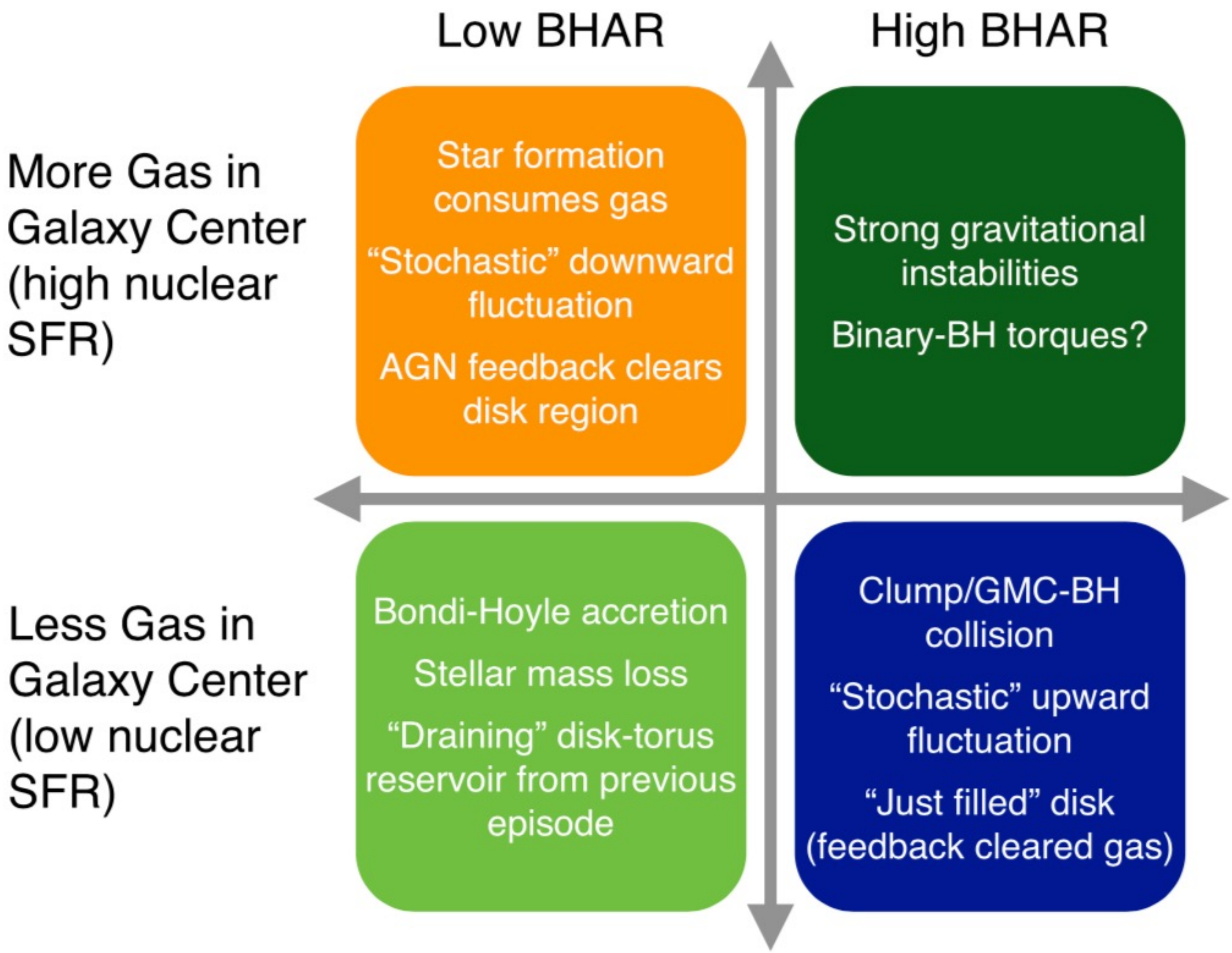
Low BHAR
High BHAR
More Gas in Galaxy Center (high nuclear SFR)
Less Gas in Galaxy Center (low nuclear SFR)
Star formation consumes gas
“Stochastic” downward fluctuation
AGN feedback clears disk region
Strong gravitational instabilities
Binary-BH torques?
Bondi-Hoyle accretion
Stellar mass loss
“Draining” disk-torus reservoir from previous episode
Clump/GMC-BH collision
“Stochastic” upward fluctuation
“Just filled” disk (feedback cleared gas)

Padovani+17

Multi-wavelength signatures of AGN

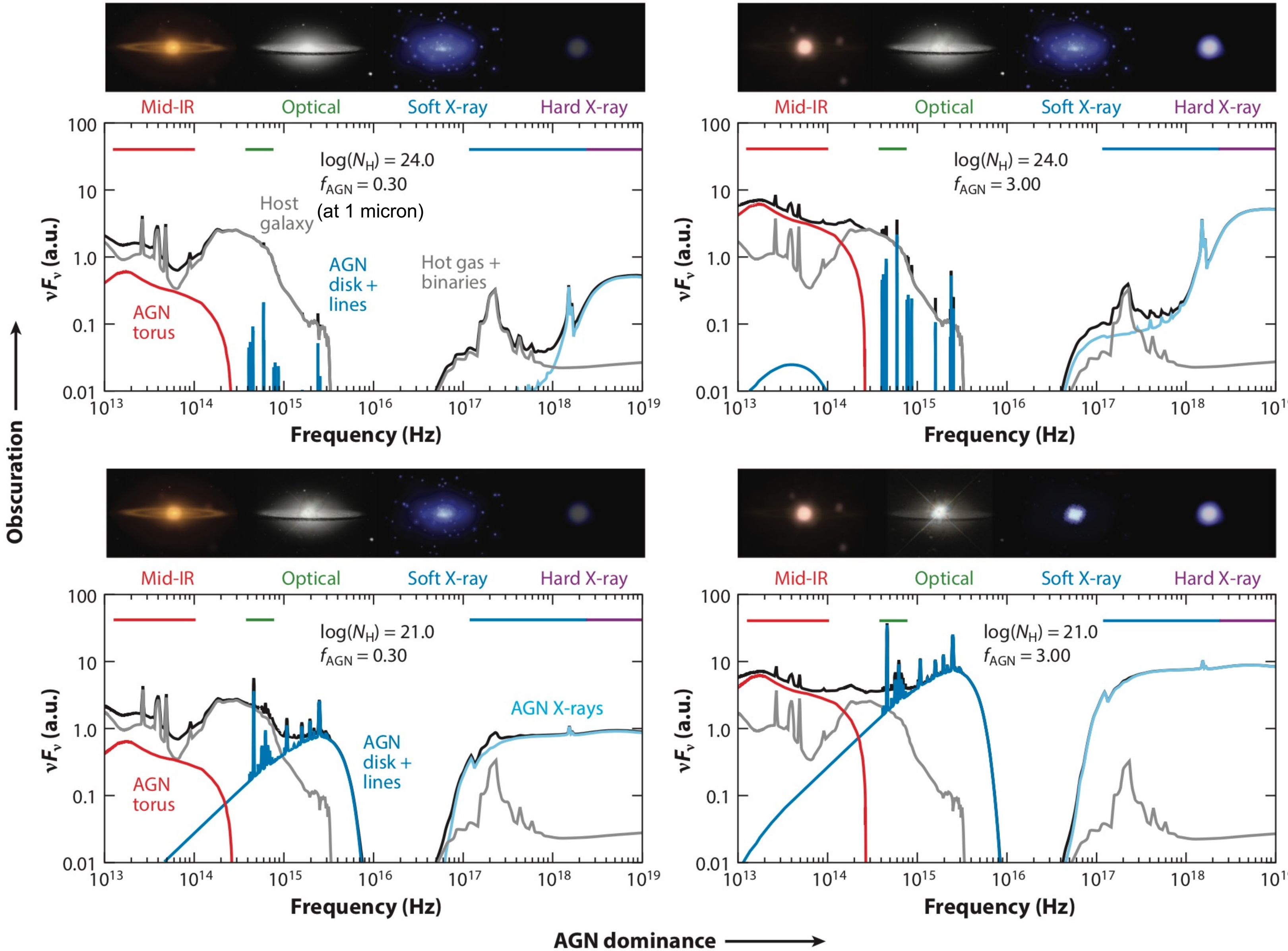

Hickox & Alexander 2018 (ARA&A)

video at https://youtu.be/82LmtccFH7E

‘Optimization’ of AGN selection

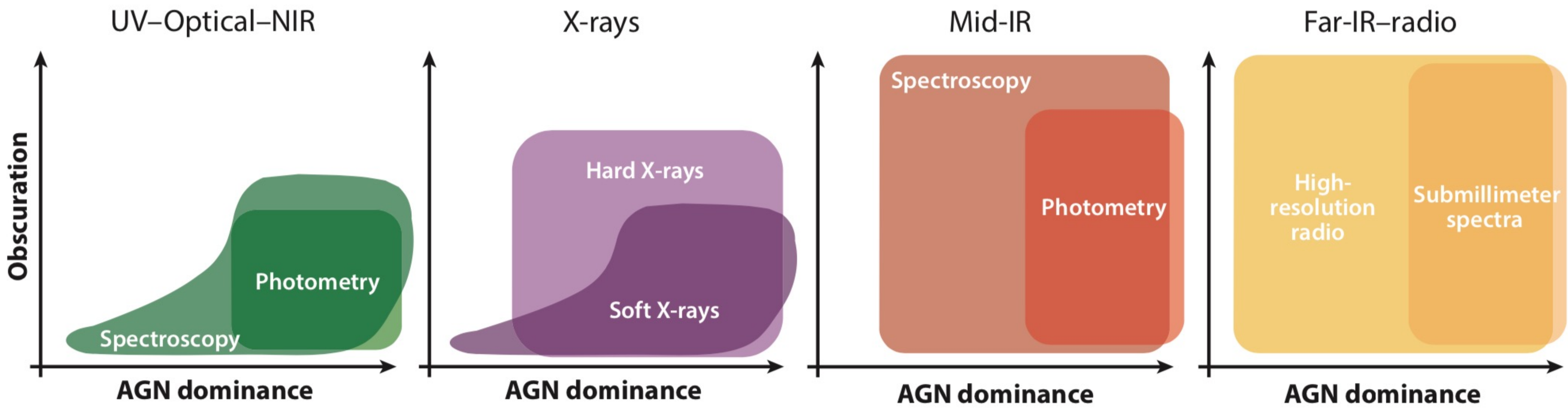

Hickox & Alexander 2018 (ARA&A)

The final picture?

A significant amount of work needs to be done

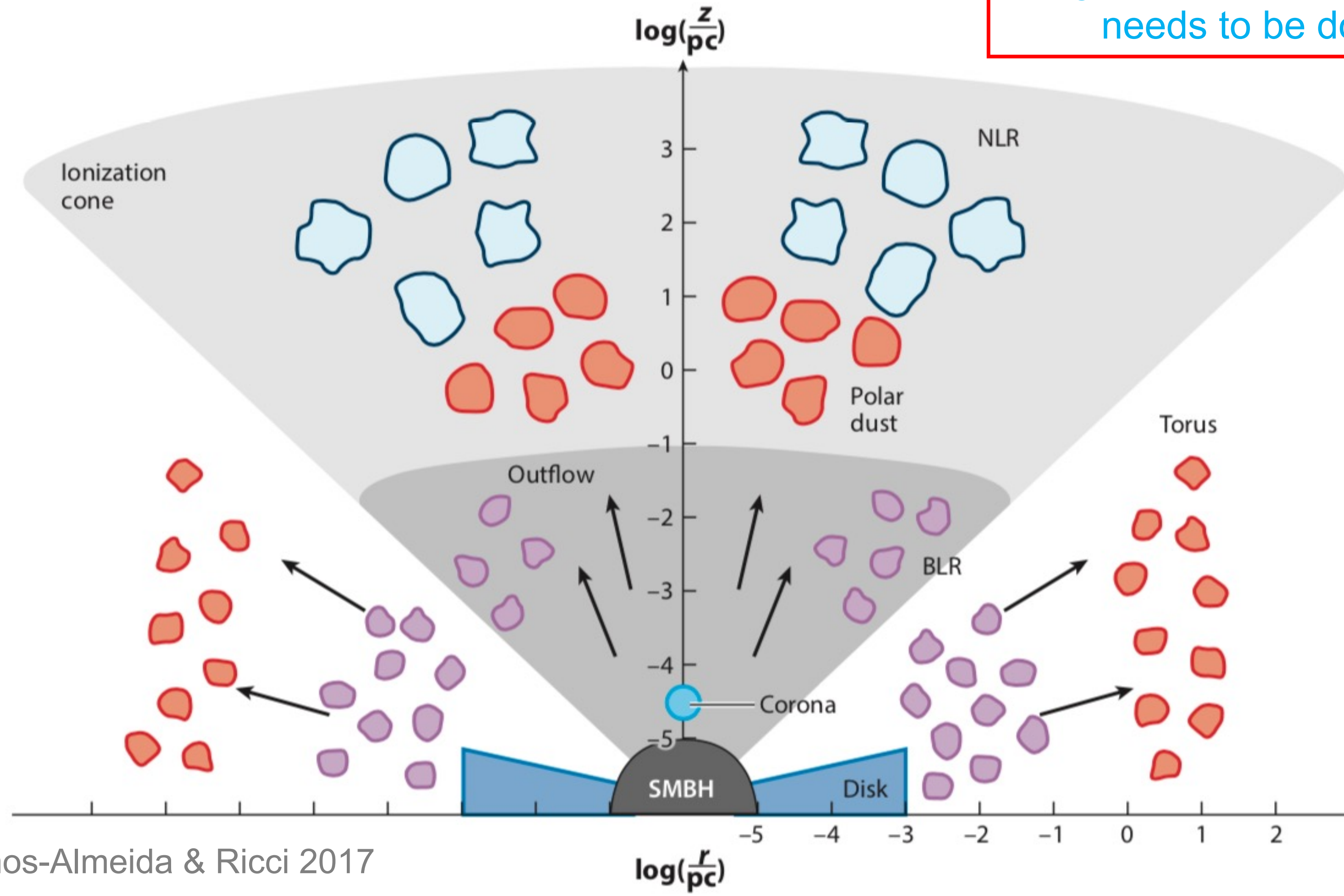

from Ramos-Almeida & Ricci 2017

The **absorber/reprocessing mater**ial is most likely **cloudy** and **filamentary** (e.g., Jaffe+04, Burtscher+13; Ramos-Almeida+11, Alonso-Herrero+, […])

Combes+18 – ALMA results, tori are disk-like on scales of ~10-30 pc + resonant rings at 100-pc scales; AGN non necessarily in the center

The quest for obscured AGN at different cosmic times

Obscured SMBH growth as a key phase in AGN/galaxy life

Needs for a ‘complete’ AGN census

X-ray surveys

- *Integral* and *Swift*/BAT surveys: limited sensitivity, mostly low z
- *NuSTAR*: more efficient and sensitive, obscured AGN up to z~3 (a few)
- Deep X-ray Surveys (*Chandra*, XMM): up to high redshift, limited by photon statistics

Combined mid-IR/opt/X-ray

- Mid-IR/optical extreme colors + X-ray spectroscopy/stacking
- Based on mid-IR as a proxy of the AGN strength

Optical spectroscopy

- High-ionization narrow emission lines as proxies of the intrinsic nuclear emission
- [OIII]$_{5007\text{Á}}$, [NeV]$_{3426\text{Á}}$, CIV$_{1549\text{Á}}$ selection in the optical
- Similar probes in the mid-IR: [NeV]$_{14.3\mu m}$, [OIV]$_{26\mu m}$

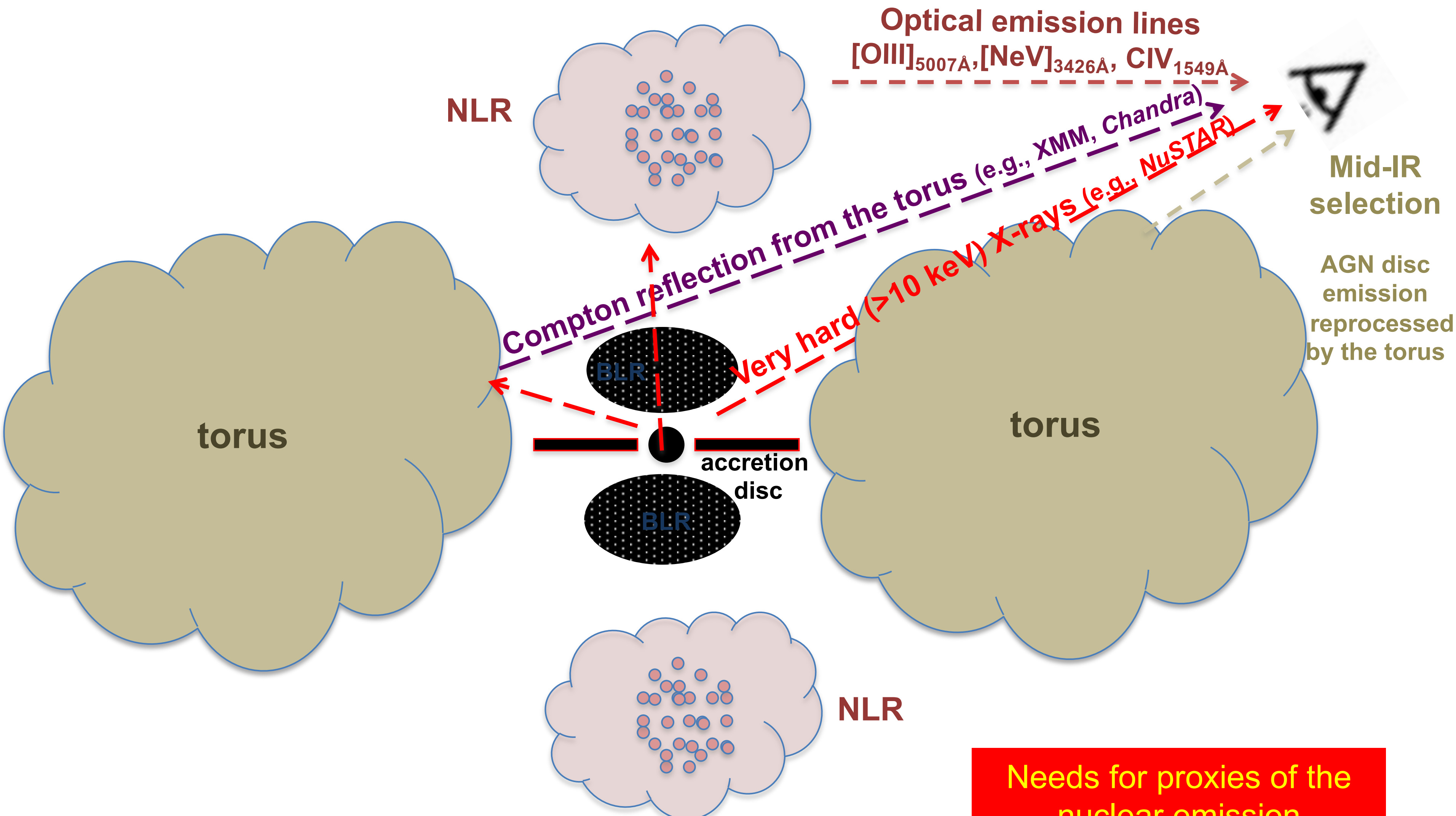

Needs for proxies of the nuclear emission

see also the review by Hickox and Alexander (2018)

CV2014

Obscured AGN searches in X-rays

- Some highlights on the search and characterization of obscured AGN in X-ray survey fields: the strength (and limitations) of X-ray spectra
- The role of imaging and band coverage above 10 keV (*NuSTAR*)
- X-ray redshift estimates in obscured AGN

A simple method to select obscured AGN

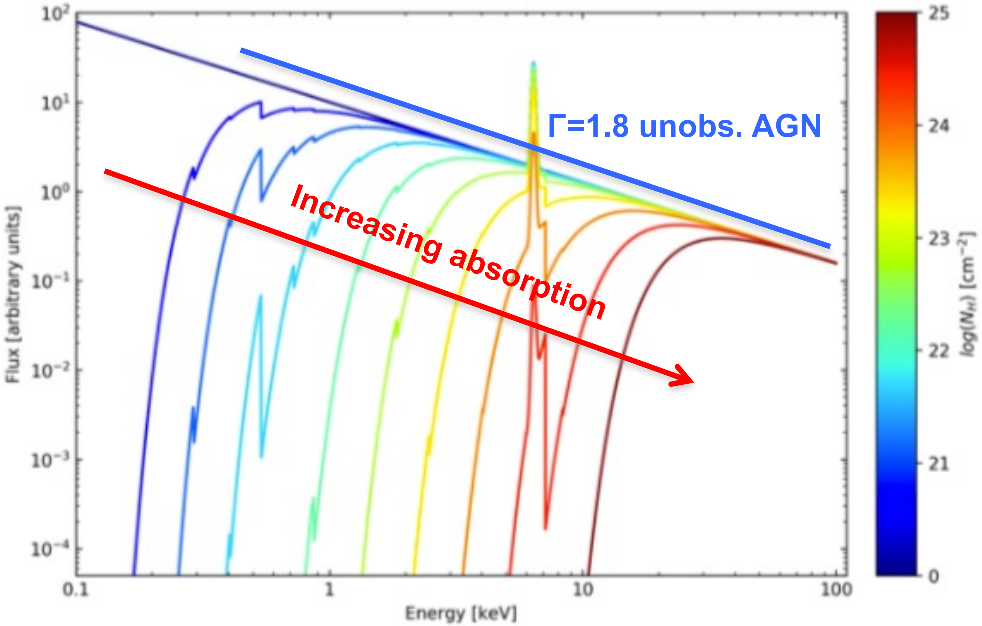

Broad band and sensitivity required

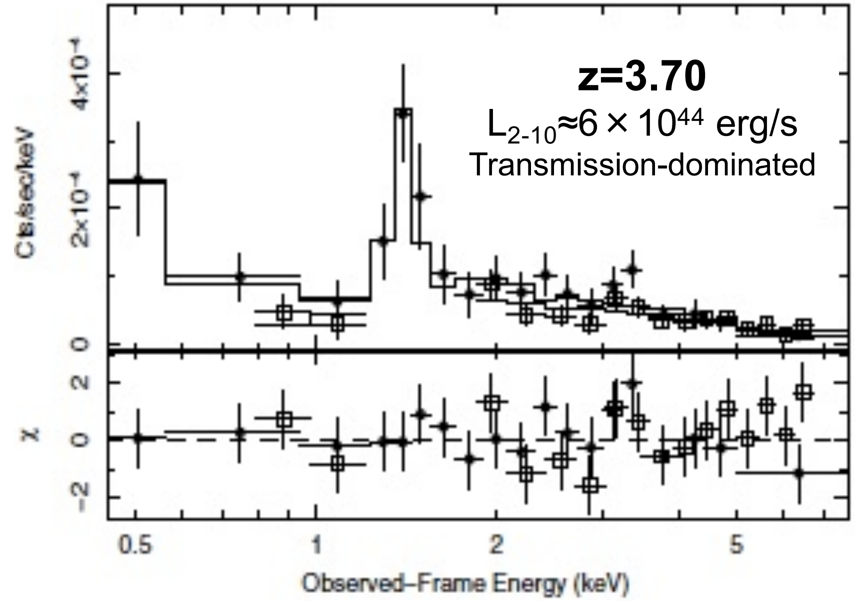

Comastri et al. (2011)

A simple, widely adopted method to search for obscured AGN (e.g., Lanzuisi+, Georgantopoulos+…):

- ❑ Flat (observed) photon index ($\Gamma<1$, i.e. much lower than $\Gamma\approx1.8$ typical of unobscured AGN)
- ❑ Strong (EW>1 keV) iron Kα emission line

Explanation: an absorbed $\Gamma\approx1.8$ power-law spectrum can be 'mimicked' by a flat X-ray continuum in cases of poor photon statistics and limited energy band

Further simplification: using X-ray colors (hardness ratio) in case of very low statistics

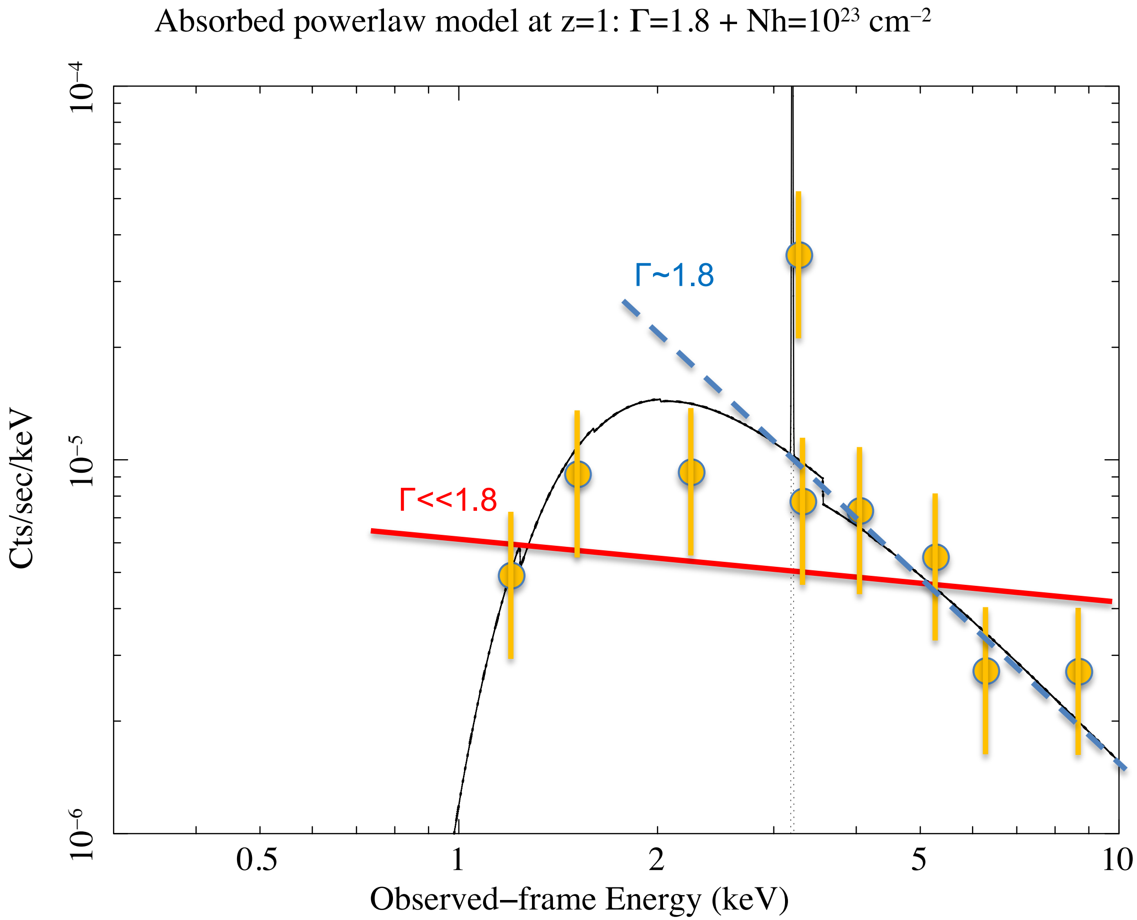

The original absorbed powerlaw spectrum with Γ~1.8 (the one typically observed in unobscured AGN and predicted by theory) can be easily fitted with a flat (Γ<<1.8) continuum in case of poor-quality X-ray spectra and when the observing band is limited

Compton-thick AGN in the COSMOS survey using XMM and *Chandra*

Searching for the most obscured AGN
Almost complete X-ray spectra coverage

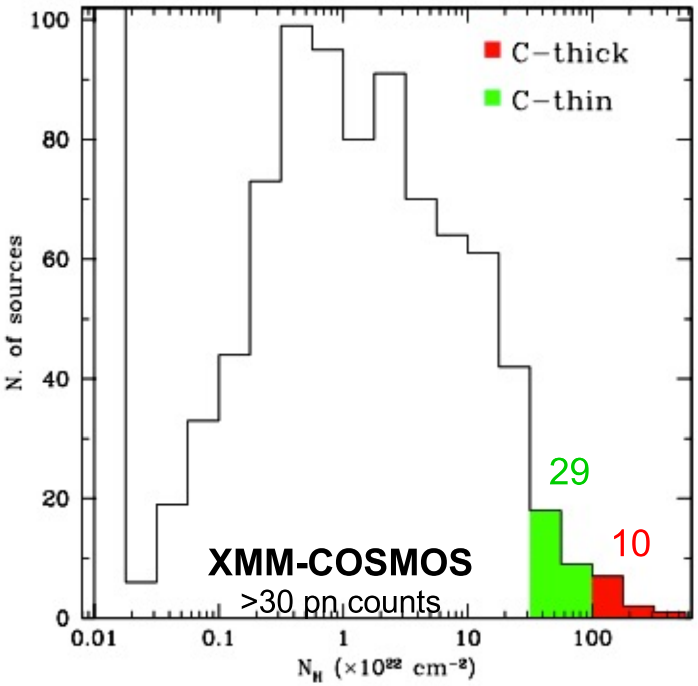

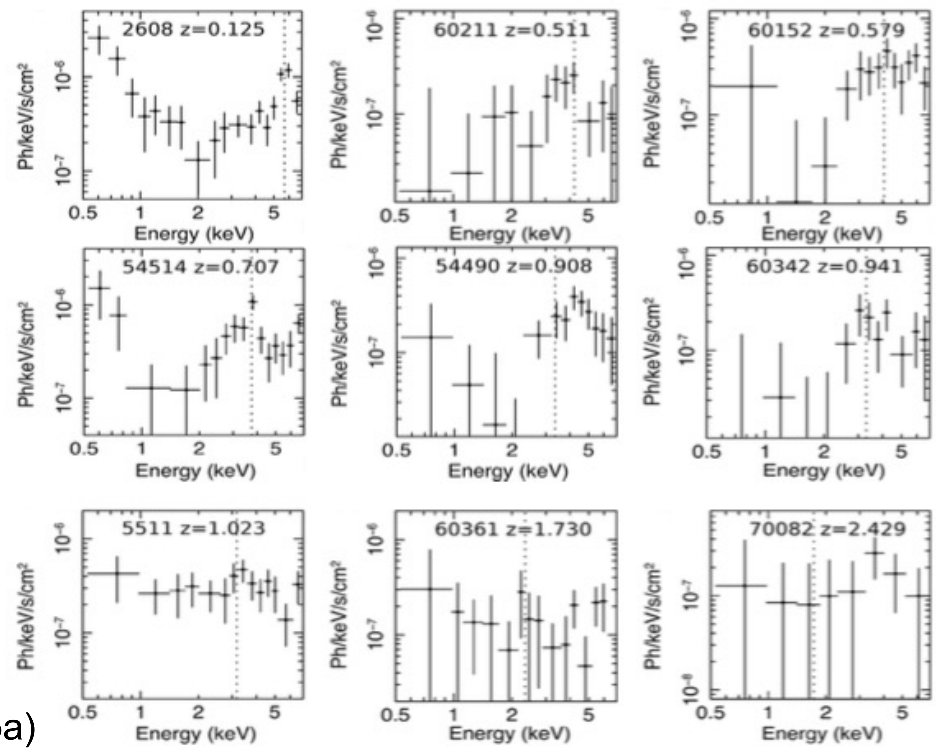

Lanzuisi et al. (2015a)

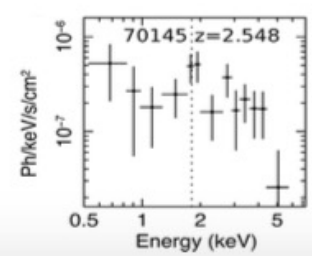

Ten CT AGN at the end
More disturbed morphologies for the hosts of heavily obscured AGN (see also Kocevski+15)

Typically, low-SNR X-ray spectra, careful modeling needed
HR selection may be not appropriate if a soft component is present at low z

$z=0.1-2.5$
$\log L_{2-10keV} \approx 43.5-45$

CT AGN at high redshift in COSMOS. I

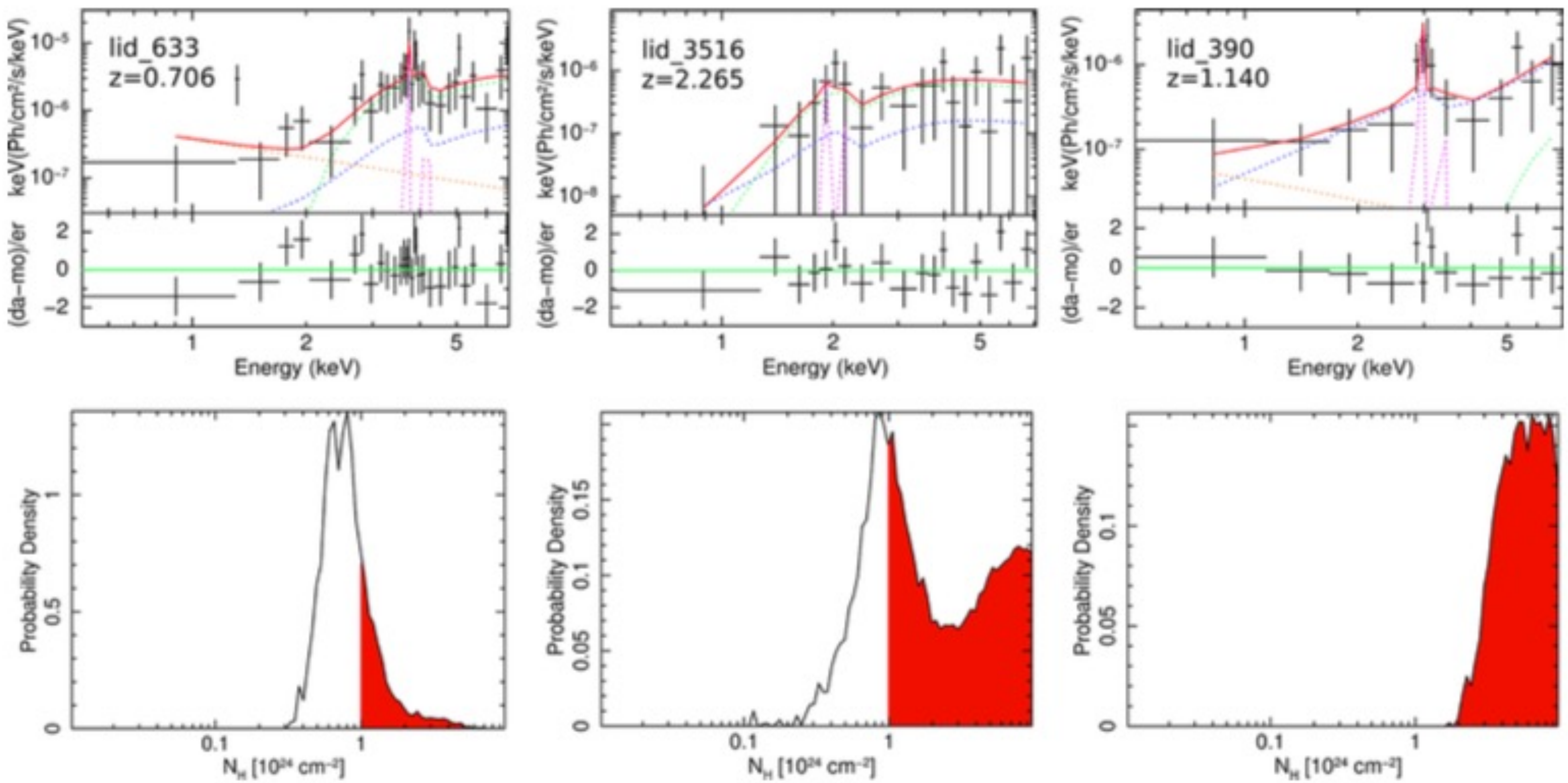

Lanzuisi et al. (2018)

Starting point: phenomenological model, then a more physical model (n>30 counts)

- ~40 CT "effective" AGN up to z~3.5 (corrected for classification bias)
- The fraction of CT AGN in mergers/interacting systems increases with redshift (once rescaled to a common X-ray luminosity range)

CT AGN at high redshift in COSMOS. II

Merger fraction vs. L_{bol}

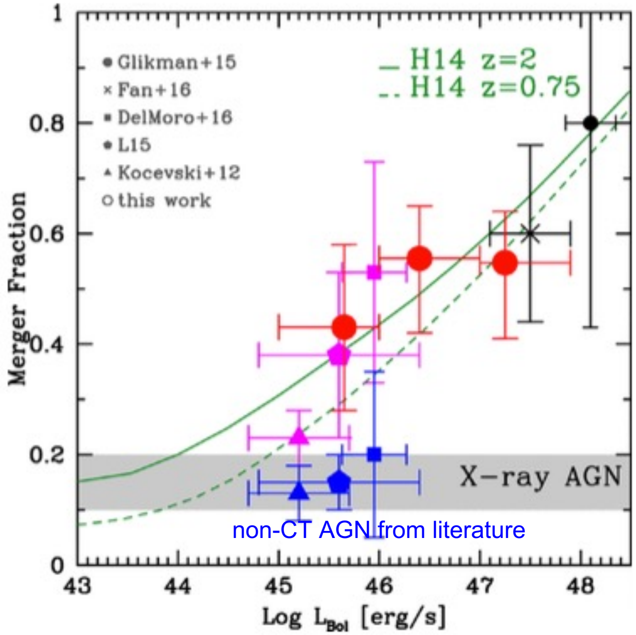

CT AGN fraction vs. z

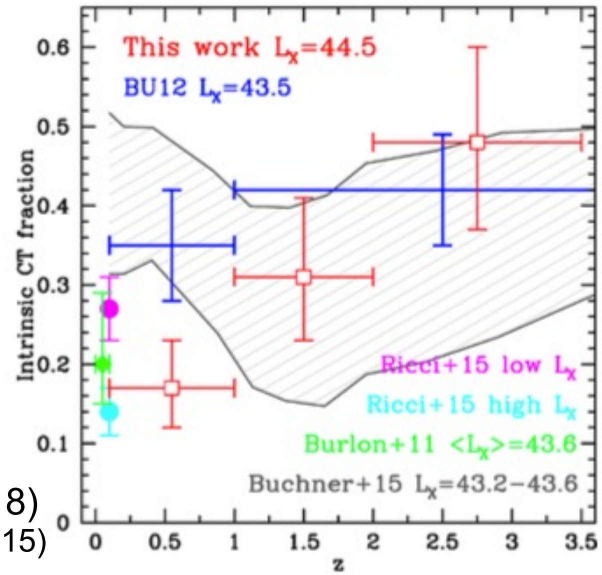

Lanzuisi et al. (2018)
see also Aird et al. (2015)

- More gas available and destabilized towards the innermost regions
- Late-state mergers have a higher fraction of heavily obscured AGN (Ricci et al. 2017, DeRosa et al. 2018)
- Similar results in the CDF-S (Vito et al. 2013, 2014, 2018) – see also Marchesi et al. (2016) for the fraction of obscured AGN at high redshift, and Marchesi et al. (2018) for estimates (*NuSTAR*-based) at low redshift

Further discussion in the high-redshift AGN lesson

Heavily obscured AGN in late-state mergers

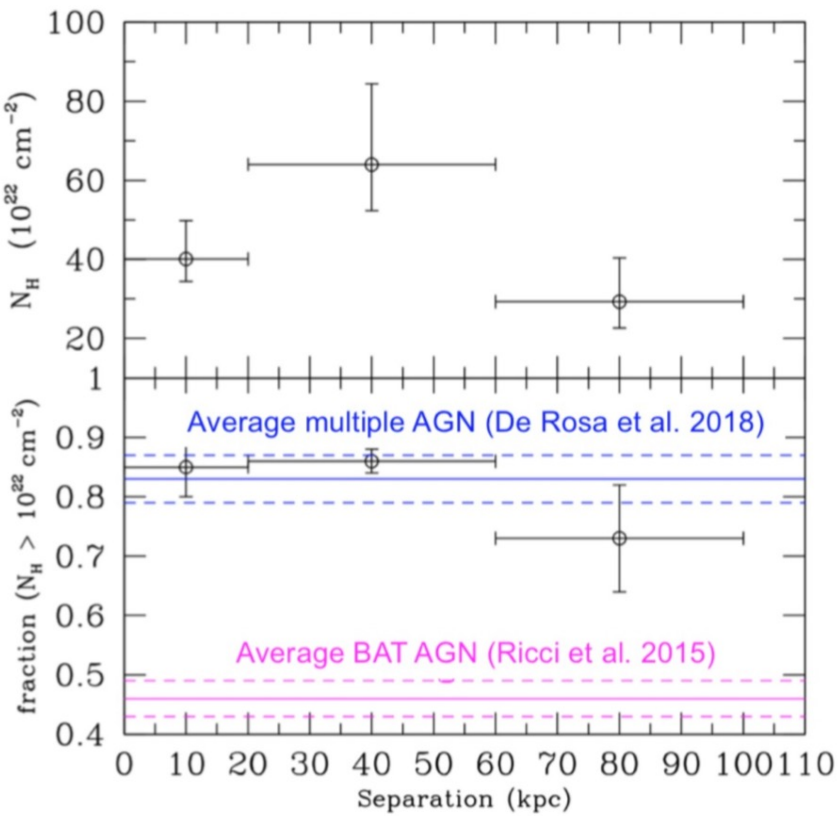

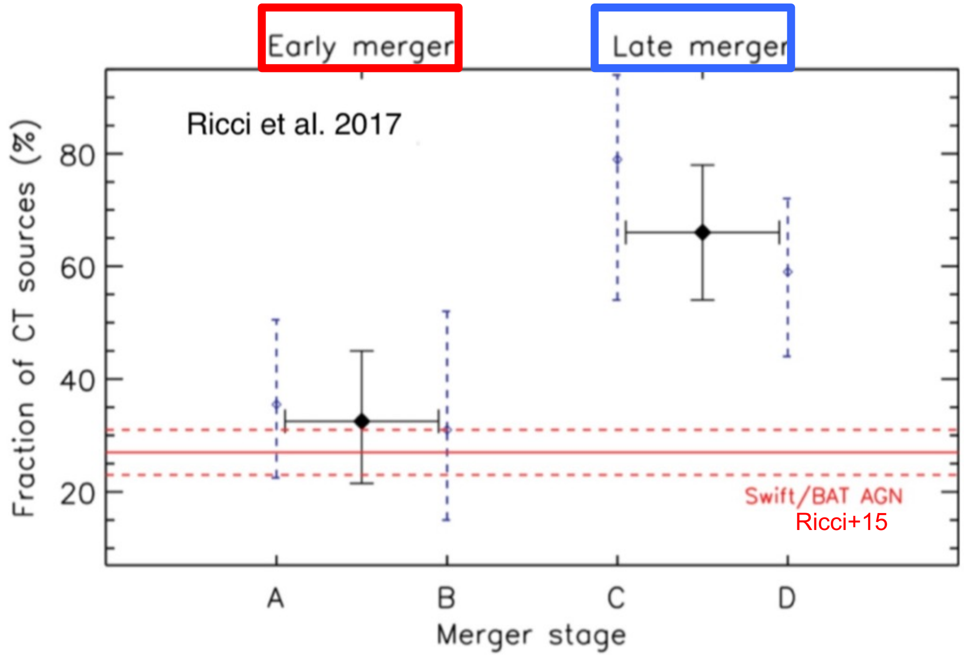

De Rosa et al. (2019) review

Higher fraction of heavily obscured AGN in late-state mergers (and, generally, higher N_H)
Is gas more easily funneled to the central regions and then provide support to accretion, hence AGN activity?
See also Ricci et al. (2021) and Tamada et al. (2021) results on the interacting galaxies in the C-GOALS sample

Obscured AGN in the J1030 field.
Estimates of redshifts through X-ray spectra and simulations. I

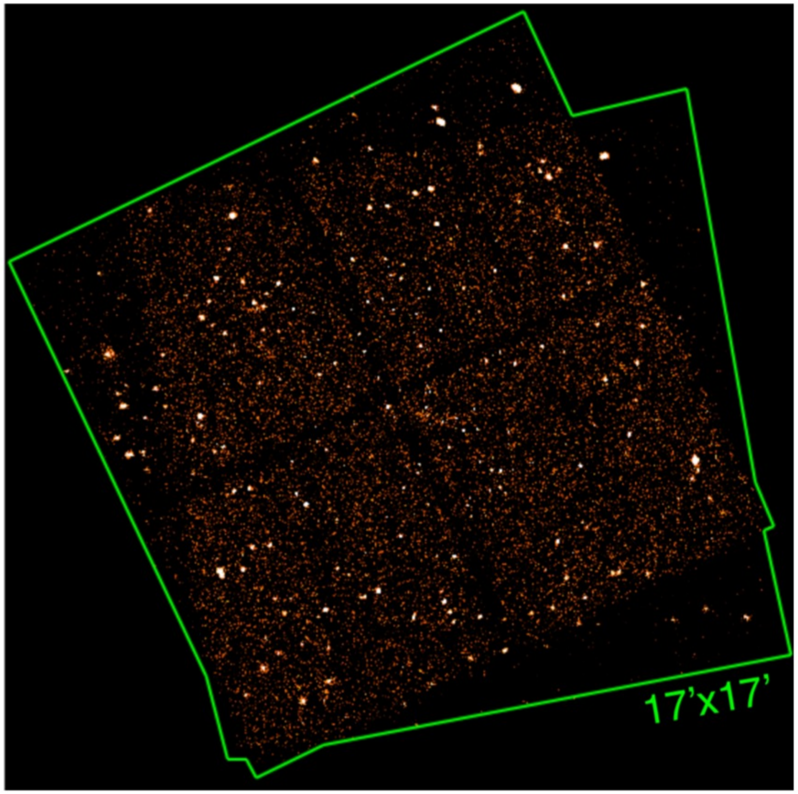

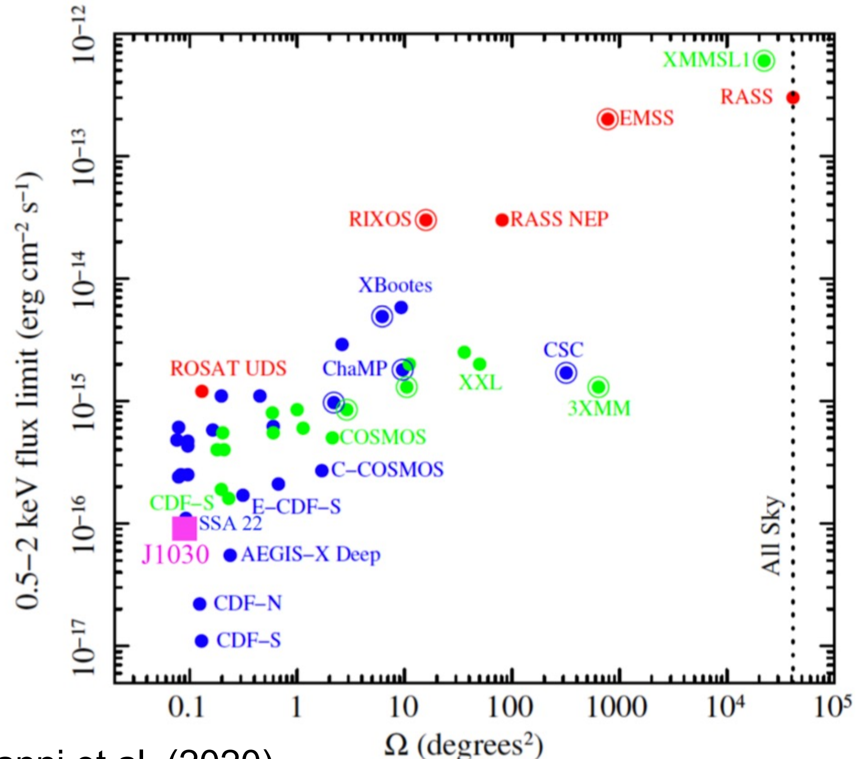

Nanni et al. (2020)

- 480 ks Chandra obs. centered on a QSO at z=6.3 with ample multi-wavelength coverage
- 256 point-like X-ray sources (Nanni et al. 2020) + some high-z candidates (Decarli et al. 2019, Mignoli et al. 2020) + protocluster at z=1.7 (Gilli et al. 2019)
- Obscured AGN searches (based on hardness ratio; Peca et al. 2021)

Hardness ratio: HR=(H-S)/(H+S)

H=counts in 2-10 keV band, S=counts in 0.5-2 keV band

HR=+1: only counts above 2 keV → likely indication of large N_H

HR=−1: counts only below 2 keV

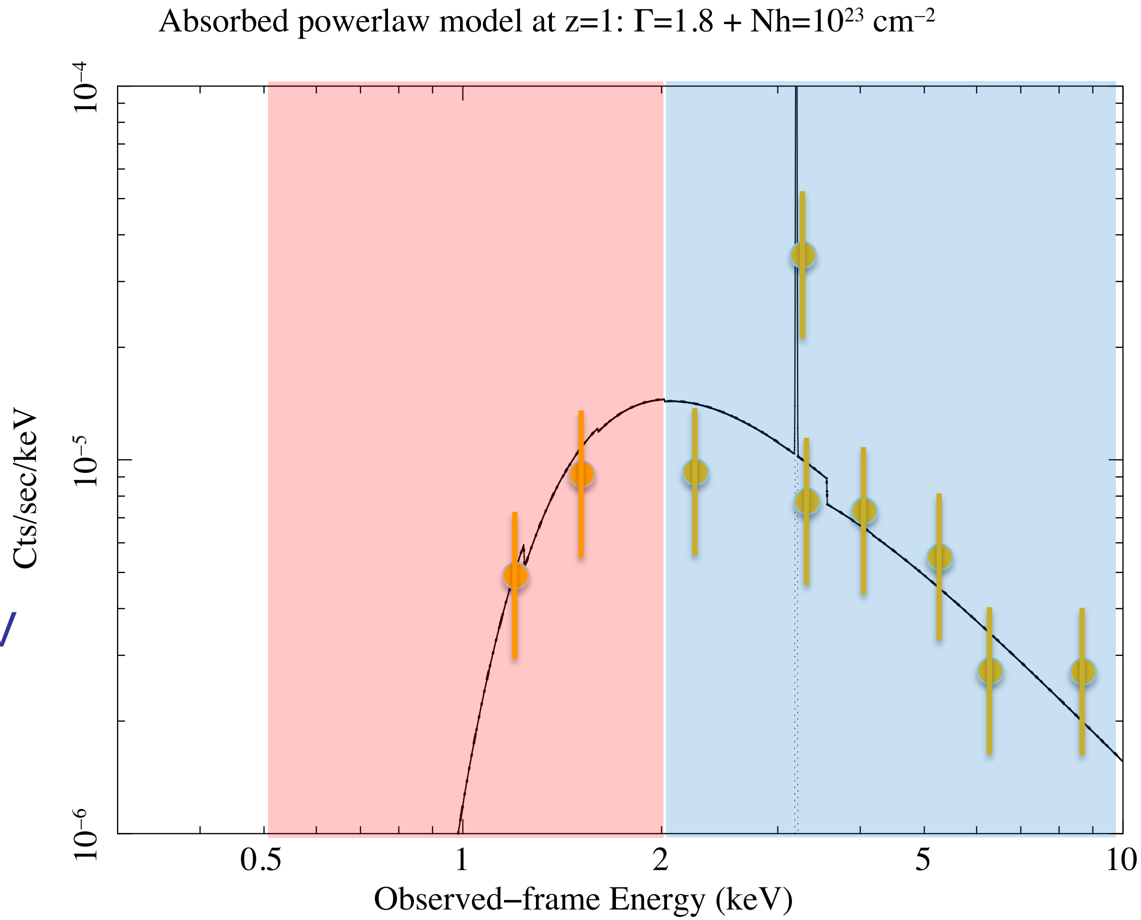

The **hardness-ratio** technique is a sort of **X-ray color**: it provides a first guess on the X-ray spectral properties of a source. Large HR means that the spectrum is harder (e.g., the soft X-ray emission is depressed by photoelectric absorption, as in the example above).

More complex models than a powerlaw may imply a more challenging HR → N_H conversion

Obscured AGN in the J1030 field.
Estimates of redshifts through X-ray spectra and simulations. II

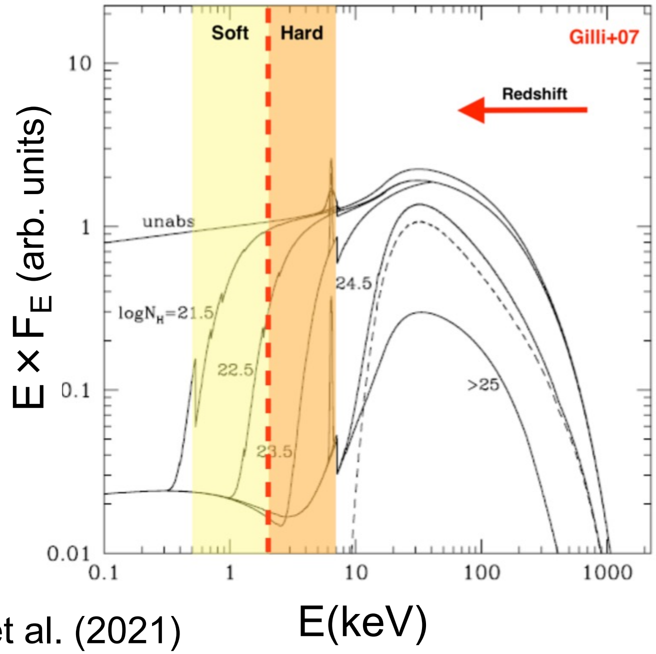

Peca et al. (2021)

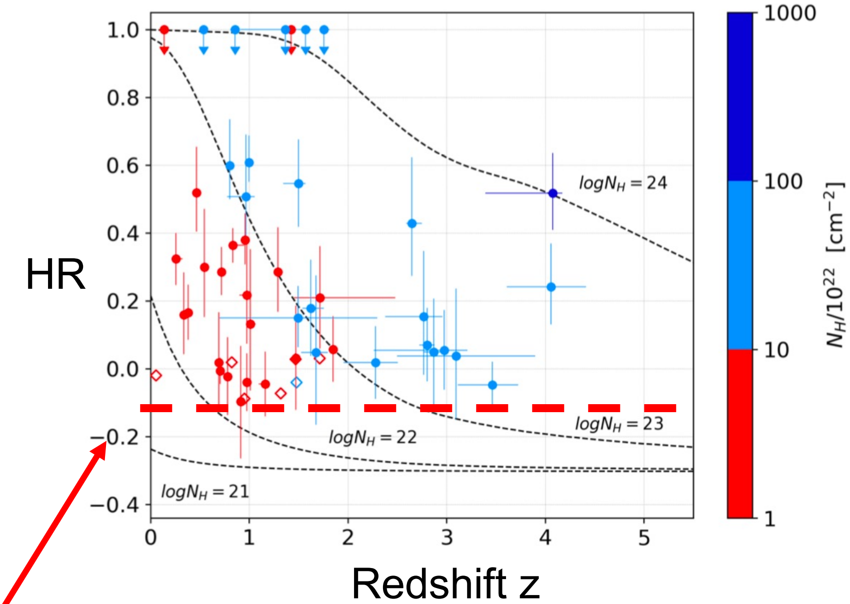

HR is a function of the redshift (presently unknown for most of our sources)

SELECTION: >50 counts (0.5-7 keV) & HR>-0.1 **+** optically faint red sources (r>27.5 & r-[3.6]>4) → 54 sources

HR>-0.1 provides a good selection of obscured AGN regardless of redshift

MAIN GOAL: use the iron **Kα line + edge + photoelectric cutoff** to estimate the **source redshift** (waiting for optical spectroscopy) – check vs. simulations
Technique already used in Iwasawa+12, 20, Vignali+15 (see also Simmonds+18), using higher photon statistics spectra

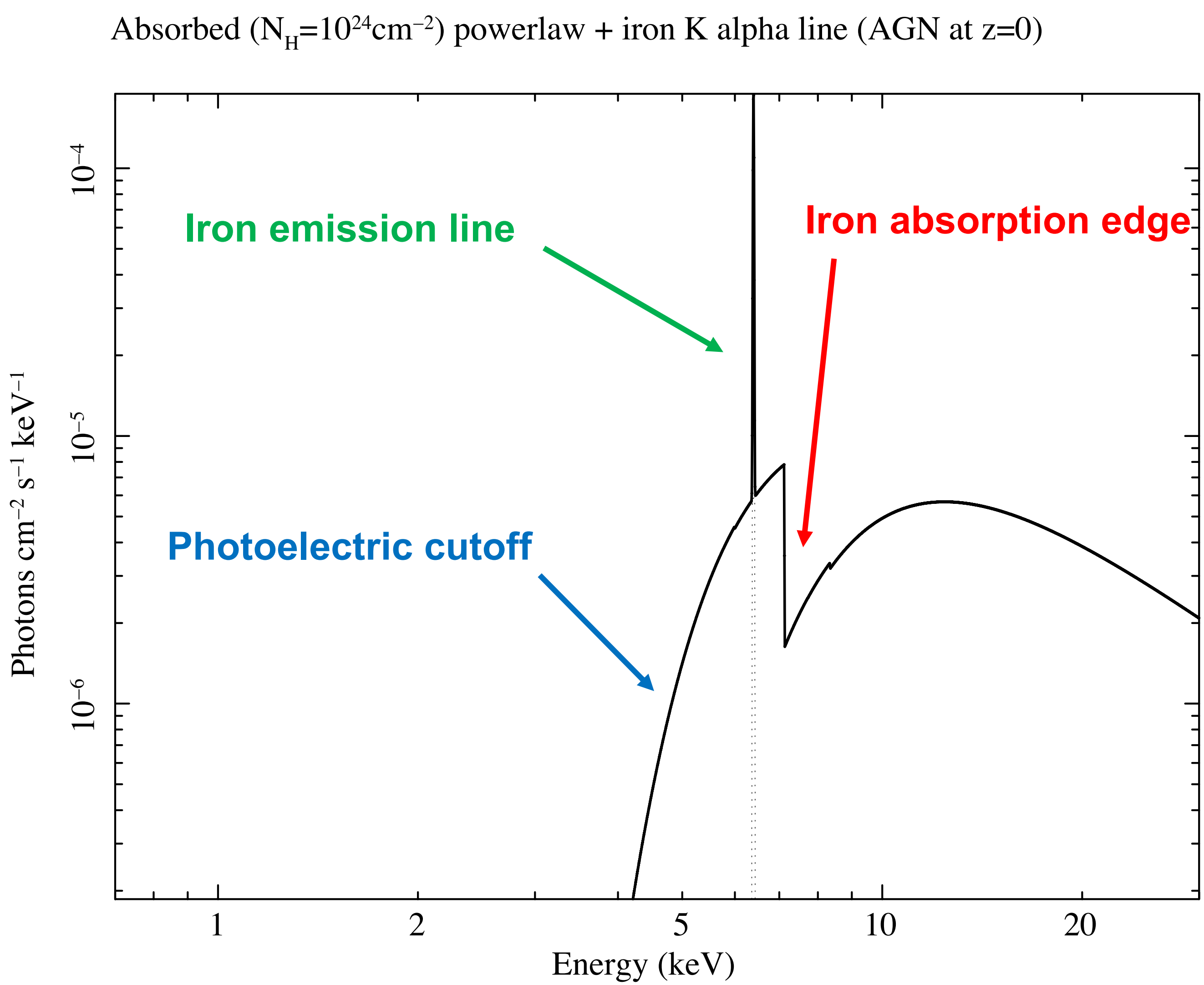

To 'anchor' X-ray redshift solutions in absorbed AGN, the following spectral 'features' can be used:

(a) photoelectric cut-off at low energy,

(b) iron emission line (if present) and

(c) iron absorption edge (whose depth is a function of N_H)

Obscured AGN in the J1030 field.
Estimates of redshifts through X-ray spectra and simulations. III

z(X)=2.55+0.32/-0.64 **z(opt. spec)=2.551** z(Hyperz)=2.28+0.20/-0.53

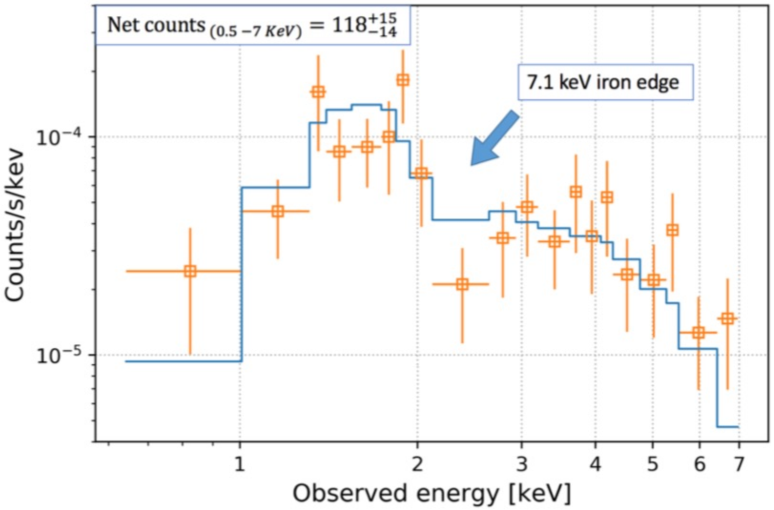

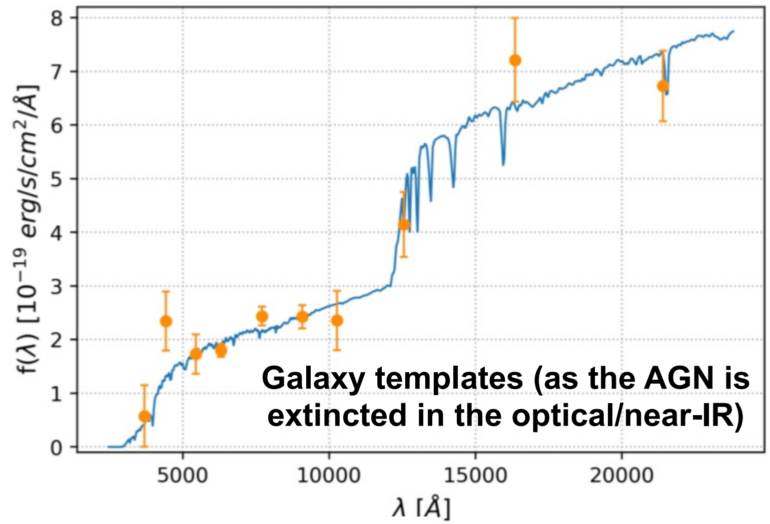

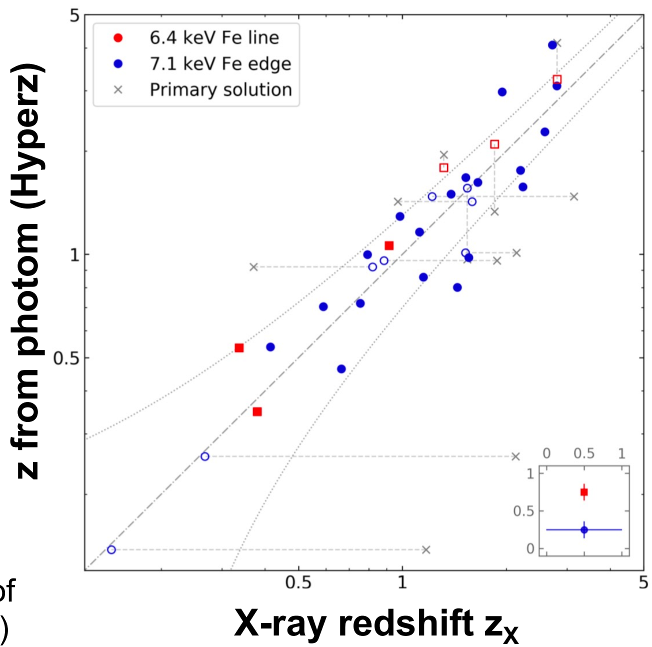

Hyperz: code for *photometric redshift* (i.e., *z* derived by matching the magnitudes of a source with appropriate (galaxy) templates)

Peca et al. (2021)

Searching for heavily obscured AGN at high redshift via color (opt/mid-IR) selection and X-ray information

- ❑ Deep silicate feature vs. X-rays (already discussed in this lesson)
- ❑ Mid-IR emission lines associated with intrinsic AGN strength
- ❑ Optical vs. mid-IR colors: from *Spitzer* to *WISE*-based selection
- ❑ The power of SED fitting, and mid-IR vs. X-ray correlations
- ❑ Obscured galaxies (with AGN) at high-redshift: from DOGs to Hot DOGs

Deep Silicate features vs. heavy X-ray obscuration

Spitzer/**IRS** spectra –
12 micron sample (RMS1993)

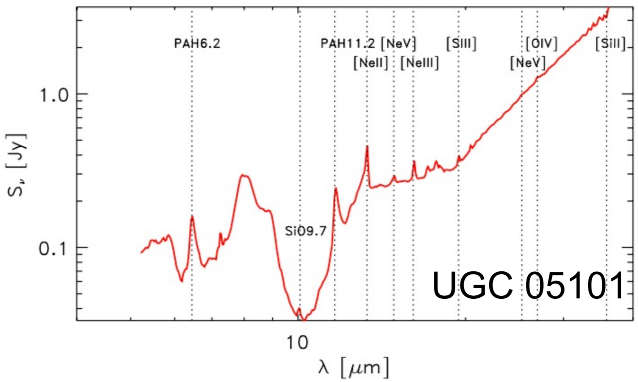

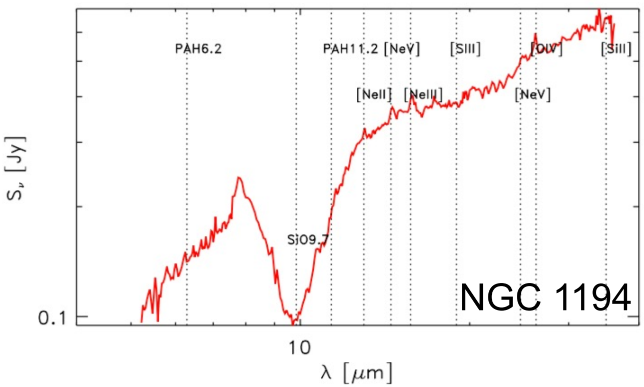

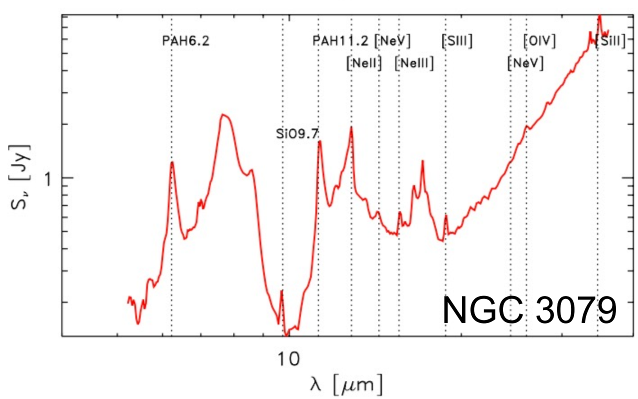

AGN presence
$[NeV]_{14.3\mu m}$, $[NeV]_{24.3\mu m}$, $[OIV]_{25.9\mu m}$ **+** mid-IR emission lines (see Spinoglio+, Tommasin+)

Is it obscured?
Deep silicate feature
Pro: low-resolution spectroscopy sufficient to reveal this feature
Con: also the host galaxy may contribute

La Caria et al. (2019); see also Gruppioni et al. (2016)

X-ray spectra: all **Compton thick**

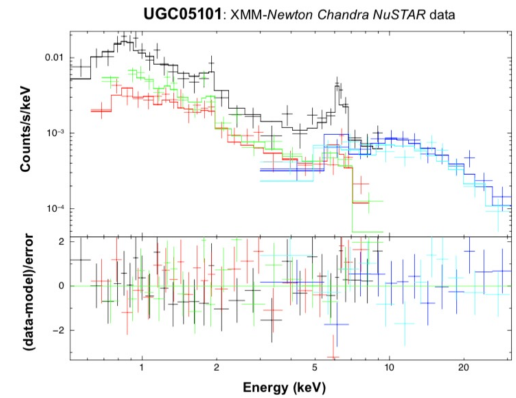

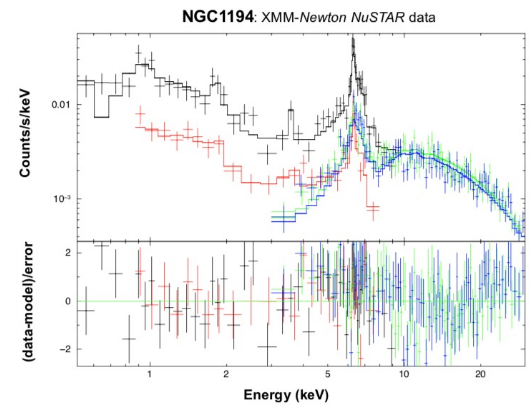

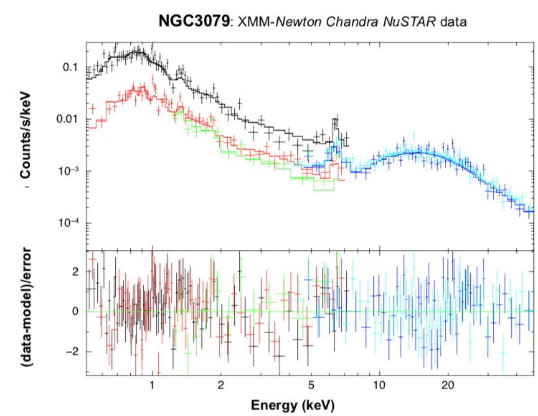

The power of high-excitation mid-IR emission lines

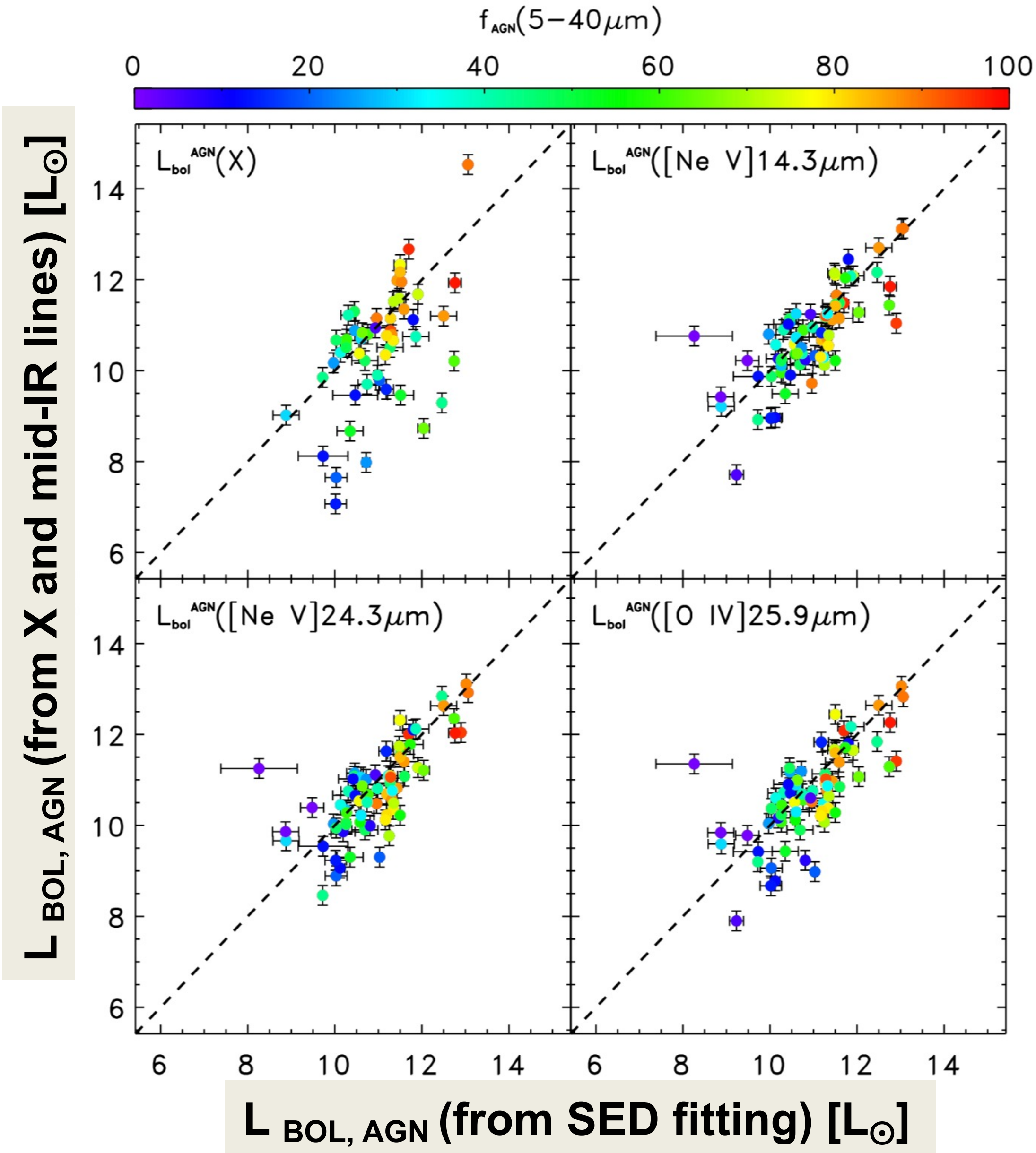

X-rays (with some expections, CT AGN and LLAGN) and **mid-IR AGN-related features** are good proxies of the intrinsic accretion-related emission – they provide a clean view of photoionization from the nucleus

Gruppioni et al. (2016)

The power of mid-IR coverage: color selection of AGN

High fraction of
X-ray detections

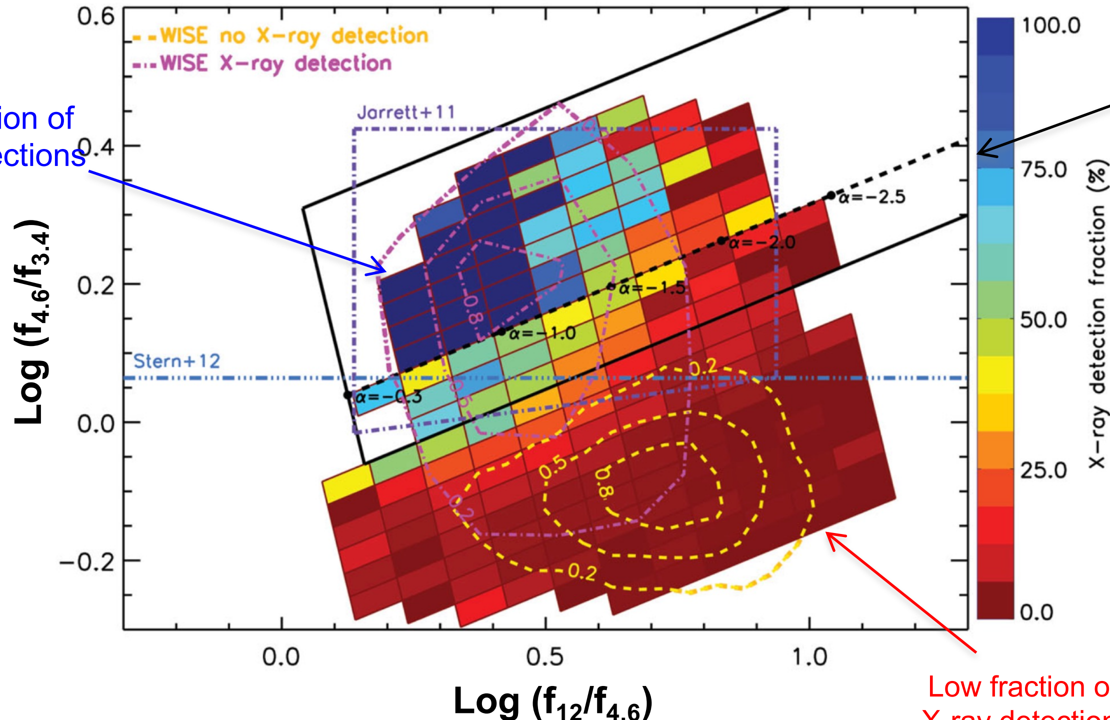

Power-law AGN
(Donley et al. 2012):
slightly a higher
fraction of obscured AGN here
(Castello-Mor et al. 2013)

No simple way to distinguish Compton-thick AGN from the Compton-thin AGN

Low fraction of
X-ray detections

Mateos et al. (2012)

Mid-IR colors to select AGN vs. galaxies and pick up the most obscured ones (based on the SED properties)
see also Donley+12, Stern+12, Mateos+13, Rovilos+13, Lacy+13, Assef+13
(and previous works based on *Spitzer*)

1. Completeness vs. reliability issues
2. Similar distribution in mid-IR wedge for Compton-thin and Compton-thick AGN
3. SED decomposition powerful (hence needed) in quantifying the host galaxy (SF) contribution to mid-IR colors

Dust Obscured Galaxies (DOGs)

DOGs: F(24μm)/F_R>1000 – *Spitzer* (Dey et al. 2008)

- Faint (extincted) in the optical, strong emission (AGN torus) in the mid-IR
- Fraction of AGN candidates increases with F(24μm)

already discussed
see Fiore et al. 2008, 2009

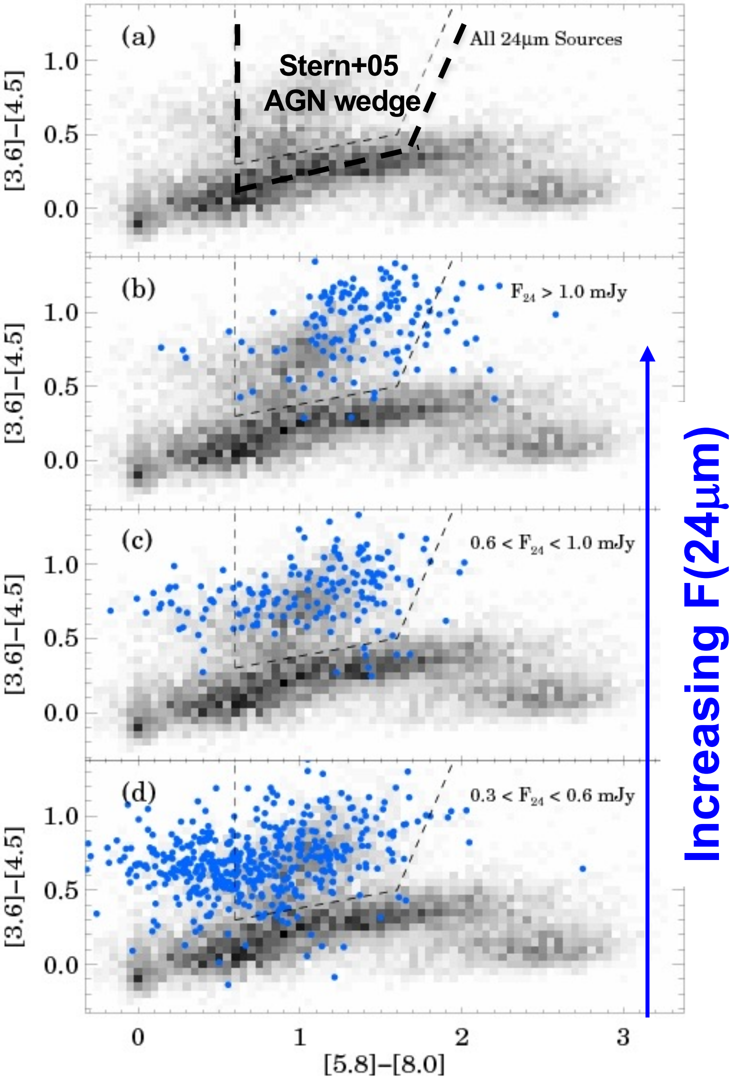

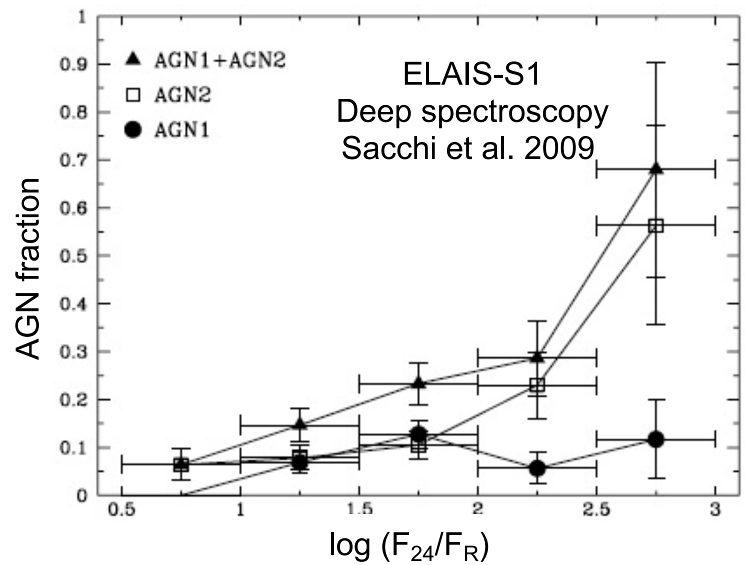

X-RAYS

- Obscured in X-rays (e.g., Lanzuisi_ et al. 2009; Fiore et al. 2008, 2009; Daddi et al. 2007)
- Hard to discriminate between Compton-thin and Compton-thick AGN with near-IR/mid-IR diagnostics alone → X-ray spectra, stacking and SED fitting required

From DOGs to Hot-DOGs

W1,W2 undetected (**W1W2 dropout**), ≈1/30 deg^2 at $F_{12\mu m}$>1 mJy, ≈1000 found, ≈100 with spec-z
(Eisenhardt et al. 2012, Wu et al. 2012, Bridge et al. 2013, Jones et al. 2014, Tsai et al. 2014, […])

AGN/SF ratio

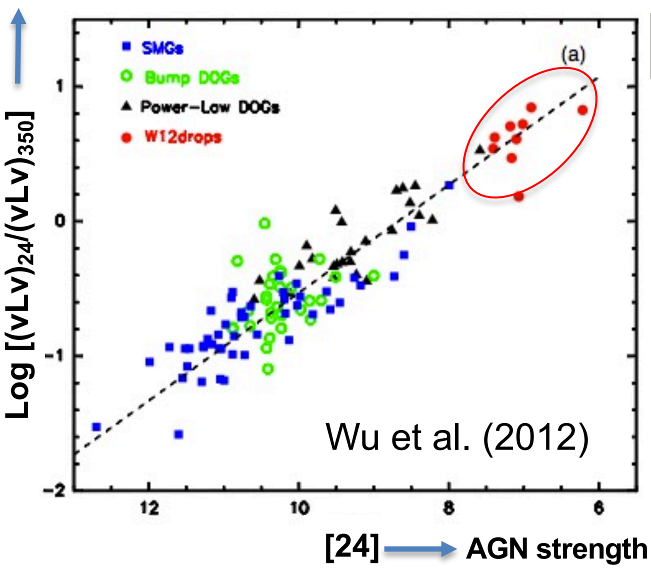

More extreme than DOGs

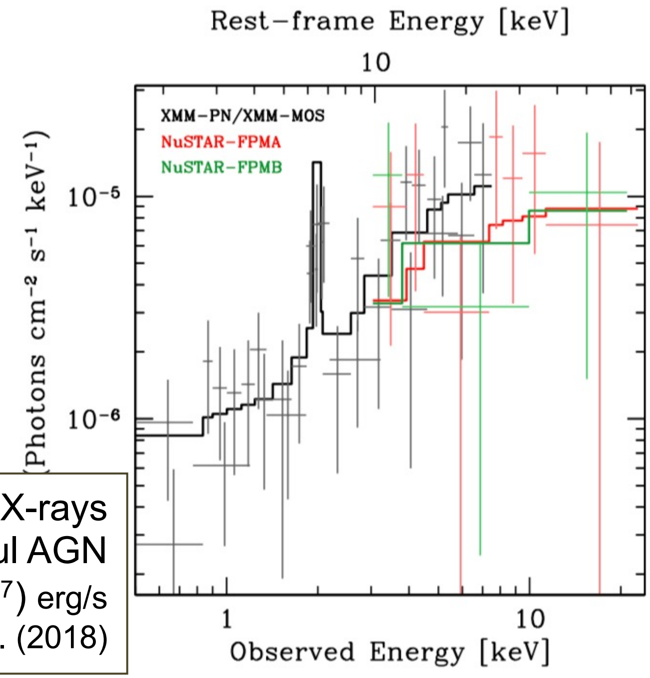

Heavily obscured in X-rays (N_H>10^{24} cm^{-2}), powerful AGN (L_{BOL}≈4×10^{47}) erg/s
Zappacosta et al. (2018)

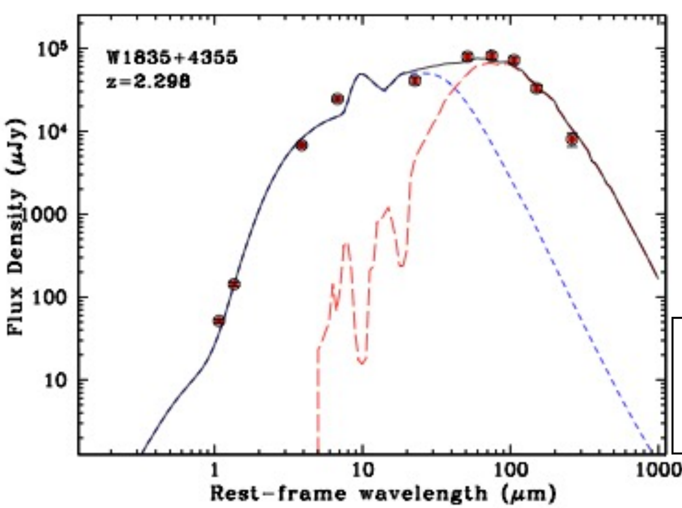

Powerful starburst
(SFR ≈3000 $M_\odot$/yr)
Piconcelli et al. (2015)

Hot DOGs: strongly accreting and star-forming systems, interpreted as late-state merger in the context of **merger-induced QSO formation scenario** (Hot DOGs eventually leading to optically bright QSOs)

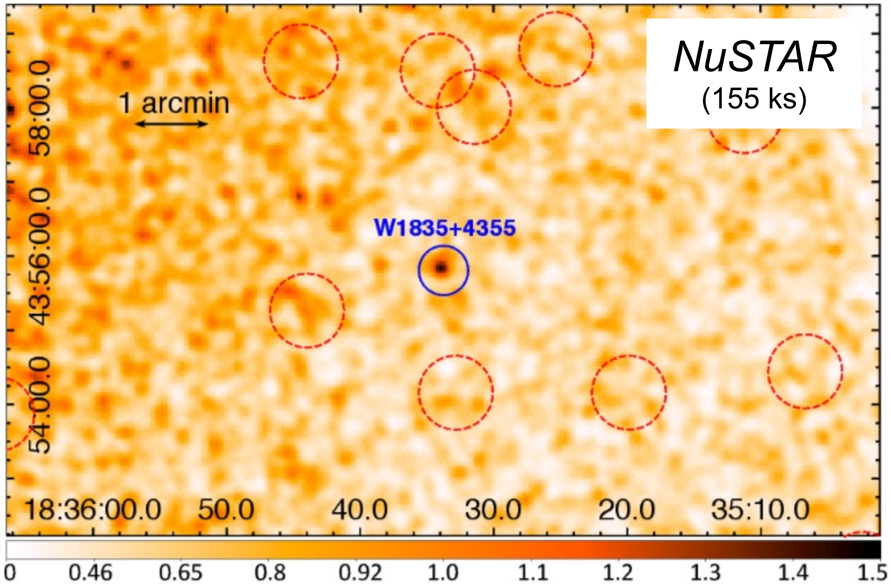

$N_H > 10^{24}$ cm^{-2}
Most obscured z>2 AGN detected by *NuSTAR*

$L_{2-10keV} \approx (1\text{-}3) \times 10^{45}$ erg/s
$L_{BOL} \approx (3\text{-}5) \times 10^{47}$ erg/s
Powerful starburst with SFR $\approx$3000 $M_\odot$/yr

Hot DOGs interpreted as late-state merger in the context of merger-induced QSO formation scenario (Hot DOGs eventually leading to optically bright QSOs)

Zappacosta+18

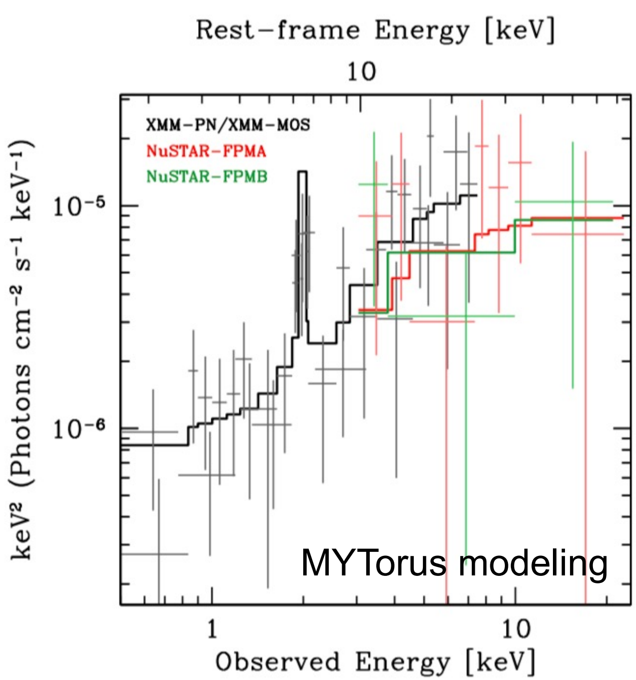

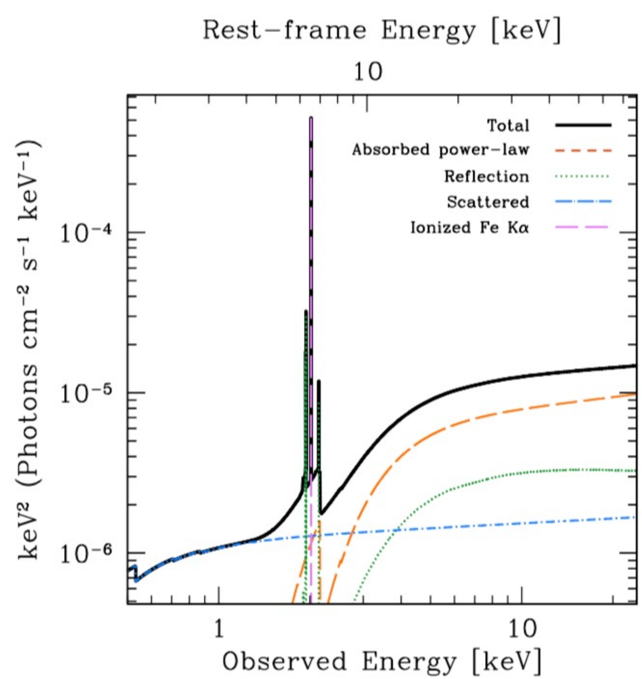

Hot-DOGs: constraints from X-ray stacking

W0116-0505 [z=3.173]

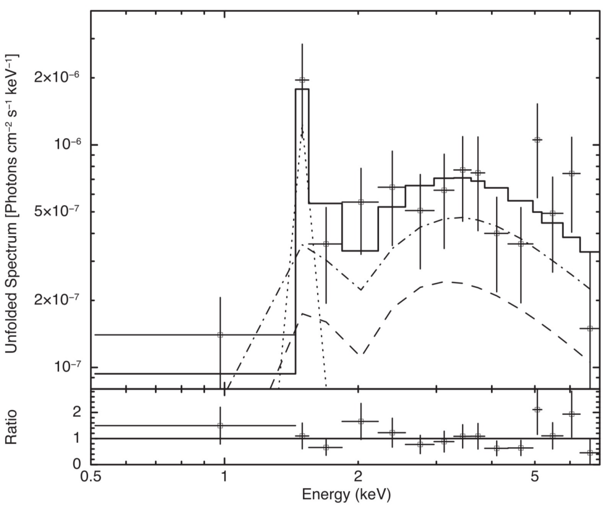

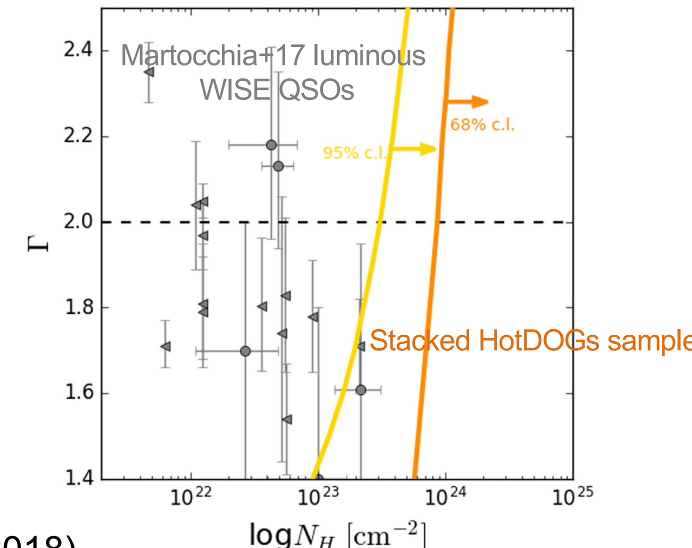

Log N_H>23.5
$L_{2-10keV}$>10^{44} erg/s

Vito et al. (2018)

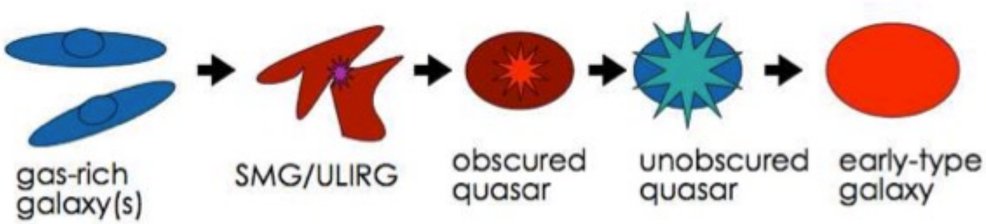

AGN-galaxy co-evolution discusse later in the course

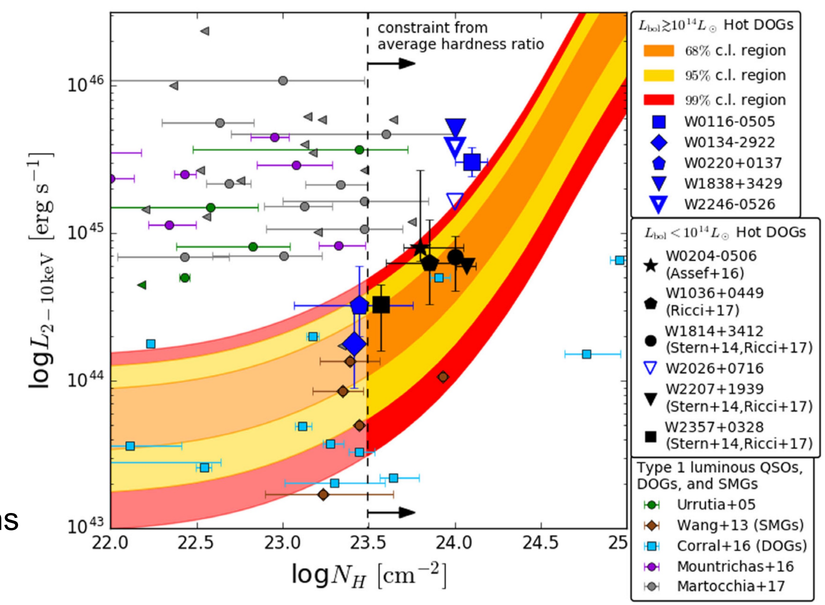

Probably weaker X-ray emission than
expected from mid-IR−X-ray correlations

The most obscured AGN in the COSMOS (field). I

The power of combining X-ray vs. mid-IR information (from SED fitting)

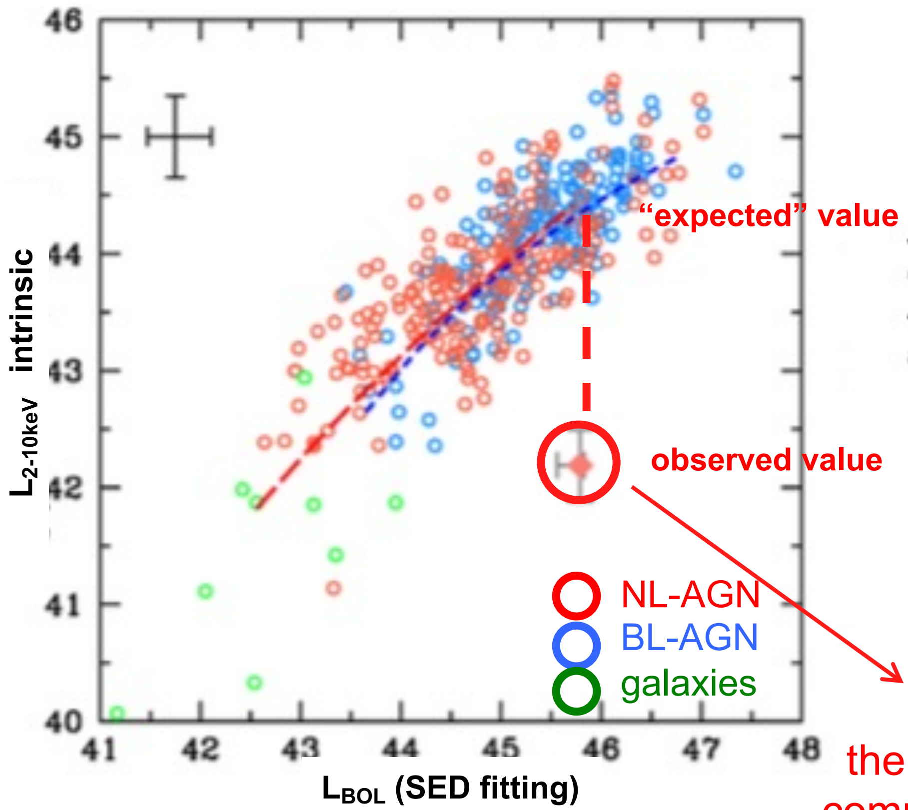

z=0.35 ULIRG in COSMOS
Similar to DOGs (MIR/O>1000) but at much lower z

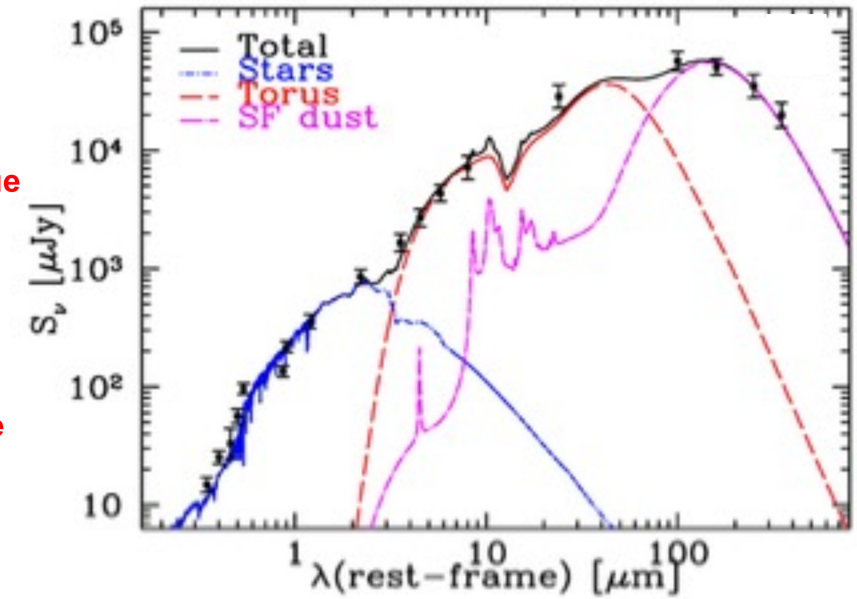

Lanzuisi et al. (2015b)

the measured L_X is too low compared to L_{BOL} assuming a "standard" (e.g., Lusso+12)

$$k_{BOL}=L_{BOL}/L_{2\text{-}10keV}$$

Typically, low-SNR X-ray spectra, careful modeling needed

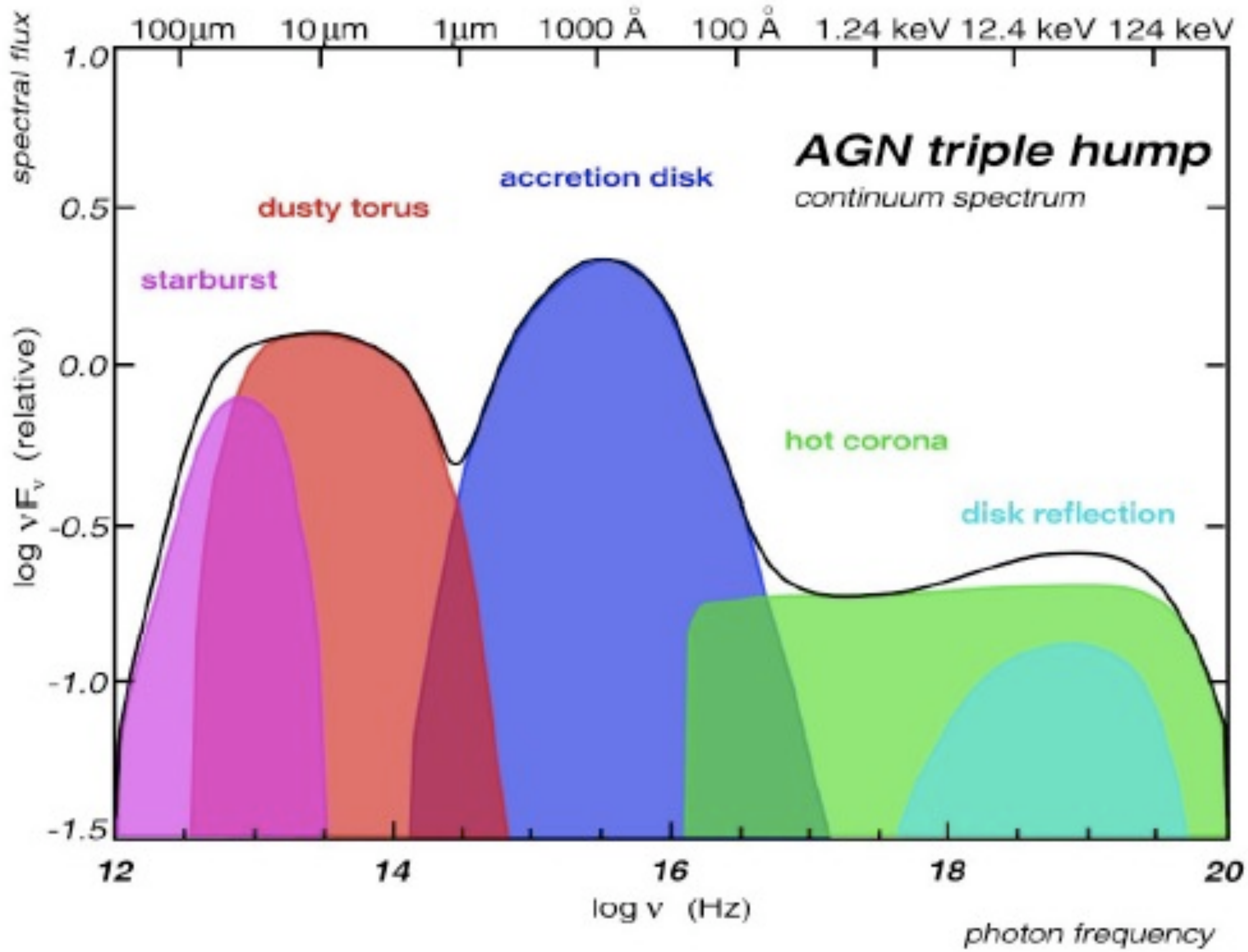

$k_{BOL}=L_{BOL}/L_{2\text{-}10\ keV}$ is a measure of the incidence of the hard X-ray emission with respect to the bolometric AGN luminosity (most of which residing in the accretion disc peak)

The most obscured AGN in the COSMOS (field). II

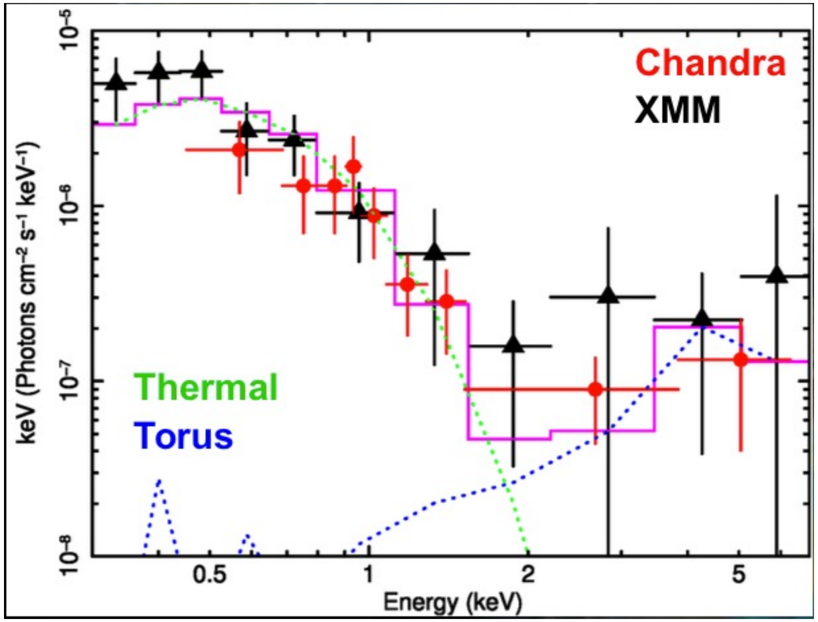

Checks with different models to account for obscuration (MYTorus, etc.)
Strong soft X-ray emission may 'hide' the Compton-thick nature of the sources in case of simple hardness ratio analysis
Extreme source (in terms of X-ray obscuration) in all diagnostic diagrams

allows comparison of intrinsic vs. observed AGN strength and finding of obscured AGN

"diagnostic diagrams"

Lanzuisi et al. (2015b)

Log N_H
vs.
$L^{obs}_{(2\text{-}10keV)}/L_{[NeV]}$

Depressed by absorption

Intrinsic AGN strength

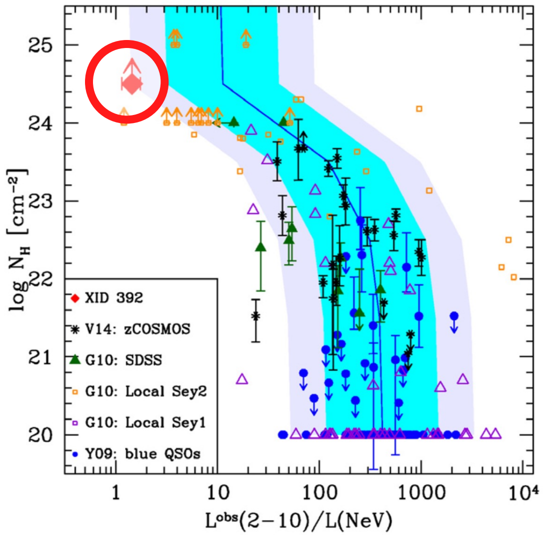

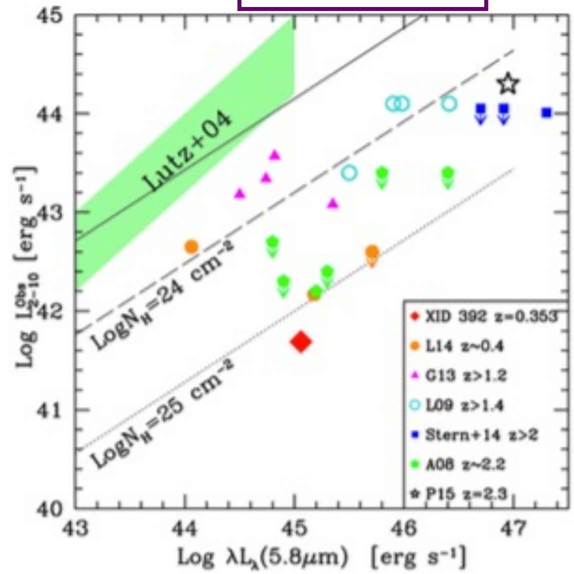

Log $L^{obs}_{(2\text{-}10keV)}$
vs.
Log λL_λ(5.8μm)

Selection of heavily obscured AGN in the Chandra Deep Fields. I

Delvecchio et al. (2015): *Herschel*-selected galaxies in GOODS and COSMOS (goal: to study BHAR vs. SF as a function of cosmic time via SED fitting)

Dalla Mura, CV, et al., in prep.

X-ray detection in 7Ms CDF-S and 2Ms CDF-N catalogs (Luo+17; Alexander+03)

X-ray spectral analysis to constrain N_H and derive intrinsic L_X

Presence of an AGN from SED decomposition (using modified MAGPHYS, SED3FIT; Berta)

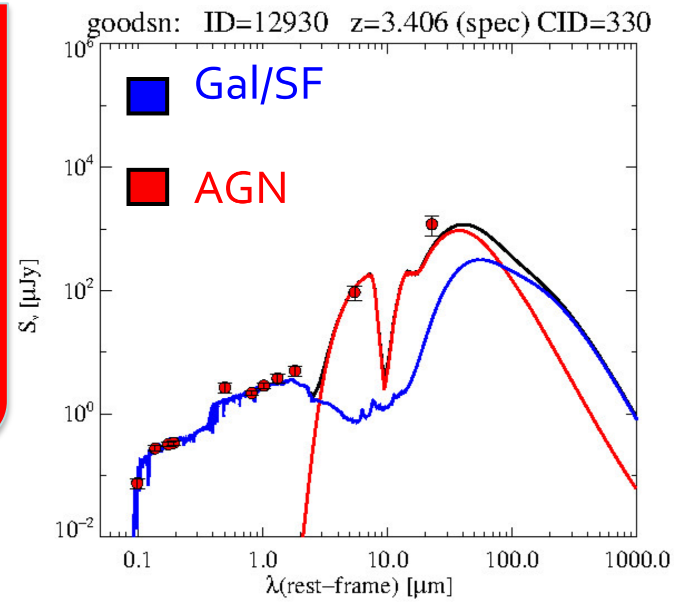

Intrinsic L_X predicted from L_{BOL} (SED fitting) + k_{BOL} $>10 \times L_{X,observed}$

Not a complete selection

Selection of heavily obscured AGN in the Chandra Deep Fields. II

CDF-S
14 obscured AGN candidates

z=0.07−3.4

CDF-N
4 obscured AGN candidates

Red + **blue** datapoints: 64 (CDF-S) and 58 (CDF-N) sources with X-ray detections and AGN highly required in the mid-IR (**SED fitting**)

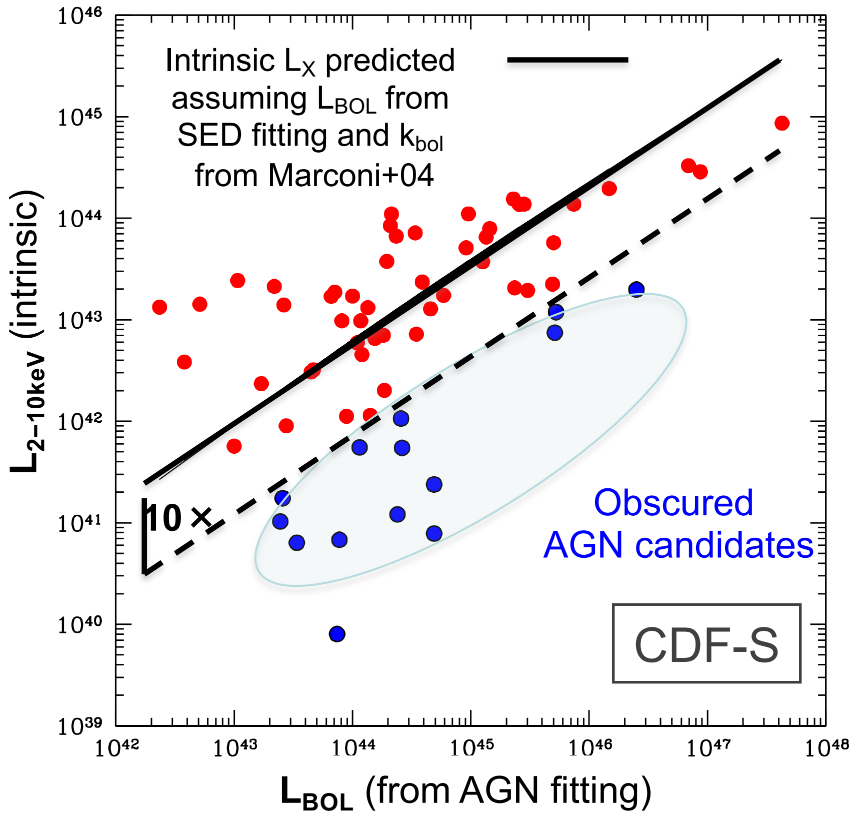

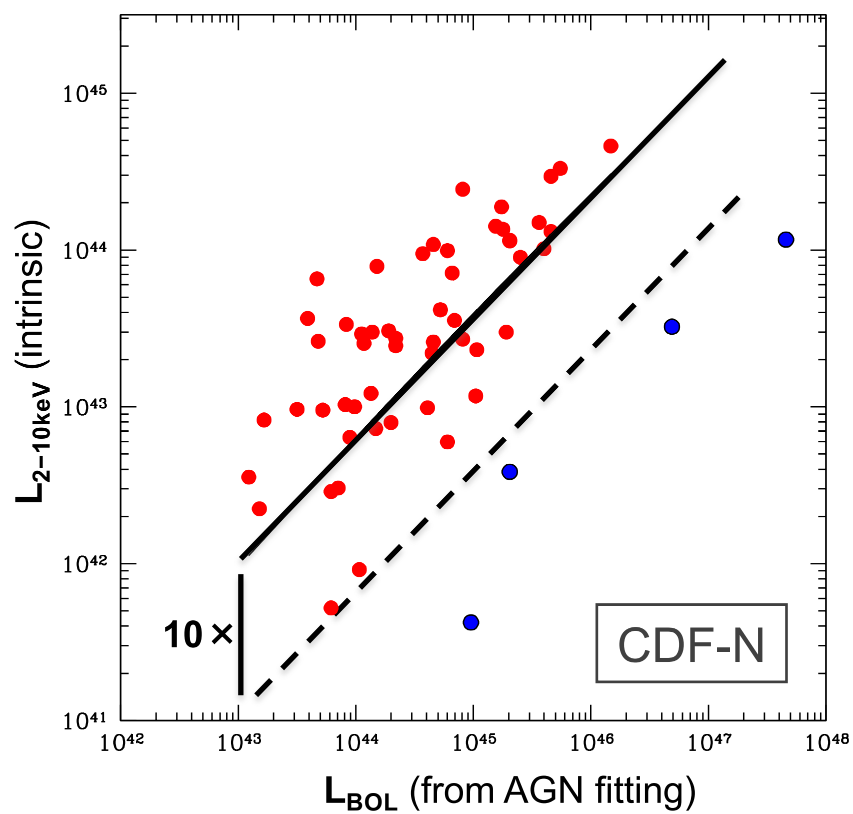

L_{BOL} → predicted (intrinsic) L_X vs. measured L_X
Difference likely ascribed to obscuration

Selection of heavily obscured AGN in the Chandra Deep Fields. III

Net counts=[40−570, median=100] **CDF-S** − [20−110, median=50] **CDF-N**

Some of the most heavily obscured AGN candidates (‘high stat’, low z)

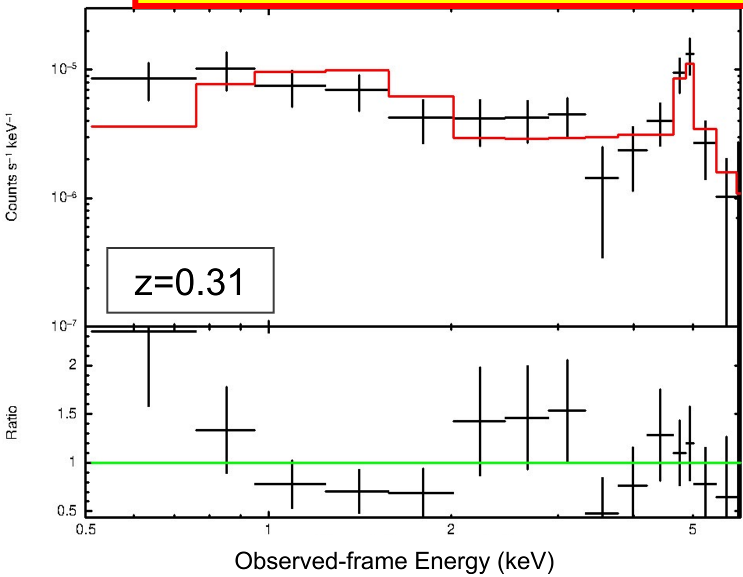

$N_H > 3 \times 10^{24}$ cm^{-2}

Proper (MYTorus) physical X-ray modeling

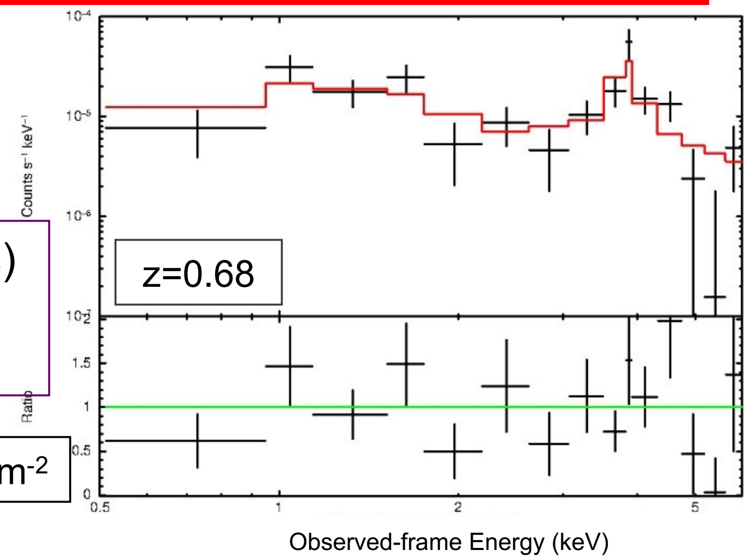

$N_H > 1.8 \times 10^{24}$ cm^{-2}

13/18 have $N_H > 10^{23}$ cm^{-2} about half are CT

see also Luo+11, Brightman & Ueda 2012, Brightman+14, Del Moro+16, Liu+17, Li+19, Corral+19 (in the *Chandra* Deep Fields)

Dalla Mura et al. (in prep.)

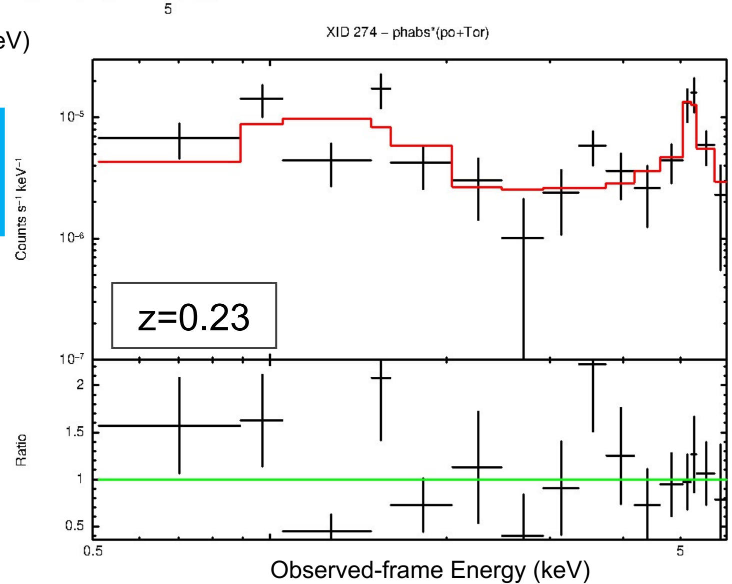

$N_H \approx 1.3 \times 10^{24}$ cm^{-2}

7Ms data CDF-S + 2Ms data CDF-N

Selection of heavily obscured AGN in the Chandra Deep Fields. IV

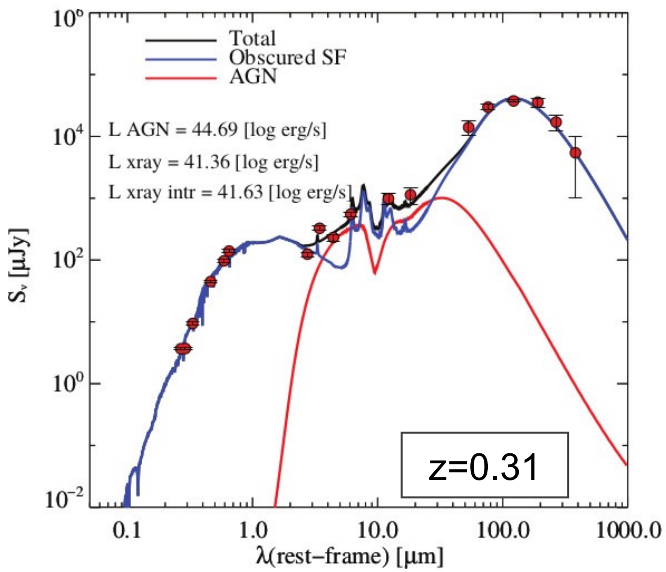

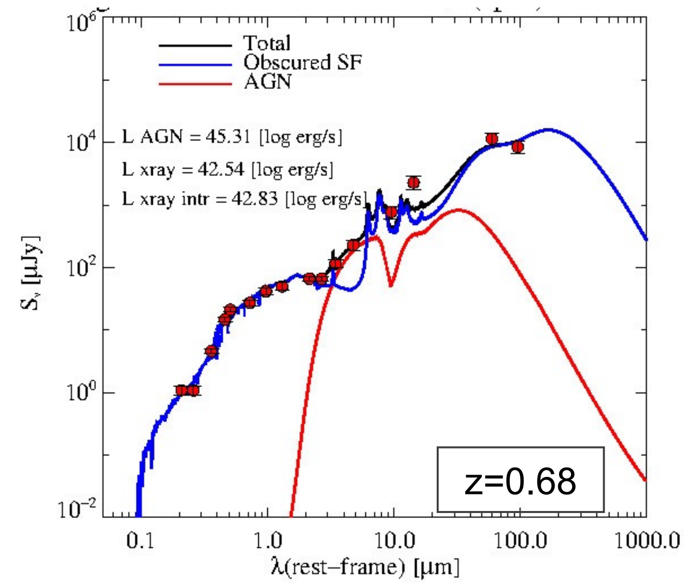

X-ray requirements

- Good photon statistics to apply physical models to X-rays (e.g., MYTorus, BORUS)

- Stacking analysis for the X-ray non-detections (but low background is needed, and SF may contribute to the signal) – *Chandra* (and deep data) is ideal

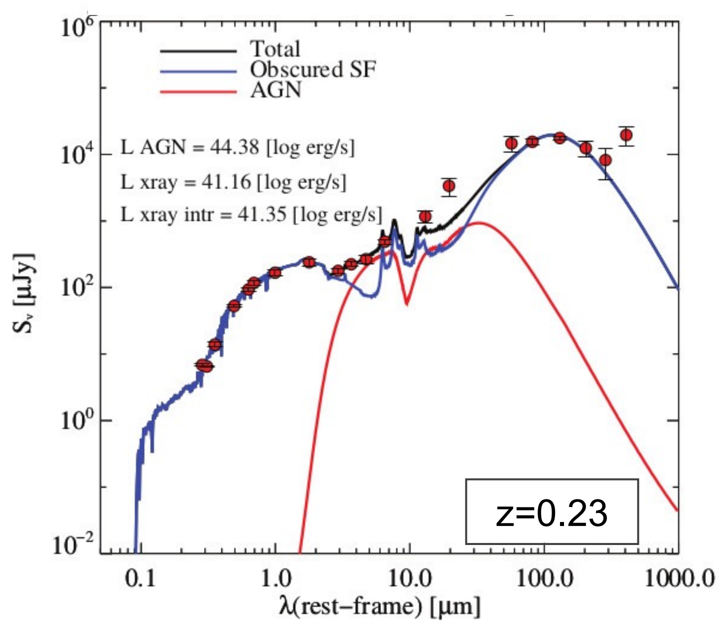

SED fitting requirements

- good photometry/low-resolution spectroscopy
- large wavelength range (to properly disentangle accretion from star formation
- model degeneracies in SED fitting under control

Importance of multi-wavelength data and joint mid-IR + X-ray info

Selection of heavily obscured AGN in the Chandra Deep Fields. V

$L_{2-10keV}$ vs. $L_{12\mu m}$

Comparison of the **X-ray luminosity** with the **AGN 12.3μm luminosity** (from SED fitting)

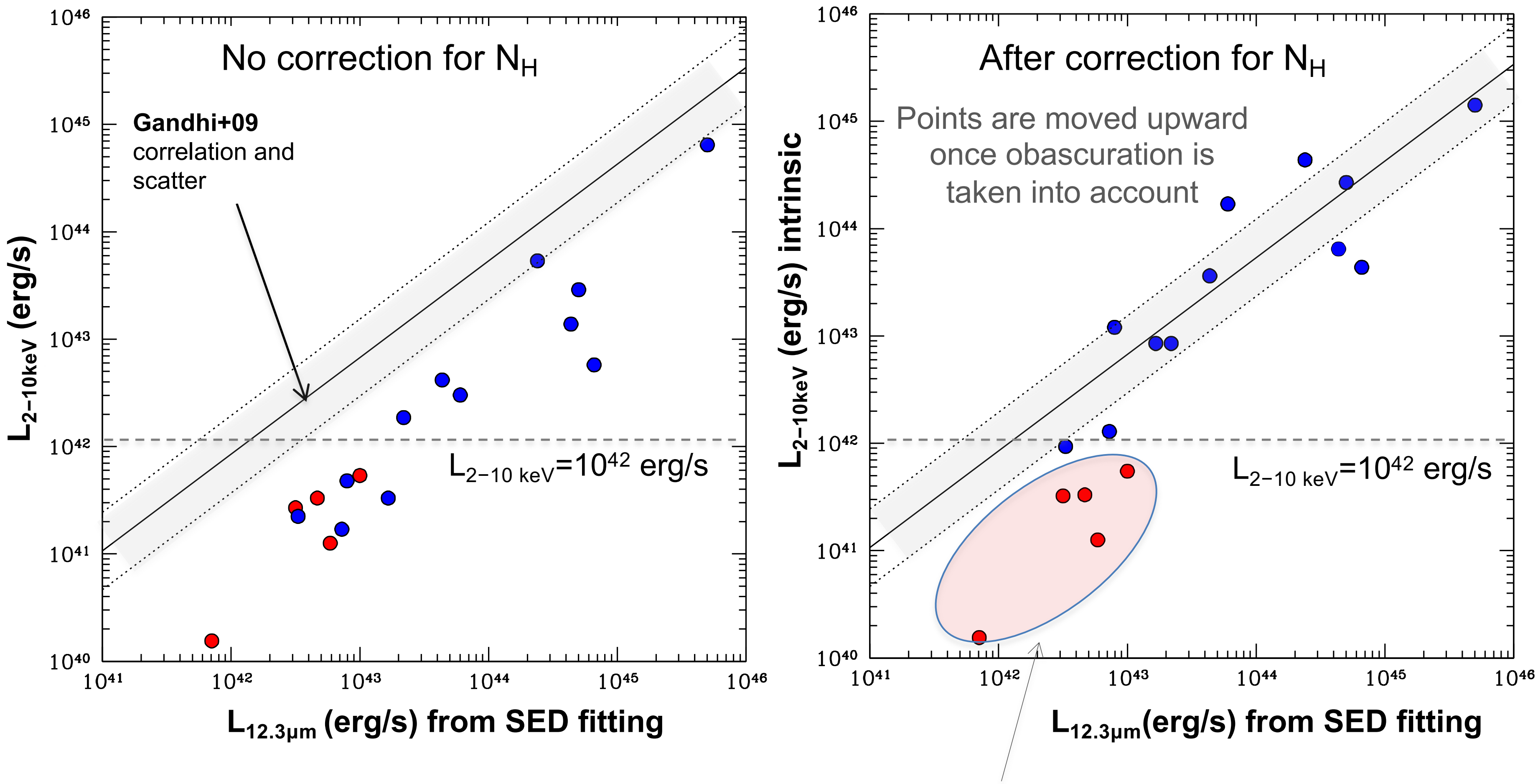

Original selection seems to pick up also few “hybrid” sources, where the AGN is not dominant.
X-ray → SFR (Ranalli’s, Mineo’s relation, etc.) ≈a factor 3 higher than SFR derived from the FIR

The quest for obscured AGN using optical spectroscopy

- Optical spectroscopy to select narrow-line AGN
- From low to high-redshift using [OIII], [NeV] and CIV lines (CIV: narrow component) and derive the space density of heavily obscured AGN
- X-rays (spectroscopy/stacking) to estimate the amount of obscuration

When the "missing" XRB was emitted?

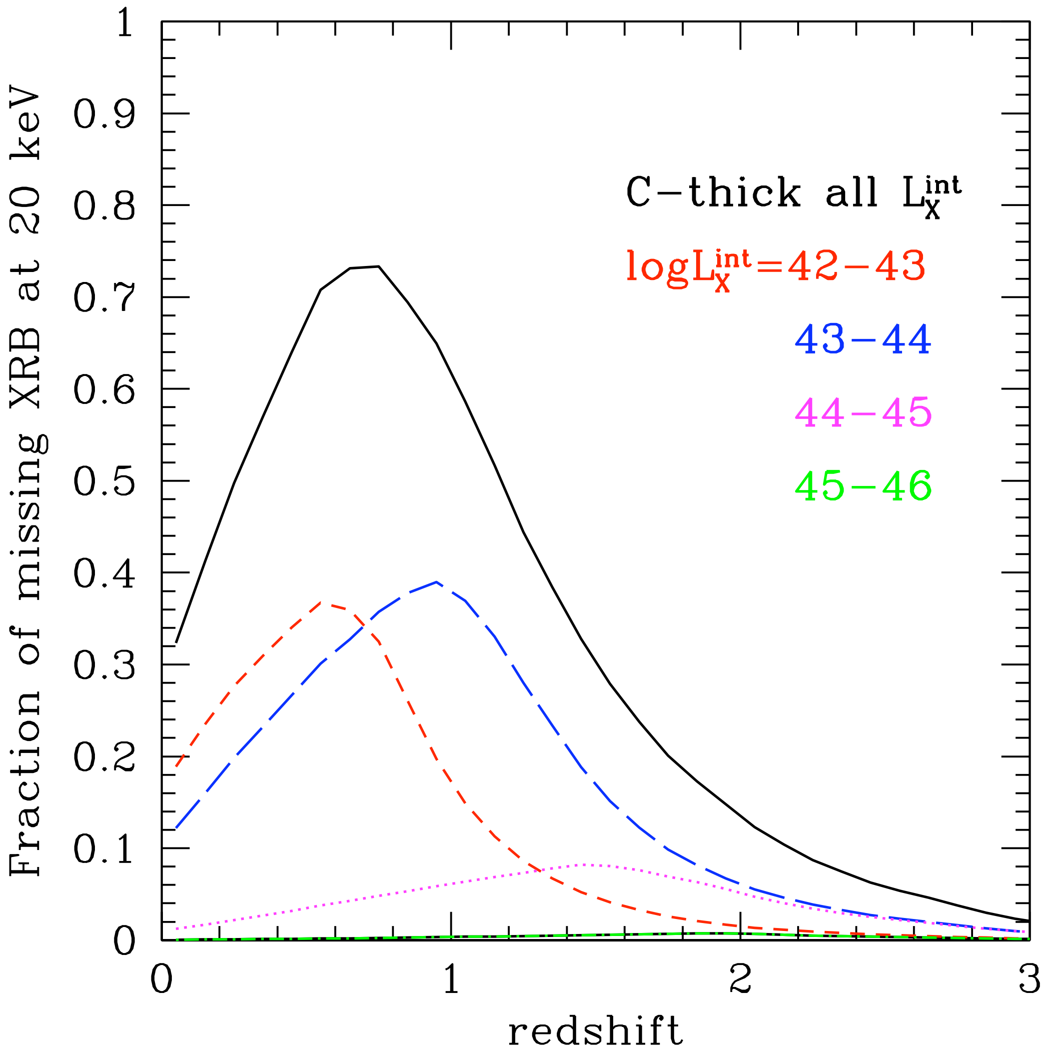

Predicted peak at z≈0.7-0.8
Mostly at $L_x \sim 10^{42-44}$ erg/s

Gilli 2013

Optical spectroscopic surveys: [OIII] vs. [NeV] selection

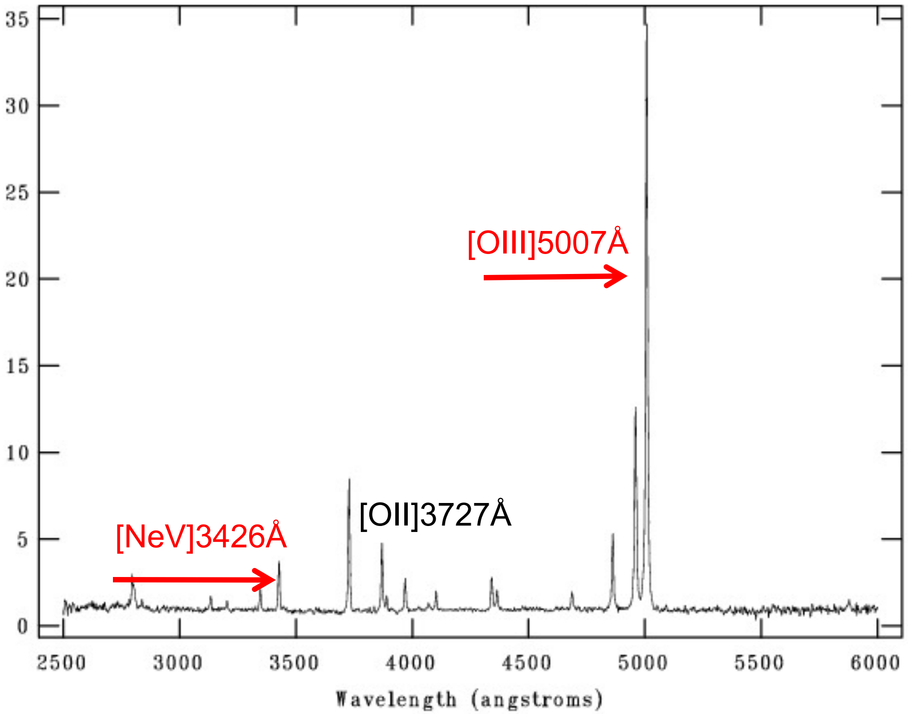

[OIII]

- **50%−65% of the SDSS Type 2** sample from Zakamska et al. 2003 at $LogL_{2\text{-}10keV}$>44.6 consistent with being **Compton thick**

  (Vignali et al. 2010; see also Ptak et al. 2006, Panessa et al. 2006, Lamastra et al. 2009, LaMassa et al. 2009)

- Extension using *NuSTAR* with no need of indirect absorption diagnostics (Lansbury et al. 2014, 2015)

limited z range (z<0.8) in SDSS

Extending the quest for heavily obscured Type 2 AGN using [NeV]

[NeV] cons

✔ It is a factor of ~9 weaker than [OIII] and suffers from heavier extinction ➔ selects only objects with “clean” NLR

[NeV] pros

✔ Unambiguous AGN marker (E_{ion}≈97 eV)

✔ Visible from z≈0.1 up to z≈1.5, while [OIII] only up to z≈0.8

X-ray properties of [NeV]-selected Type 2 AGN. I

Mignoli et al. (2013),Vignali et al. (2014); see also Gilli et al. (2010) using SDSS

COSMOS data

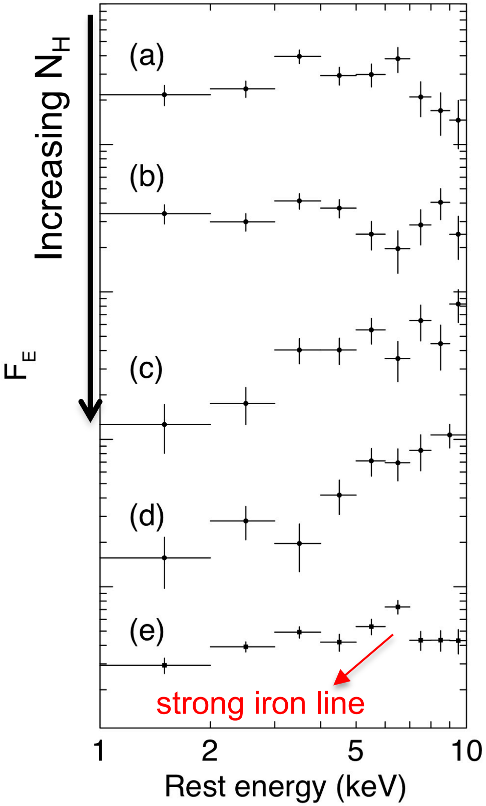

- 23 NL-AGN detected by *Chandra* (10-300 net counts, ~70 on average), 49 X-ray undetected
- 9/72 (13%) are **good C-thick candidates** (**X/[NeV]<15**)
- X-ray stacking + Monte-Carlo simulations indicate that **the overall fraction of Compton-thick AGN is ≈43%**

(a), (b), (c), (d): spectra of [NeV]-selected AGN with most X-ray counts
(e) Sum of 19 spectra of [NeV]-selected AGN with poor X-ray statistics (likely more obscured)

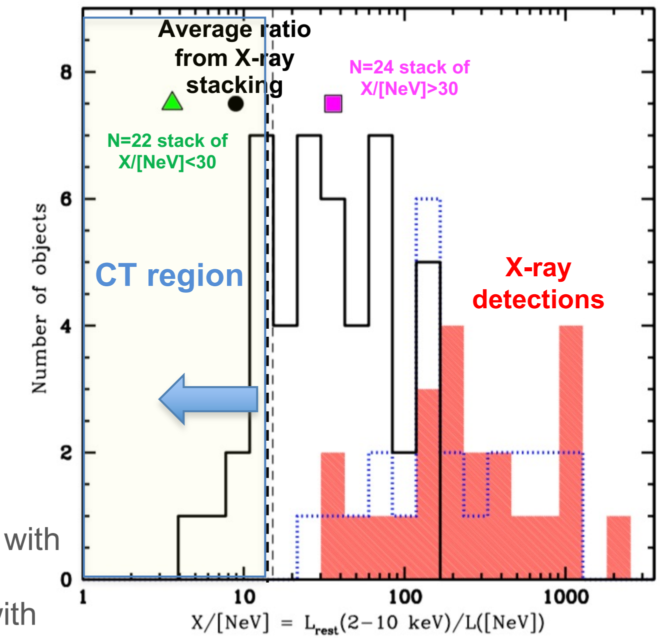

Main issue:
use the [NeV] optical emission line as a proxy of the intrinsic AGN strength

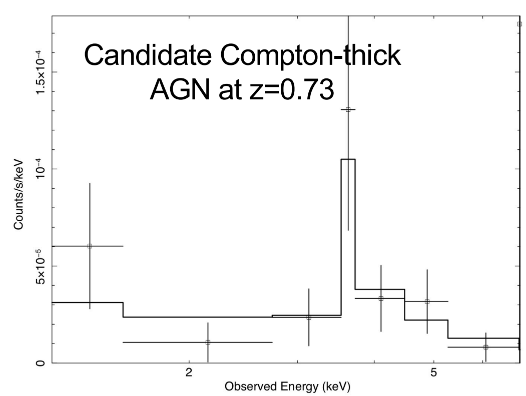

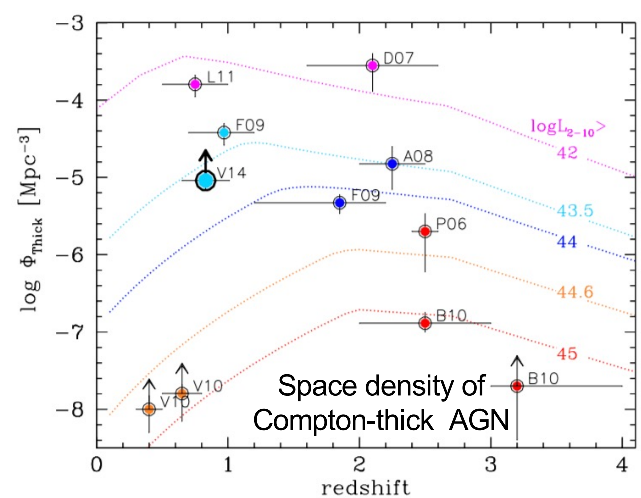

X-ray properties of [NeV]-selected Type 2 AGN. II

COSMOS-Legacy data ('estension' of the previous work)

Barchiesi (PhD student)

- 36 NL-AGN detected by *Chandra*
- 20% of the sources (including non-detections) are likely Compton-thick
- Half of the sample is in strong phase of accretion

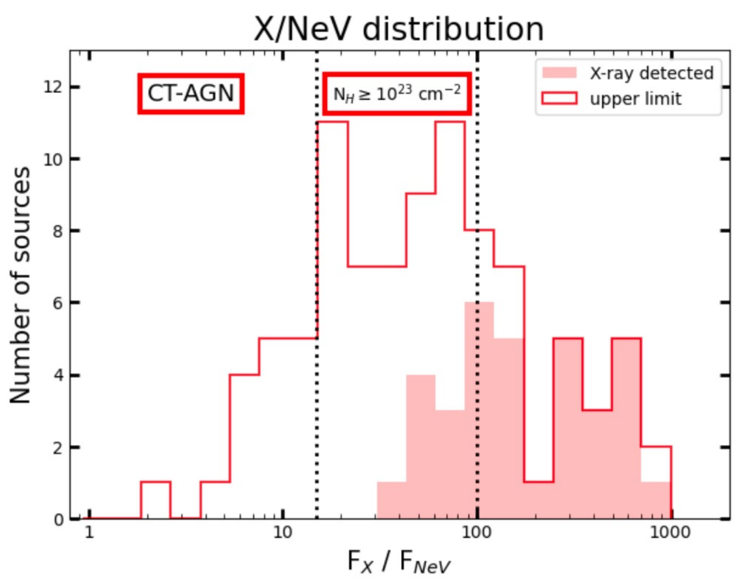

AGN and host galaxy interplay

Study of the impact of the AGN in shaping the properties of the host

→ The [NeV]-selected sample is preferentially in SF galaxies (lack passive galaxies)

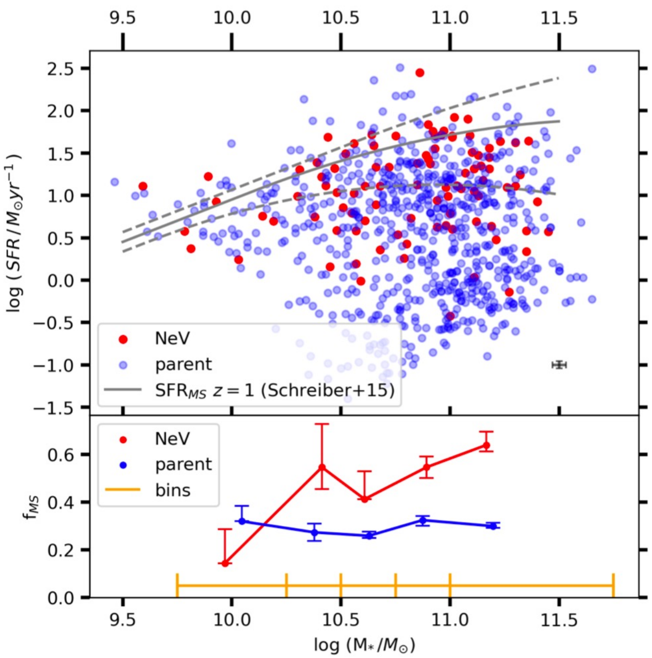

Barchiesi et al. (in prep.)

Search for high-z Type 2 AGN in COSMOS via CIV$_{1450Å}$
Pushing the search for obscured AGN via optical spectroscopy to z=3

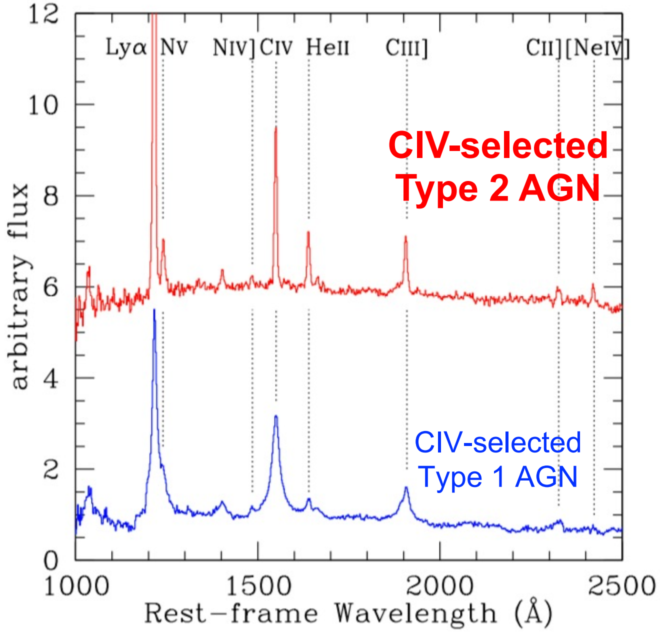

- 90 Type 2 AGN, z~1.5-3.0
- 51/92 are X-ray detected (50 counts on average)
- $N_H > 10^{22}$ cm^{-2} for X-ray detected Type 2 AGN
- $N_H > 10^{23}$ cm^{-2} for the X-ray individually undetected Type 2 AGN

Mignoli et al. (2019)
Vignali et al. (in prep.)

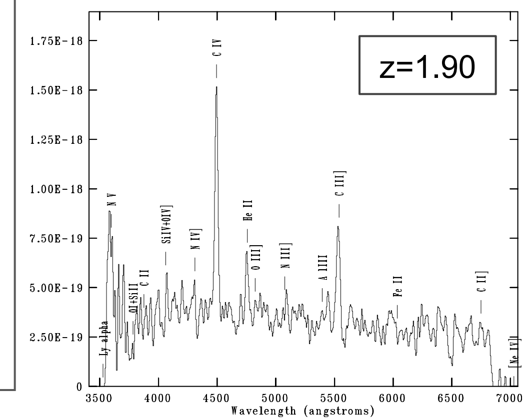

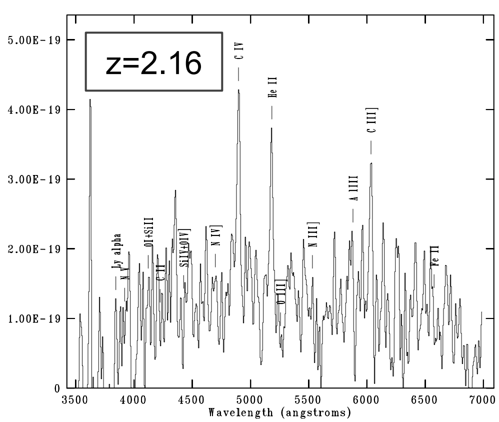

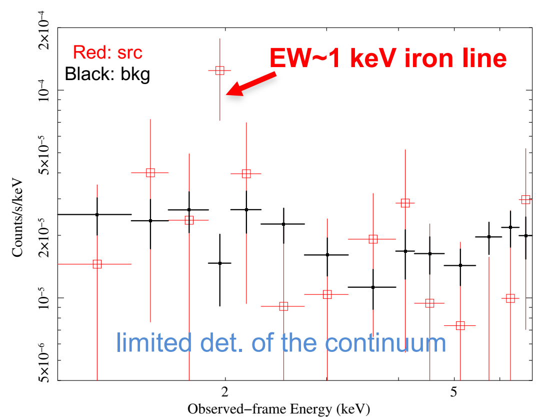

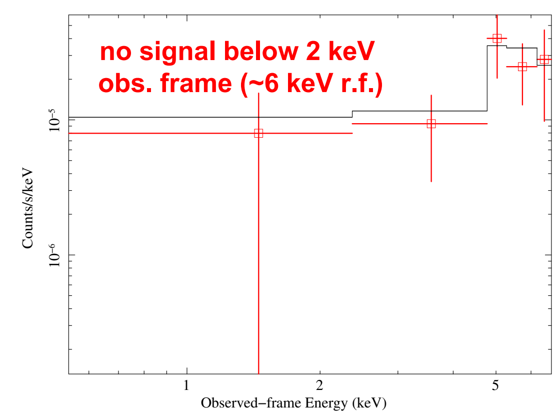

High redshift and obscuration prevent from a detailed X-ray spectral analysis → working in low-count regime

What about the far-IR/millimeter? I

Topic: molecules

Search for dense ($n_e > 10^4$ cm^{-3}) molecular gas tracers (cloud cores, fuel for SF and possibly AGN): HCN, HNC, HCO^+, CN (Gao & Salomon 2004; Imanishi et al. 2016)

These molecules are radiatively excited by mid-IR photons and can reveal the presence of obscured AGN

Higher ratios in HCN/HCO+ may imply the presence of an (obscured) AGN

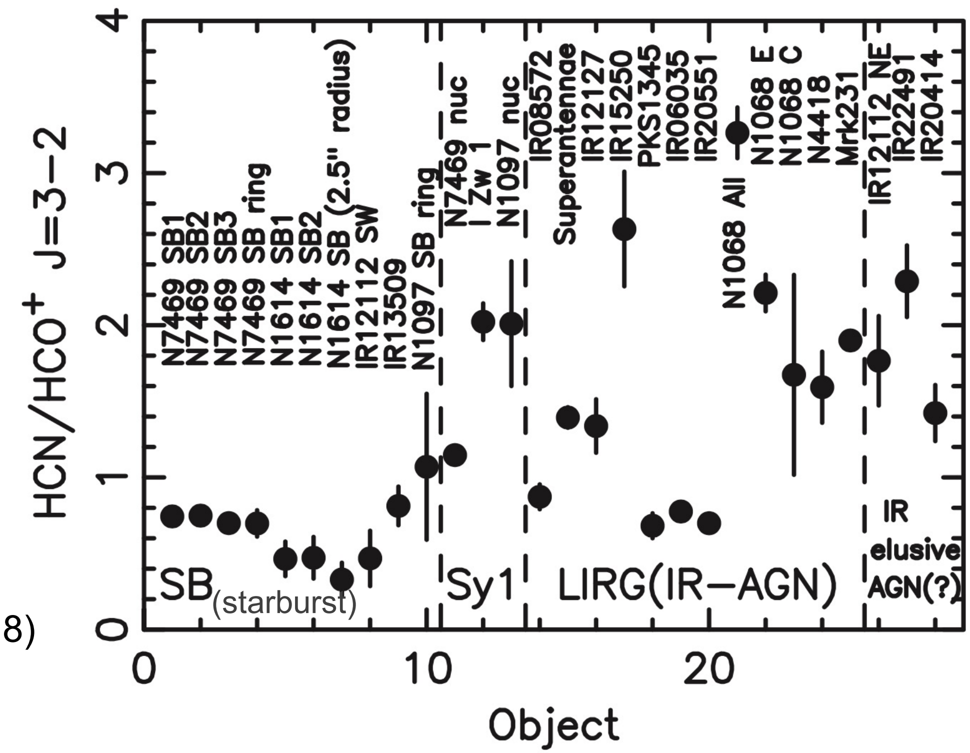

Imanishi et al. (2016, 2018)

What about the far-IR/millimeter? II

Situation is far from being assessed: hard X-ray (*NuSTAR*) data indicate that there is no clear correlation between the HCN/HCO^+ ratio and the AGN fraction → this line ratio may not be driven by the energetic dominance of the AGN → unreliable proxy for SMBH?

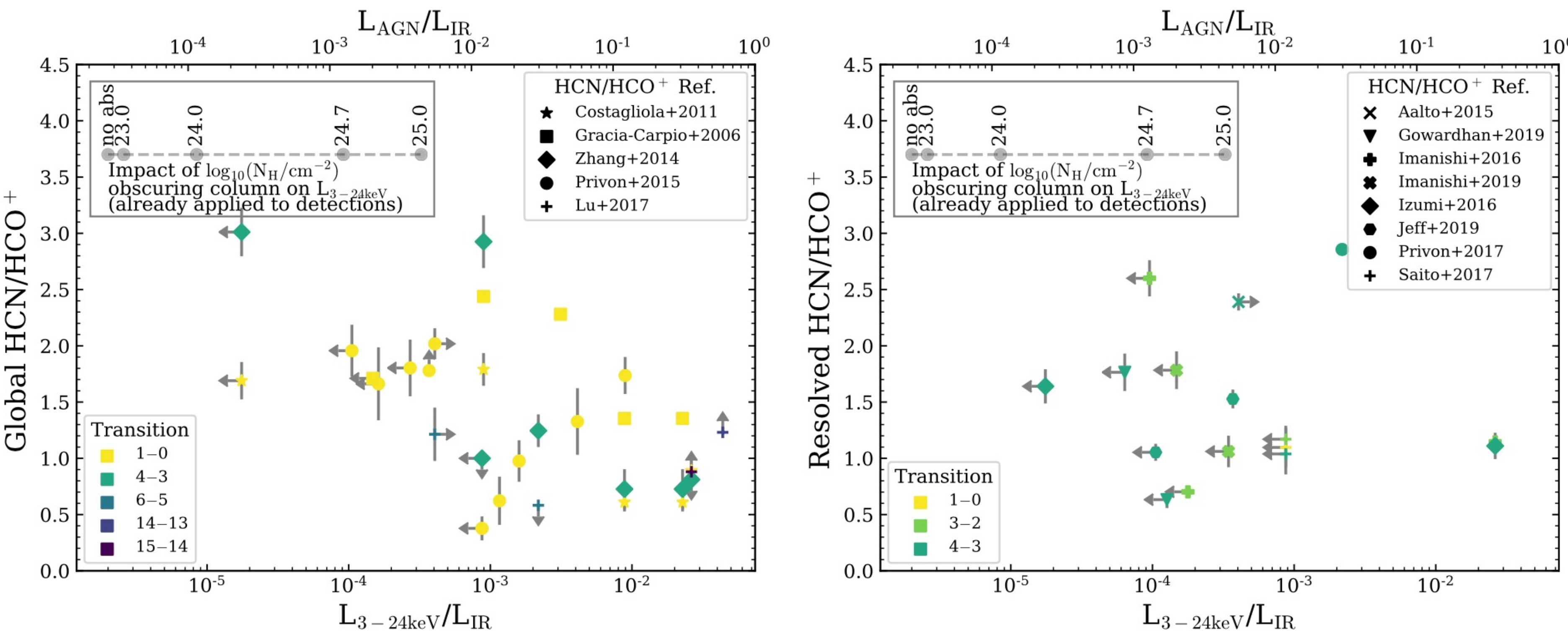

Privon et al. (2020)

What about the far-IR/millimeter? III

Topic: CO spectral energy distribution (COSLED)

Use the CO SLED to probe the 'nature' of the galaxy (SF vs. AGN/QSO) and provide hints on the underlying physical processes

A high ratio of high-excitation to low-excitation CO lines (*CO excitation ladder*) can indicate heating from an AGN

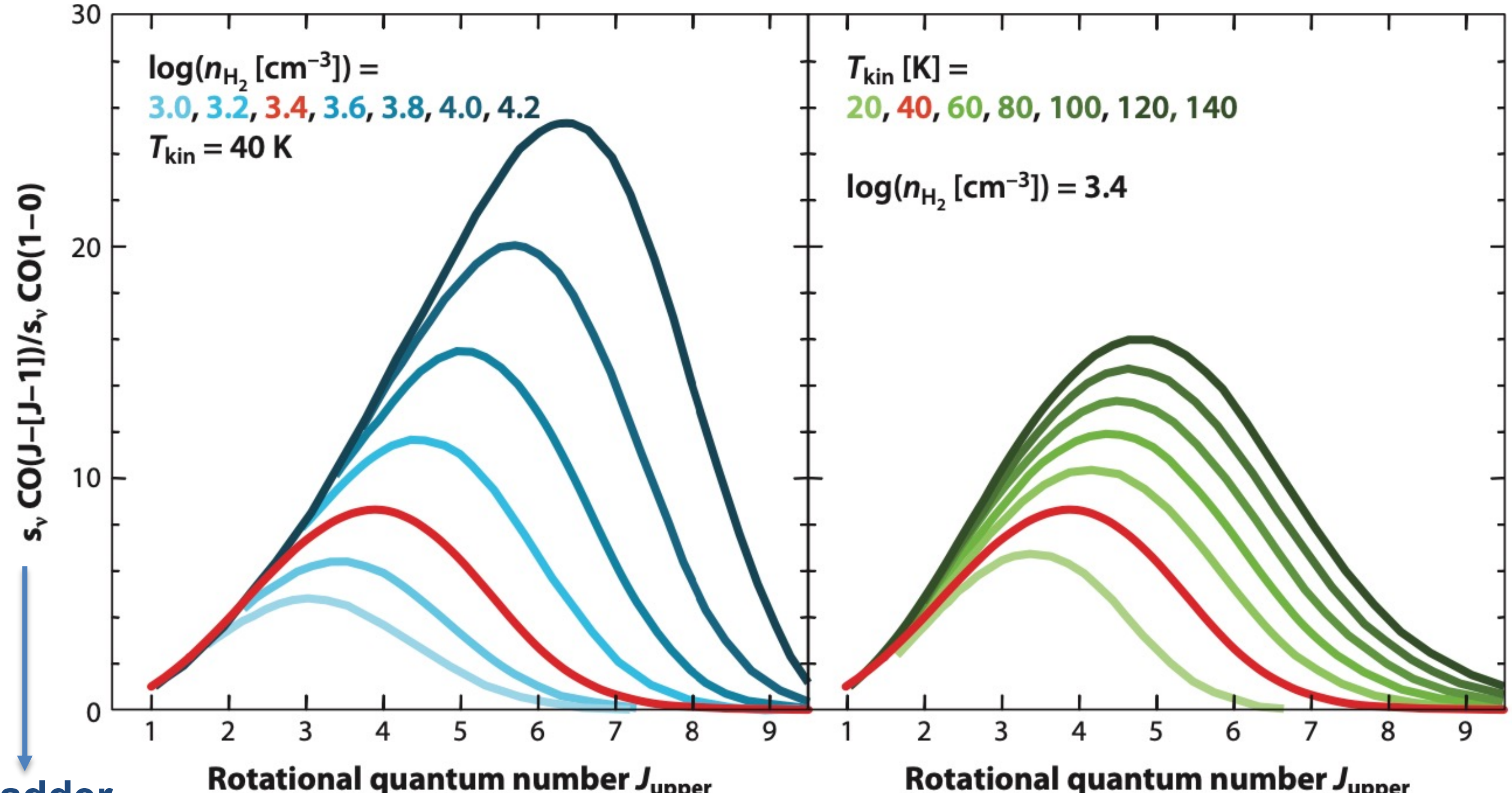

CO excitation ladder

Quantified rotational states

Carilli & Walter (ARA&A, 2013)

$$J \rightarrow J-1 : \Delta E_{rot} = h\nu_{line}$$

What about the far-IR/millimeter? IV

Different trends in the CO excitation ladder according to the type of object (galaxy, SFG,SMG, AGN)

Higher J reached by AGN (but shocks can be important as well)

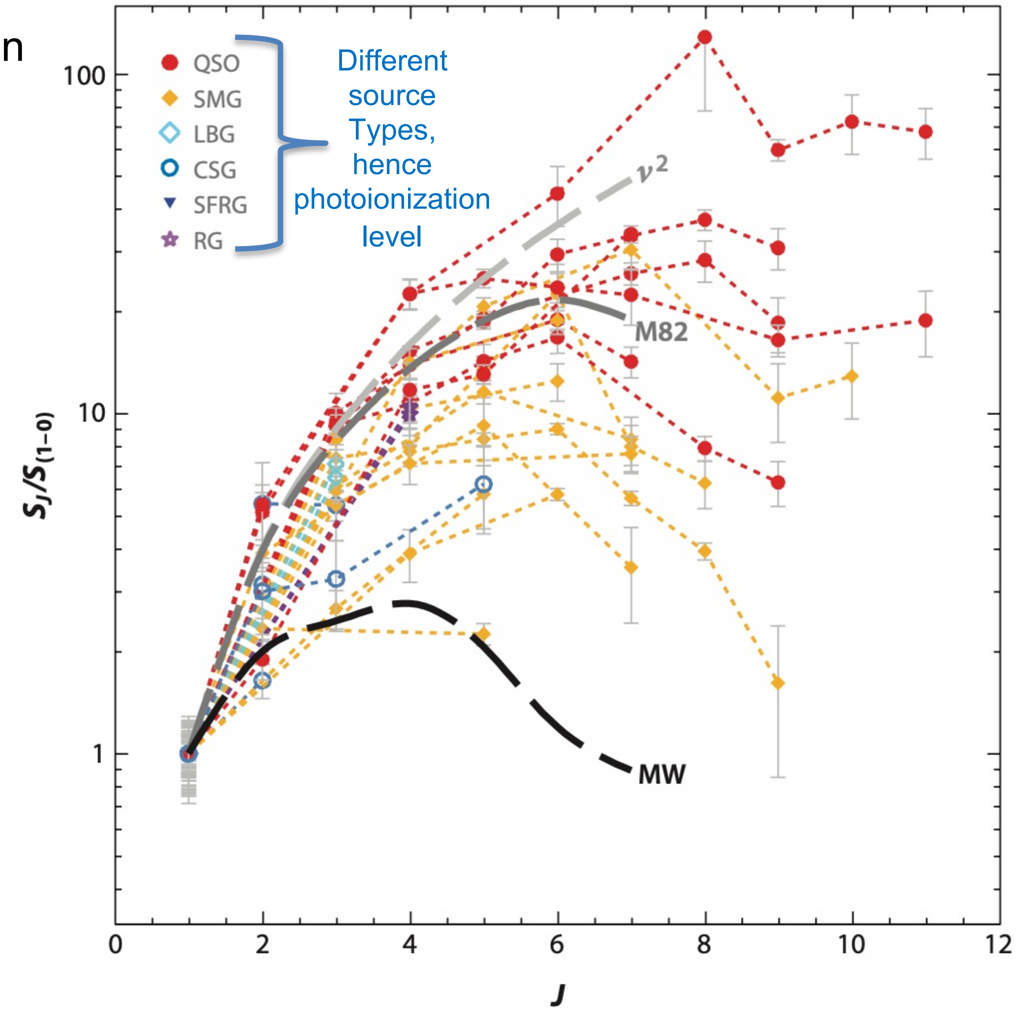

Carilli & Walter (ARA&A, 2013)

What about the far-IR/millimeter? V

Seyfert 2 galaxies at low redshift

z>6 QSO

NGC 7130

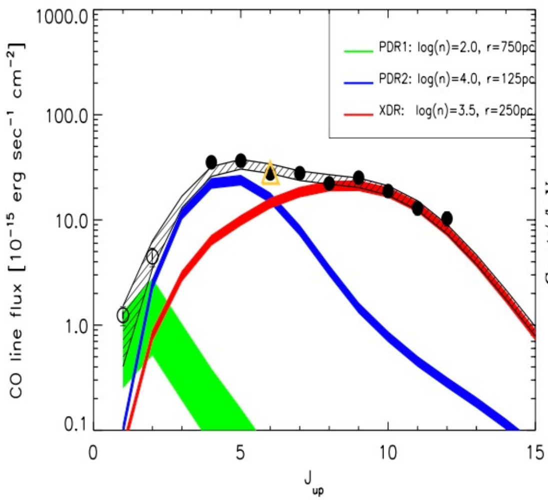

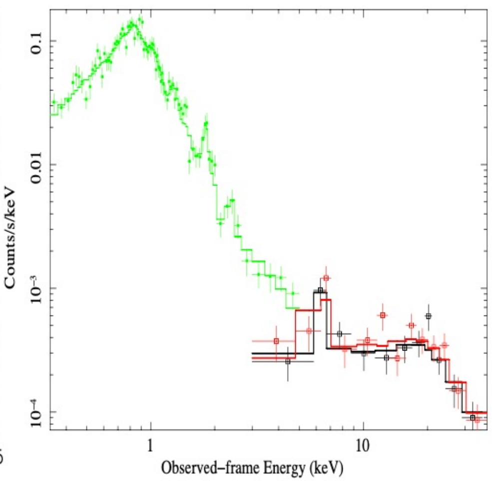

Pozzi et al. (2017)

Link the emission of AGN (including hard X-rays) to the micro-physics of the ISM

PDR: *photo-dissociation region* (regions dominated by stellar UV photons)

XDR: *X-ray dominated region* (regions dominated by high-energy photons)

Z=6.4 QSO

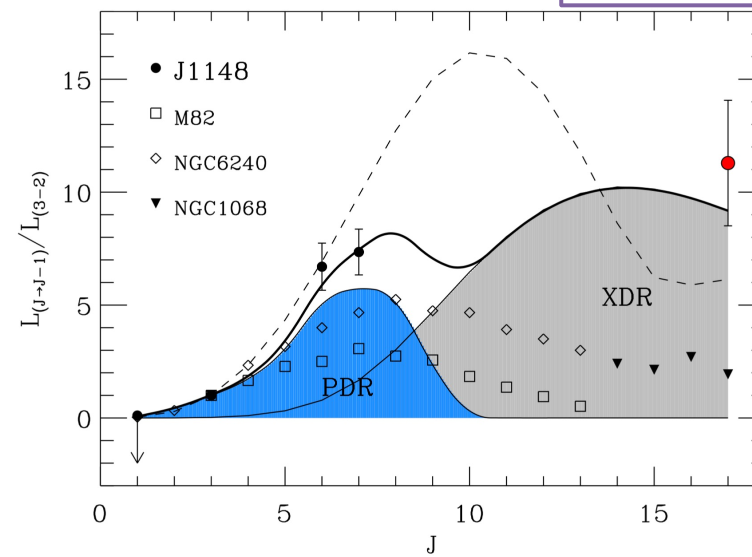

Gallerani et al. (2014)

NGC 34

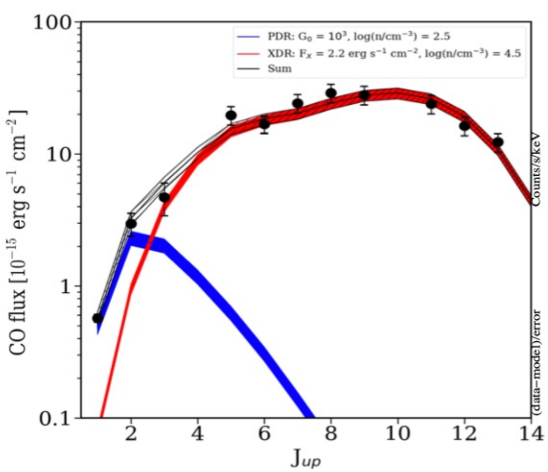

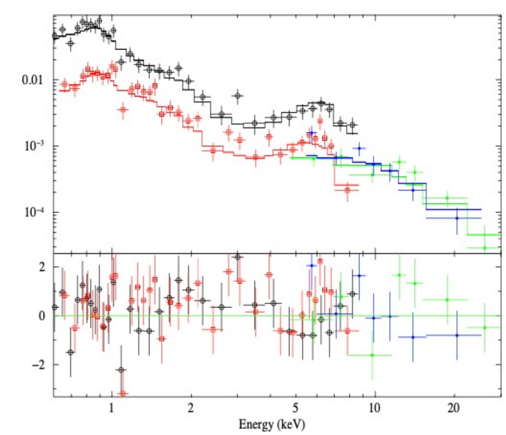

Mingozzi et al. (2018)

What about the far-IR/millimeter? VI

Observed COSLEDs (mostly local objects)

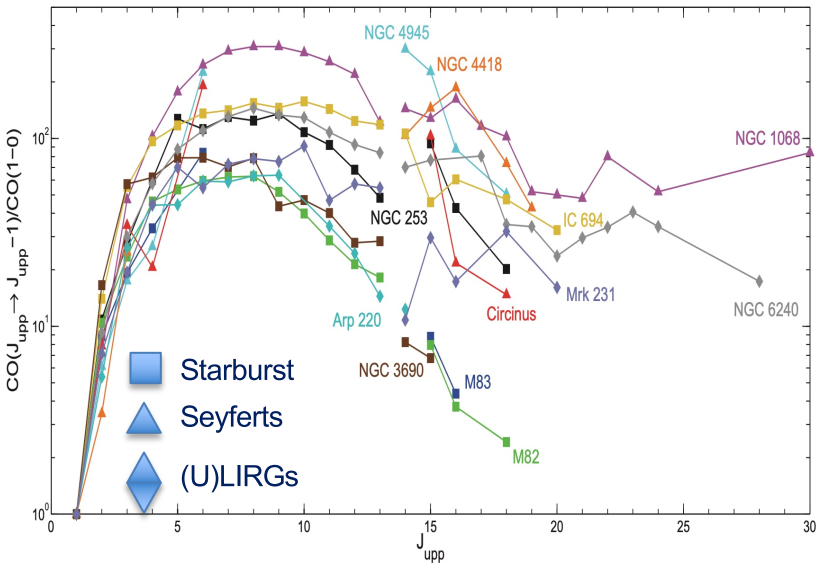

Mashian et al. (2015)

Theoretical COSLEDs

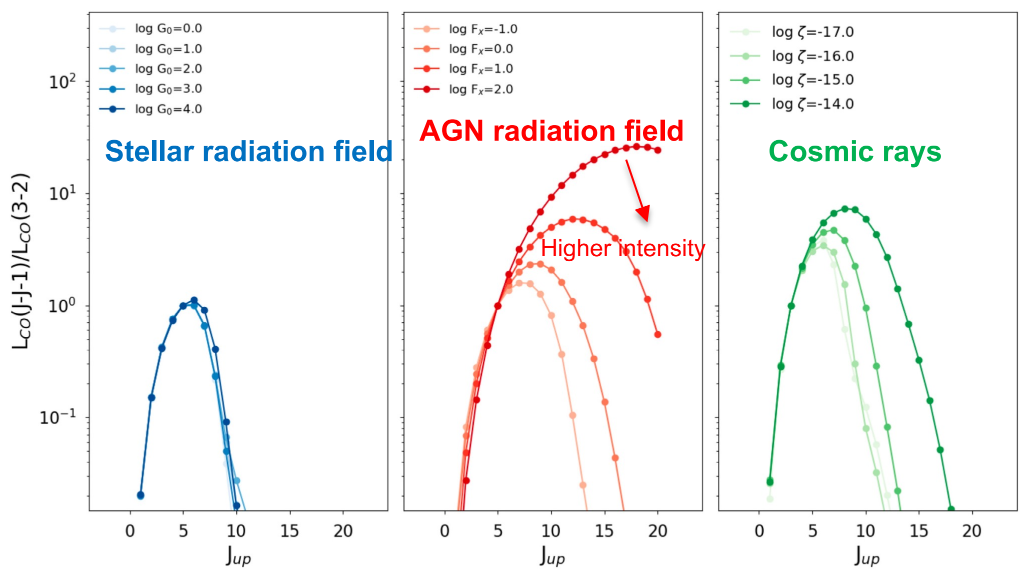

Vallini et al. (2019)

What about the far-IR/millimeter? VII

RADIO: both AGN and star formation can concur to the radio emission
Hard to discriminate at faint radio fluxes (unless the clear structures of a radio galaxy are observed)

Technique: selection of sources with '**radio excess**' with respect to that expected from SF-related processes, up to z~3 (Del Moro et al. 2013)

- Dominant AGN component in the mid-IR from SED fitting
- Detection of a compact radio core in deep VLBI observations in some cases
- About half undetected in deep X-ray data → heavily CT AGN candidates

Possibly, a still missing heavily obscured AGN population even in deep X-ray survey fields (see X-ray survey and XRB lesson)

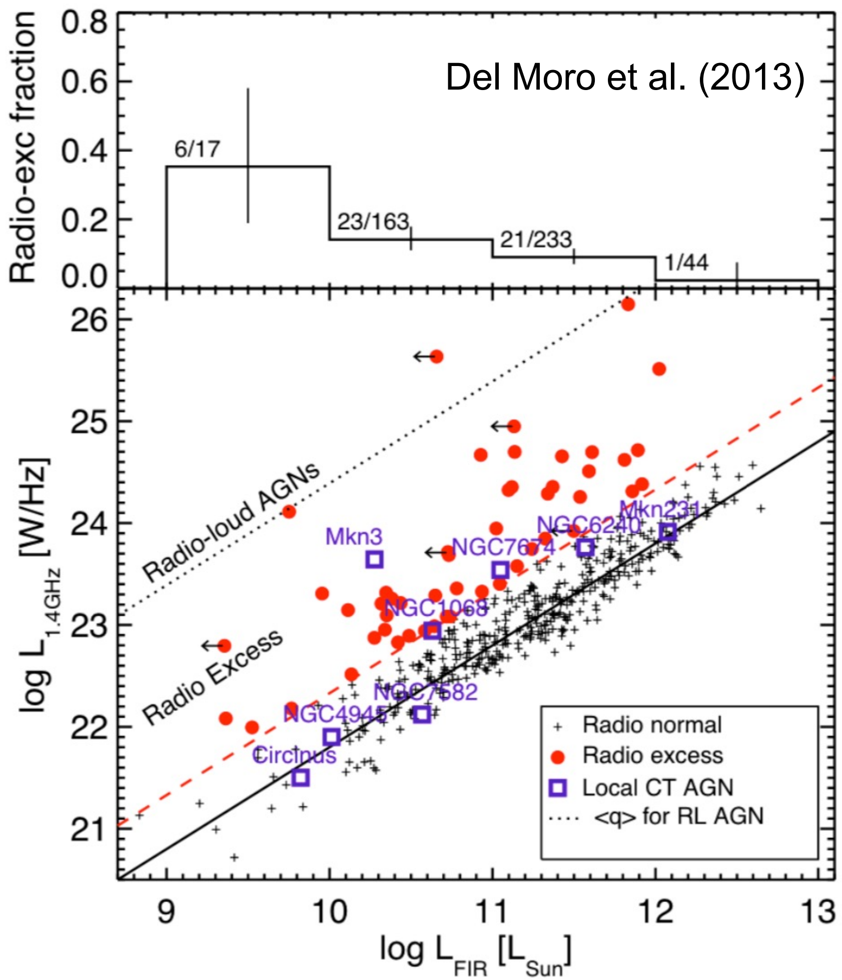

‘Optimization’ of AGN selection (including heavily obscured AGN)

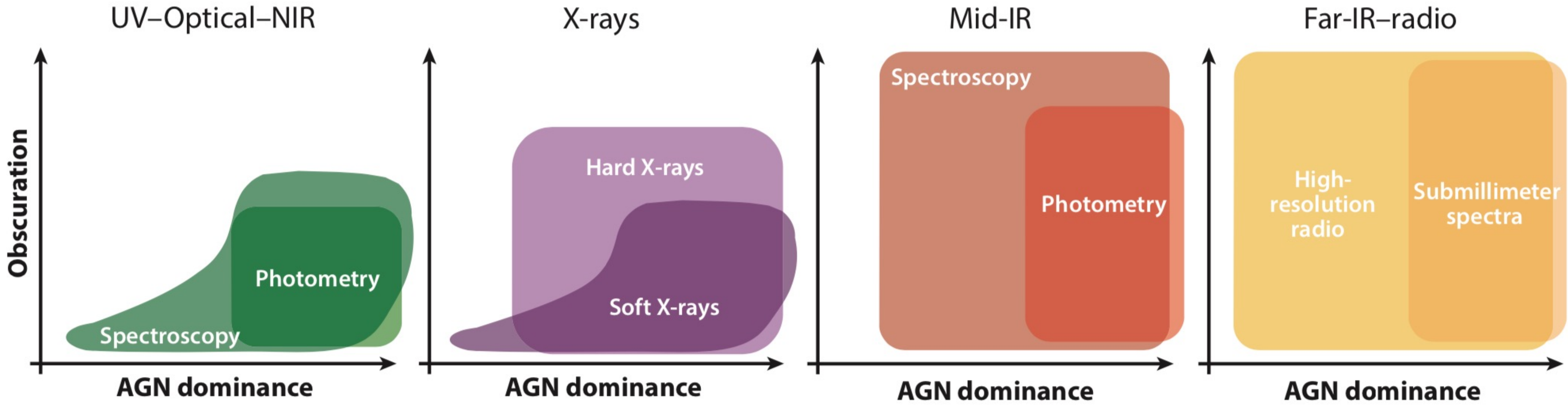

Hickox & Alexander 2018 (ARA&A)

UV/optical/near-IR selection criteria

COMMON ULTRAVIOLET/OPTICAL/NEAR-INFRARED SELECTION CRITERIA FOR OBSCURED AGN

Commonly used criteria for identifying AGN in this waveband include:

- a high ratio of high-excitation to low-excitation emission lines;
- detection of very high-excitation emission lines (e.g., [NeV]); and
- UV, optical and/or near-IR colors characteristic of an AGN accretion disk.

Once AGN have been identified, common criteria for classifying the sources as obscured include:

- width of permitted emission lines $<1{,}000$ km s^{-1};
- high nuclear extinction from spectral analysis or multiwavelength SED fitting; a typical criterion is $A_V > 5$ mag; and
- weak UV/optical/near-IR emission compared to AGN luminosity identified in other wavebands (e.g., X-ray, mid-IR).

Hickox & Alexander 2018 (ARA&A)

X-ray selection criteria

COMMON X-RAY SELECTION CRITERIA FOR OBSCURED AGN

Commonly used criteria for identifying AGN in this waveband include:

- observed or intrinsic X-ray luminosity higher than expected for stellar processes (hot gas and X-ray binaries) in the galaxy; a typical criterion is soft (0.5–10 keV) $L_X > 10^{42}$ erg s^{-1}, which is sufficient for all but the most extreme host galaxies; and
- identification of an X-ray point source in high-resolution imaging of the nucleus of the host galaxy (for nearby galaxies, although note the caveats in Section 2.2).

Once AGN have been identified, common criteria for classifying the sources as obscured include:

- X-ray spectral fitting results implying $N_H > 10^{22}$ cm^{-2}, or equivalent measurements using X-ray hardness ratios;
- a low ratio of observed X-ray luminosity to intrinsic AGN luminosity (usually determined from IR or optical data); and
- a high equivalent width of the Fe Kα line.

Hickox & Alexander 2018 (ARA&A)

Mid-IR selection criteria

COMMON MID-INFRARED SELECTION CRITERIA FOR OBSCURED AGN

Commonly used criteria for identifying AGN in this waveband include:

- color diagnostics from mid-IR photometry;
- a significant contribution of AGN to mid-IR emission, from measurement of features in the mid-IR spectrum or fitting of AGN and galaxy templates to the mid-IR SED;
- detection of very high-excitation emission lines (i.e., [NeV], [NeVI]); and
- identification of a point source in high-resolution observations of a galactic nucleus (for nearby galaxies).

Once AGN have been identified, common criteria for classifying the sources as obscured include:

- red UV–optical–mid-IR photometric colors;
- high nuclear extinction (for example, $A_V > 5$ mag) from spectral analysis or optical/IR SED fitting; and
- detection of solid-state absorption features in the mid-IR spectrum (particularly the Si features at 9.7 and 18 μm).

Hickox & Alexander 2018 (ARA&A)

Far-IR/radio selection criteria

COMMON FAR-INFRARED–RADIO SELECTION CRITERIA FOR OBSCURED AGN

Commonly used criteria for identifying AGN in this waveband include:

- a significant AGN contribution from fitting of AGN and galaxy templates to the mid-IR–far-IR SED;
- a large ratio of high-excitation to low-excitation CO lines or the detection of dense gas tracers (i.e., HCN, HCO^+);
- a high observed radio power (i.e., $P_{1.4\ \mathrm{GHz}} > 10^{25}\ \mathrm{W\ Hz^{-1}}$);
- a flat radio spectral index; and
- an excess of radio emission beyond that predicted for star formation.

Due to low optical depth in the radio, most criteria to classify AGN as obscured rely on other wavebands after identification in the radio, but one technique is the detection of absorption from neutral hydrogen determined through the 21-cm line.

Radio is the least-biased waveband for AGN selection but is largely unable to classify an AGN as obscured without any further indication from other criteria/wavelengths

Some of these issues will be discussed further in the course

Hickox & Alexander 2018 (ARA&A)